GEOLOGY OF THE CHLORIDE MINING DISTRICT

MOHAVE COUNTY, ARIZONA

by

Larry G. Eaton

Submitted in Partial Fulfillment
of the Requirements for the Degree of
Master of Science in Geology

New Mexico Institute of Mining and Technology

Socorro, New Mexico

June, 1980

TABLE OF CONTENTS

PLATE

TABLES

FIGURES

ABSTRACT

The Chloride mining district is located in northwestern Arizona and occupies the northern part of the Cerbat Mountains, an eastward-tilted fault block. The principal rock type is a 1.35 b.y. old granite gneiss which is uniform in composition but has diverse textures and typically is porphyroblastic. Supracrustal rocks of amphibolite, quartzite and biotite gneiss are exposed. In the central portion of the area the 1.2 b.y. old sill-like Chloride granite is crosscut by a Precambrian metarhyolite dike. In addition, dikes of various lithologies transect the Precambrian units, with the most abundant type being pegmatitic.

Structurally, amphibolite outlines three periods of Precambrian folding (F1, F2, F3), with the Chloride granite occupying the core of F1. The folding episode developed the initial fracture patterns, which were reactivated during later orogenic tectonics allowing metal-bearing hydrothermal fluids to be injected along them. Foliations of the Precambrian units strike north-northwest and have steep dips. The more massive units exhibit cataclastic deformation. Metamorphic grades during dynamothermal metamorphism approached the

high-temperature part of the medium grade facies (500° C to 600°C).

Native gold, silver complexes and sulfides are concentrated in "hydrothermal veins" characterized by open-space filling, brecciation, and quartz gangue, but the same minerals are also detected in "alteration zones". These zones are typified by iron-stained fractured outcrops. Both types of ore horizons were deposited in reactivated fractures. Mineralization may have started as early as Jurassic and appears to have continued well into Tertiary time.

ACKNOWLEDGMENTS

I would like to thank the many individuals for their prodigious help during this study. Dr. C. T. Smith provided stimulating conversations, persistent equanimity in editing this manuscript and many long hot hours in the field. Dr. Jamie Robertson contributed much help with the geochemical and metamorphic sections and Dr. David Norman assisted with the economic section; both also critically reviewed the manuscript.

I would also like to thank Bill Wyman for his help with the geochemical analyses, Robin Harrover for editing the thesis and enduring my ever-changing moods, and my colleagues too numerous to list.

Special thanks go to Arizona Juno Resources Inc., for their generous financial support so this project could be undertaken and to Dr. Richard Wyman, president of the company, for his constant hospitality. Finally I would like to acknowledge my parents for their unfailing moral support throughout these long years of college.

INTRODUCTION

Purpose

The purpose of this study is to: 1) construct a comprehensive geological map at a scale of 1:6000 of the Chloride mining district 2) describe the general geology of the area, and 3) study the relationship between the mineralized vein system and the geology.

Method

The field area covering 6 square miles was mapped between May 1979 and August 1979, at a scale of 1:6000. The geology was drafted on a contoured base map with mylar overlays for sample locations, data points and complex structure.

Over 540 data points were taken with particular emphasis around the Juno Mine (a patented claim owned by Arizona Juno Resources Inc., Boulder City, Nevada). A total of 149 rock samples were collected. From these 48 thin sections were prepared for detailed petrographic analysis to determine mineralogy and petrofabric. Ten samples were selected for whole-rock geochemical analysis

to help define the units and aid in structural interpretations.

Location and Accessibility

The study area is located in the Wallapai mining district, Mohave County, northwestern Arizona (Fig. 1). It occupies the northern part of the Cerbat Mountains which extend north-northwestward from Kingman for about 30 miles. The map area surrounds the small town of Chloride (the Chloride mining district) and includes sections 2, 3, 4, in T23N and sections 33, 34, 35 in T24N, R18W. The thesis area is 4 miles east of U.S. 93; it is served by Arizona 62, a paved highway. In addition several dirt roads mostly in poor condition, extend to many of the mines of the study area.

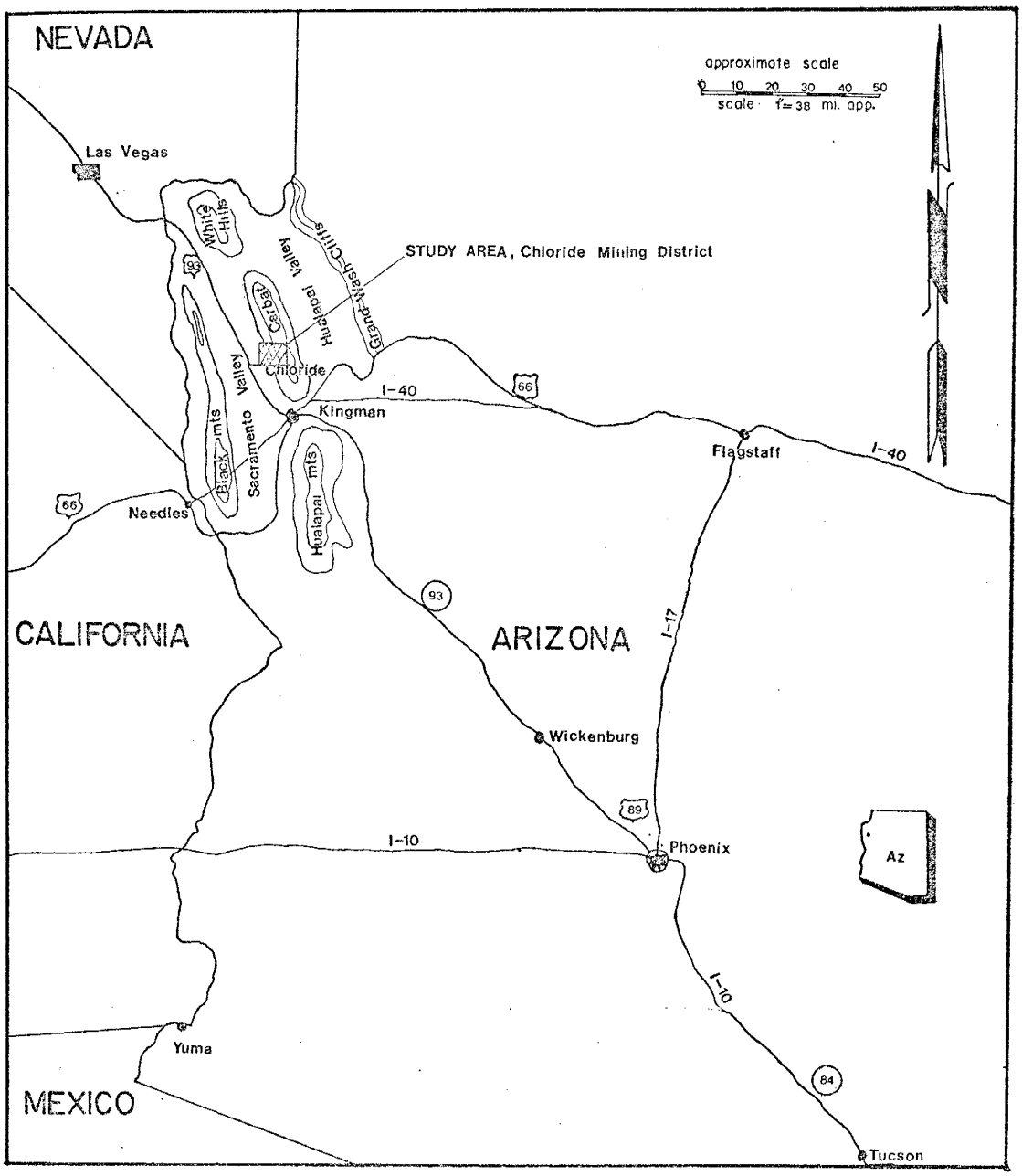

Figure 1. Index map of northwestern Arizona, showing location of the study area and the major physiographic features near it. Adapted from Boone, 1967.

Topography, Climate and Vegetation

The Chloride mining district is on the west slope of the Cerbat Range whose lower slopes are concealed by the alluvium of the Sacramento Valley. Relief is subdued and within the map area does not exceed 2000 feet. Summer months are hot, but low humidity, cool nights and a constant breeze moderate the heat. Precipitation is low and is mainly concentrated during the late summer in the form of cloudbursts. Winters are mild with little or no snow.

Vegetation is sparse consisting mainly of cacti, sage, yucca, greasewood, and scanty growths of grass. Pinon, juniper, and scrub-oak grow on the upper slopes of the Cerbat Mountains and provide cover for a variety of wildlife including deer, rabbit, small rodents, quail, hawk, rattlesnake, white-tailed dove, and a variety of song birds.

History

According to folklore the first prospect discovered in the area was Silver Hill. The discovery was made by two men who were later massacred by the Hualapai Indians after they had only explored the surface of their claim. Their graves can be found today on the west slope of Silver Hill.

The report of gold and silver in 1865 prompted other prospectors to explore this region. Ore minerals crop out as enriched accumulations in the oxidized part of hydrothermal veins; the oxidized exposures are relatively easy to trace on the surface. This led to several small mines in the district. Argentite cerargyrite, galena and gold were the principal ore minerals recovered between 1865 and 1890 (Dings, 1951). The early mining was profitable despite the enormous cost resulting from shipping the ore to Swansea, Wales, for smelting. Not until 1890 with a decline in silver prices did many of the operations in the district close. However in 1906 an increase in demand for base metals revived the district. This active period of mining continued through World War II, but post-war adjustments in the economy eventually led to the closure of most mines in the area.

Around 1958 Dr. Harrison A. Schmitt, a consulting geologist for Duval Corporation discovered a porphyry copper-molybdenum deposit at Ithaca Peak (known today as Mineral Park), 5 miles south of Chloride, Arizona. Currently it is the only active mine in the area.

Previous Work

Lee (1908) recorded the first general geological observations of the district in a study of western Arizona. This study was followed by Schrader (1909) who did a major geological reconnaissance of the Wallapai district; the work is of particular value since most of the mines were accessible at that time. Bastin (1925) considered the origin of the rich silver minerals and their persistence at depth. Hernon (1938) reinvestigated the ore deposits of the district, for the Arizona Bureau of Mines.

The most detailed work in the area was done by Dings (1951), which resulted in a large scale (1:24000), map of the Cerbat Mountains. Within the Precambrian, Dings separated three main units: amphibolite, undifferentiated granite, schist and gneiss, and the Chloride granite. In addition he studied the nature of the metallization and its paragenetic sequence. At

roughly the same time, Thomas (1949a) investigated the geology and ore deposits of the Wallapai district; part of the information was used as his Ph.D. thesis at California Institute of Technology. In 1953, Thomas published his work on the Wallapai district in the Bulletin of the Geological Society of America, (Thomas, 1953).

Using Rb:Sr, Damon and Giletti (1961) dated the Chloride granite (1.2 b.y.) and the Diana granite (1.35 b.y.). The latter unit is a coarse grained gneiss that was separated from the Cerbat complex by Thomas (1949a). Mauger and Damon (1965) dated Ithaca Peak porphyry (72 my.) by K:Ar method, supporting its genetic difference from the Chloride granite. Finally, Drake (1972) made a study of the ore forming fluids at Mineral Park (Ithaca Peak), 5 miles south of Chloride, including samples from a few mines in the Chloride district.

REGIONAL GEOLOGY

The Cerbat Mountains are an eastward tilted fault block located in the Basin and Range Province (Drake, 1972). On the east, the range is flanked by the Hualapai Valley and farther east by the Grand Wash Cliffs. The latter constitute the break between the Colorado Plateau and the Basin and Range Province. To the west of the Cerbat Mountains is the Sacramento Valley flanked by the Tertiary volcanic Black Mountains farther west. South of the Cerbat Mountains are the Hualapai Mountains and north, the White Hills; both are Precambrian gneissic complexes (Fig.1). The principle rock type of the Cerbat Mountains, is a Precambrian granite gneiss, characterized by diverse textures and structures but relatively uniform in composition (Thomas, 1953). Less abundant but widely distributed are layers of amphibolite, gneiss and dikes of various lithologies. In addition pegmatitic lenses and dikes are very common throughout the district. In the Chloride area a large sill-like granitic mass known as the Chloride granite is Precambrian in age. The central portion of the range is a 72 m.y. old quartz monzonite stock, part of which is host to the porphyry copper-molybdenum deposit, at Mineral Park.

Structurally the Cerbat Mountains have a pervasive north- northwestward trending foliation that dips steeply to the east. Folding is common on a small scale, as illustrated by the ptygmatic gneiss (Fig. 9). In the Chloride area a large (greater than 2 miles across) antiformal fold is present; it may represent a Precambrian refolded fold. The most interesting structural feature of the district is the fissure faults (trending mostly north-south) along which mineralized veins have formed. Thomas (1949a) suggests a north-south trending fault, just west of Chloride known as the Sacramento fault, which may be responsible for the present uplift of the Cerbat Range and which may control many of the younger structures in the district.

PRECAMBRIAN ROCK TYPES

The study area is composed of essentially Precambrian rocks, which have been divided into 6 major units; from oldest to youngest they are: 1) amphibolite; 2) undifferentiated granite gneiss complex, containing three rock types: quartzite, biotite gneiss, and granite gneiss; 3) non-foliated granite; 4) Chloride granite; 5) garnetiferous alaskite, a border facies of the Chloride granite; and 6) metarhyolite. The six units are shown on the geological map (plate 1).

Amphibolite

Schrader (1909) made the first recorded observation of amphibolite in the district. Thomas (1949a) described the rock, but Dings (1951) was the first person to map it as a separate unit. Thomas (1949a) believed the amphibolite was Archean in age. Field observations however, suggest the amphibolite outcrops are large blocks "rafted" in the 1.35 b.y. old granite gneiss complex; thus the amphibolite is older but its actual age is not known.

The amphibolite is primarily brown hornblende, with a well developed foliation and is resistant to weathering. Outcrops of amphibolite can be traced easily on the surface often outlining major structural features. The unit varies in thickness from a few meters to over 120 meters, and can be traced for several miles (Thomas, 1949). Contacts of the amphibolite are normally sharp and concordant with the granite gneiss and the Chloride granite, but some discordant characteristics occur. An excellent example of of the latter is exposed in an arroyo due east of the Schenectady mine (Fig. 2). At this location granite belonging to the undifferentiated granite gneiss complex has intruded and partially assimilated the amphibolite unit, leaving fragments of the amphibolite detached from the main body and "floating" in the homogeneous granite. The very weak linear fabric seen in the granite at this location may be due to late magmatic or tectonic deformation (Compton, 1962).

Outcrops of amphibolite vary from dark black to gray, depending on the amount of felsic material present locally. The amphibolite weathers light brown to reddish brown and due to its resistance to weathering forms prominent ridges. Many exposures contain fine-to

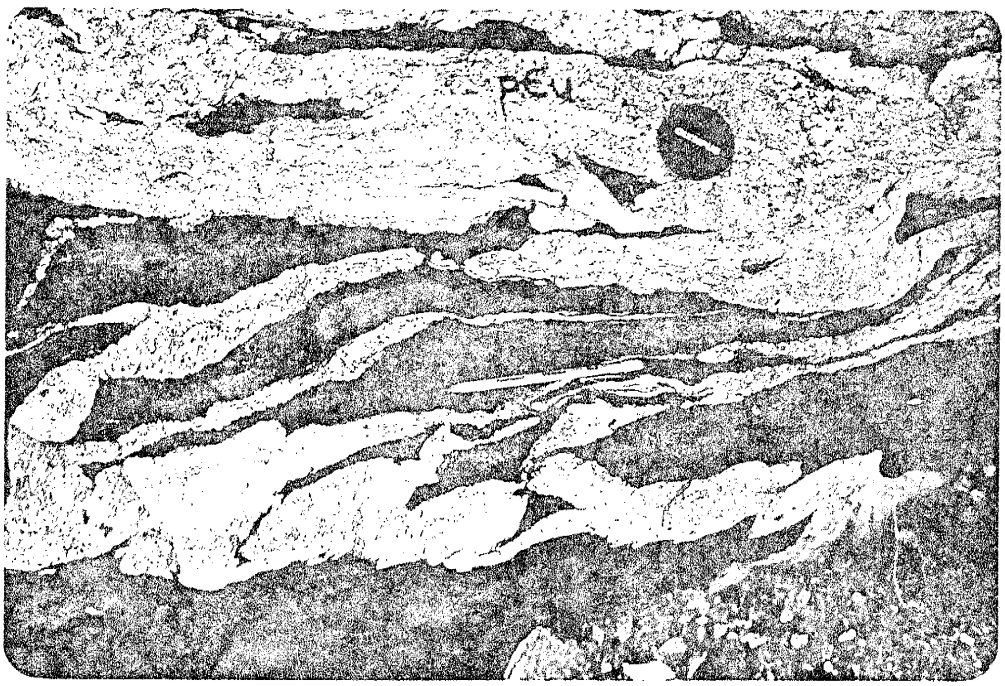

Figure 2 Igneous contact between younger granite gneiss (pEu) and amphibolite (black). The amphibolite foliation passes into the granite gneiss without deflection. The amphibolite is being assimilated by the intruding granite gneiss. Location section 25, T24N, R18W, east of the Schenectady mine.

medium-grained quartzo-feldspathic veins which vary from less than 4 mm to greater than 30 cm wide. These veins commonly exhibit ptygmatic patterns (Fig. 3). In contrast, many outcrops also have at least two generations of light colored bands that occur at oblique angles to each other (Fig. 4). The bands appear to have formed from hydrothermal fluids moving through the unit; this action preferentially alters augite as seen in thin section (Fig. 5).

Approximately 1/4 mile west of the Juno vein system the amphibolite has medium grained quartzo-feldspathic layers alternating with hornblende rich bands, and could be more aptly described a hornblende gneiss. This type of rock is very minimal in the field area. Elsewhere the amphibolite can grade into a more schistose unit depending on the amount of biotite present (Thomas, 1949). Normally, the amphibolite occurs as outcrops of foliated rock that is fractured and displays a conjugate set of joint patterns. An excellent exposure of a massive outcrop is located east of the Tennessee wash (Fig. 7). This black butte rises over 90 meters and can be seen for several kilometers (Thomas, 1949).

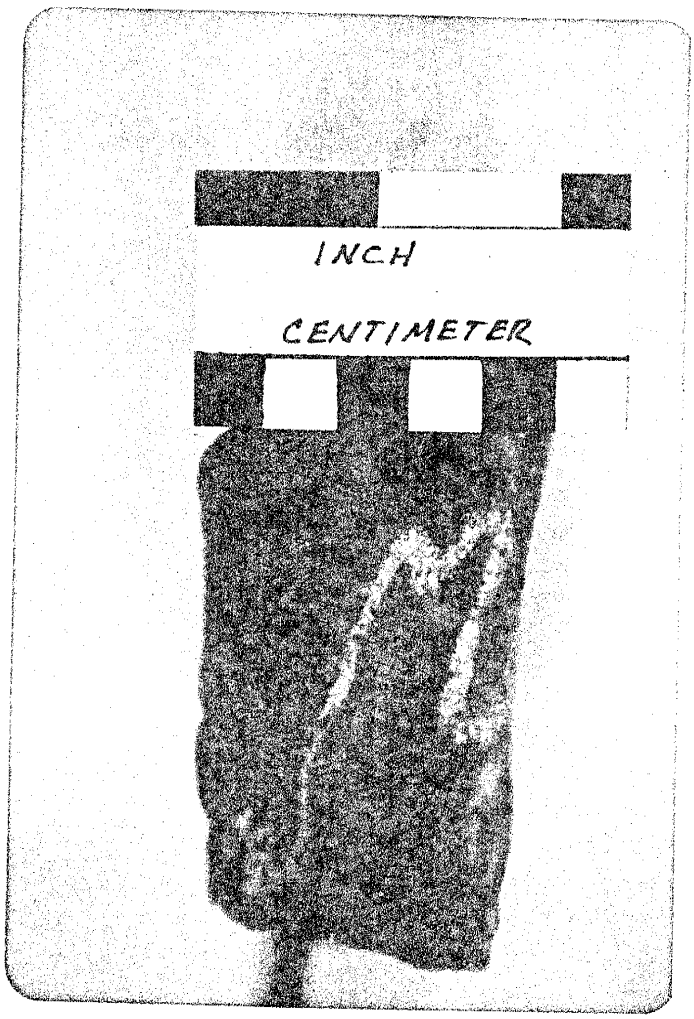

Figure 3 Ptygmatically folded quartzo-feldspathic vein within the amphibolite unit. The vein lies within the plane of foliation.

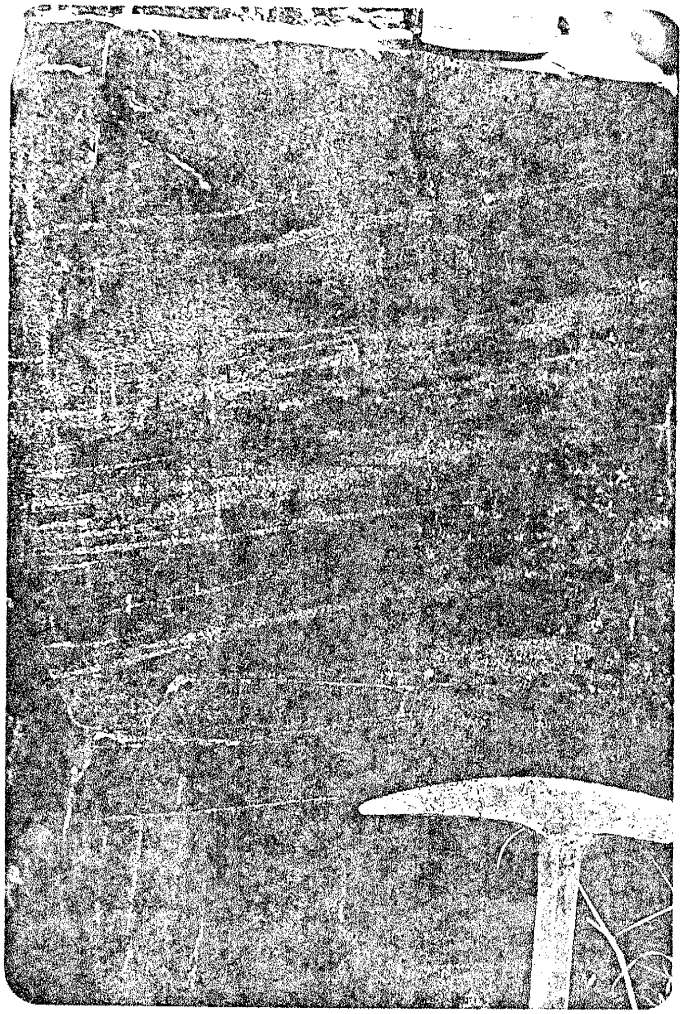

Figure 4 Amphibolite unit with two (1 and 2) generations of light colored bands, composed of felsic material, at oblique angles to each other. Band number 2 is contained within the plane of foliation. Location section 34, T24N, R18W.

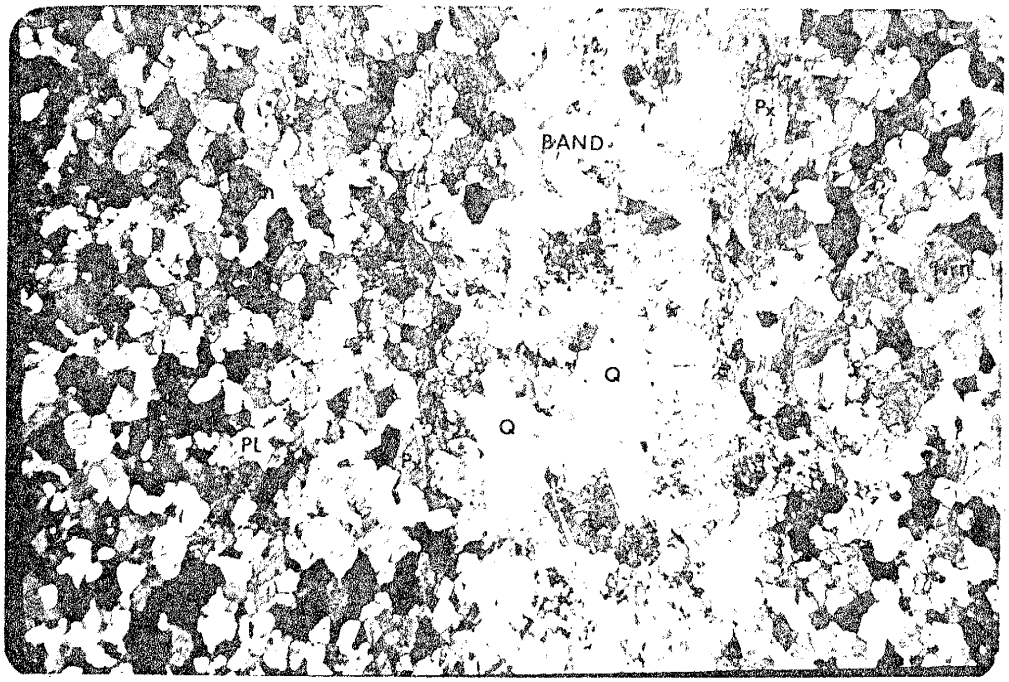

Figure 5 Photomicrograph of bands seen in figure 4. Band is composed of quartz (Q), altered feldspar (F) and altered pyroxene (Px). The host is mainly hornblende (Hrn), plagioclase (PL) and pyroxene in a granoblastic to decussate texture. 2.5 mag., x-nicols, sample # 14.

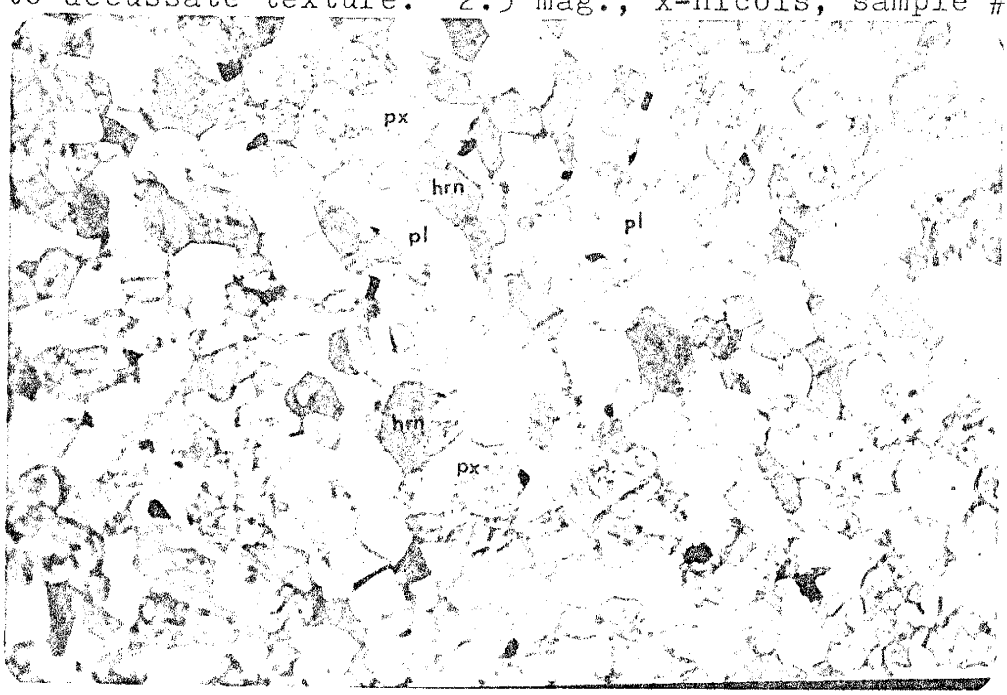

Figure 6 Photomicrograph of pyroxene (px) altering to hornblende (hrn). Texture is granoblastic; plagioclase (pl), 2.5 mag., uncrossed nicols, sample # 13.

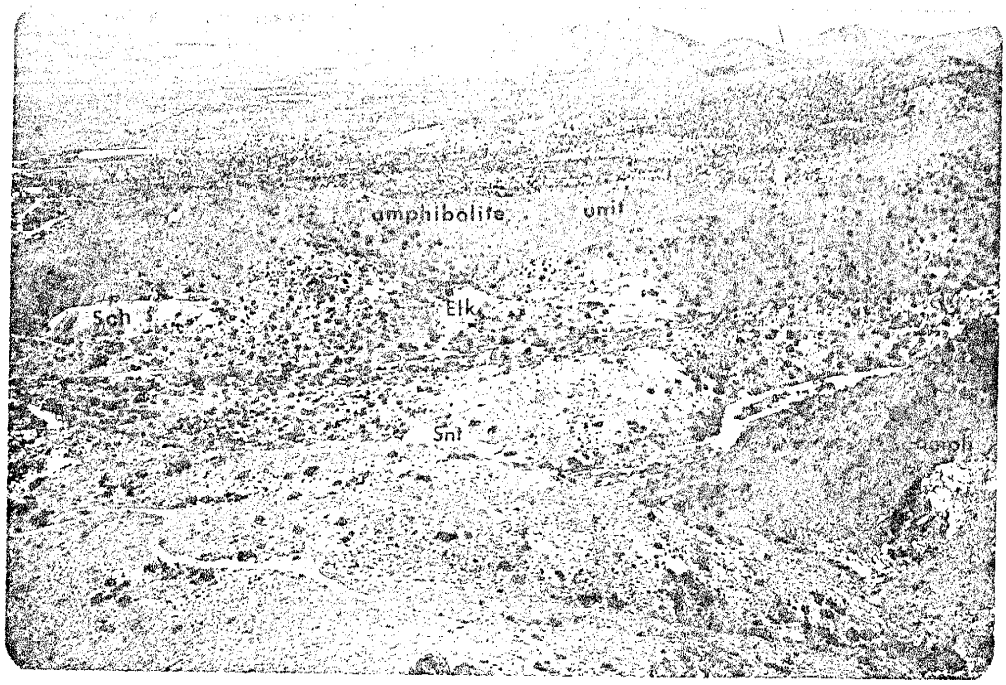

Figure 7 Massive outcrop of amphibolite (amph) striking north-south, with steep dips to the east. The Schuylkill mine (Sch), Elkhart mine (Elk) represent one continuous hydrothermal vein. Schenectady mine (Snt). Looking west.

The amphibolite is from 30 to 40% hornblende (see table 1), 15 to 30% augite and 15 to 30% andesine averaging An35. The augite content depends upon how much pyroxene has been converted to hornblende during metamorphism. From 1 to 5% of pleochroic dark green to brown biotite and 2 to 7% magnetite comprise the varietal minerals. Traces of zircon and apatite are the accessories.

The overall texture ranges from granoblastic to decussate depending upon the habit of the hornblende crystals. In some thin sections a distinct foliation is present, produced by the preferential alignment of hornblende laths and biotite flakes. Most minerals are poikiloblastic with inclusions of magnetite.

The average grain size of the hornblende crystals is 0.5 mm; however, laths up to several millimeters in length do occur (Thomas, 1949). Hornblende has been formed at the expense of augite (Fig. 6) and occasionally the amphiboles alter to chlorite. Augite has a neutral color, with a high relief and commonly shows twin planes {100}. In samples 6 and 10 the amount of pyroxene exceeds the amount of hornblende (table 1), as compared to sample 7, where almost all the pyroxene has been converted to hornblende. Plagioclase occurs as

Table 1 Modal analyses of Amphibolite samples in the Chloride district. Trace minerals are sericite, zircon, sphene, chlorite; tr = trace amount.

Sample #	Hornblende	Augite	Plagioclase	Magnetite	Biotite
3	41	24	28	2.6	4.4
4	44	21	29	4	2
6	23	31	35	6.2	4.8
7	42	15	32	7.2	3.8
8	50	21	20	5.2	4.8
9	34	31	23	6.8	6
10	36	40	18	4.8	2.2
11	49	18	28	3.4	1.6

subidioblastic laths averaging 0.5 mm in length and occasionally shows myrmekitic textures. Plagioclase can have a combination of albite and pericline twinning, giving the laths a "cross-hatched" appearance. Combined carlsbad- albite twinning is also observed, as well as untwinned plagioclase grains. Plagioclase shows sericitic alteration and often has inclusions of pyroxene, zircon and apatite. For thin section descriptions of the amphibolite unit see appendix I, sample numbers 3-15.

Compared to the other Precambrian units the amphibolite shows little hydrothermal alteration. However, secondary products after hornblende such as chlorite, magnetite and biotite are seen in thin section. In addition, Thomas (1949a), reported actinolite-tremolite and epidote after pyroxene as well as calcite, epidote and zoisite after feldspar. Hematitic staining derived from magnetite is common in all specimens.

The amphibolite contains contorted quartzo-feldspathic veins as small as a few millimeters wide (Fig. 3). These veins are composed of quartz, orthoclase, microcline and plagioclase. The grains average 0.6 mm in diameter (Thomas, 1949) and are irregularly intergrown with the bordering amphibolite

host. The alkali feldspars in the veins normally show perthitic textures and the plagioclase may exhibit bent twin lamellae. Quartz shows undulatory extinction along with some of the feldspars. The quartzo-feldspathic veins are more intensely sericitized than the amphibolite host. The veins can either be concordant with the amphibolite foliation or crosscut the foliation at oblique angles. Often ptygmatic patterns are observed in the veins with no direct relationship to the regional foliation and structure.

Undifferentiated granite gneiss complex

The predominant rock type of this group is a fine to medium-grained granite gneiss which is typically porphyroblastic (Spry, 1976, pp.137) and has a weak to moderate foliation. The complex also contains a well banded biotite gneiss and discontinuous layers of quartzite. The complex forms approximately 40% of the study area but represents roughly 90% of the Cerbat Range (Thomas, 1949a). A coarse grained granitic facies (Diana granite) of this complex has been dated at 1.35 b.y. (Damon and Giletti, 1961).

Quartzite -- Lee (1908) was the first to record quartzite beds in the Cerbat Mountains, Thomas (1949a) also observed quartzite in the region and did a very complete description of the rock type. Thomas (1949a) mapped the quartzite as part of the Archean metamorphic-igneous suite. The quartzite represents one of the oldest rock types in the district and because of its spatial association with other Proterozoic rock types in the area, it is assumed to be similar in age.

The quartzite is a massive light gray unit composed of greater than 95% quartz, with subrounded grains. The quartzite occurs as narrow beds usually 1 to 3 meters wide that are discontinuous in the granite gneiss complex. Normally the beds parallel the regional foliation of the area. The best outcrop is exposed in the northwest corner of section 35, just north of the Dardanelles mine. At this location the bedding (?) strikes N61° E and dips 70° to the east. This measurement is not in strict agreement with the regional foliation. Elsewhere in the area, outcrops of quartzite are rare and probably represent less than 1% of the total rock type of the district. Contacts of the quartzite with the granite gneiss are concordant and sharp and the quartzite is usually more resistant to erosion than the surrounding gneiss.

Outcrops of quartzite are typically light gray and weather to a light brown. Discrete grains that are subrounded and less than 1 mm in diameter give a granular (psammitic) texture (Thomas, 1949). The bedding (?) is accented by thin (less than 5 mm thick) dark bands probably composed of biotite, chlorite and magnetite (Fig. 8) (Thomas, 1949).

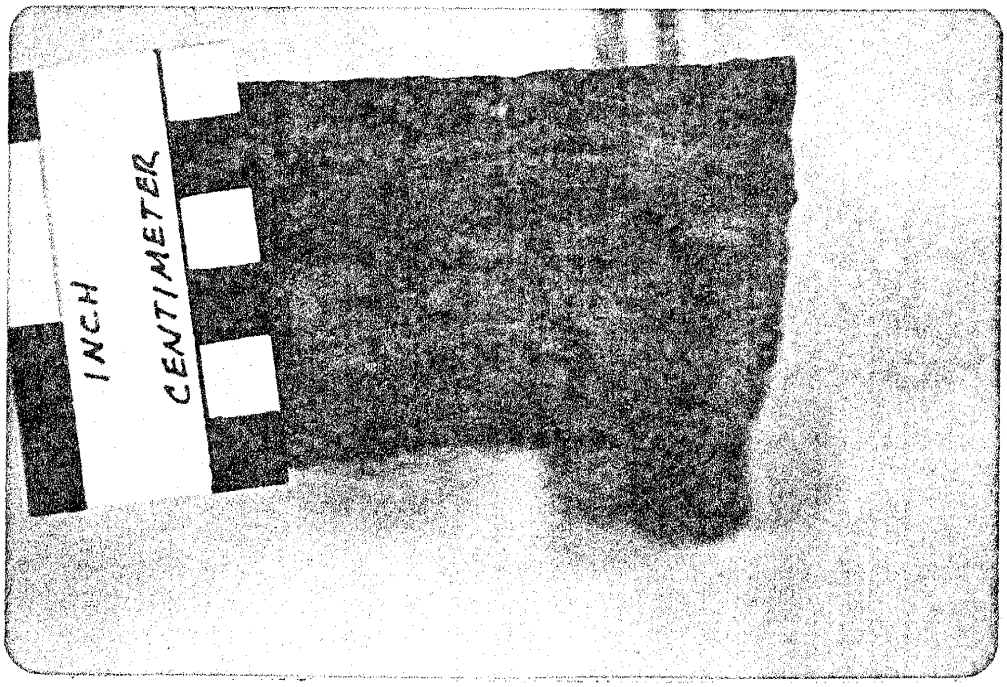

Figure 8 Quartzite unit with relict planar bedding. Dark bands are mainly composed of magnetite.

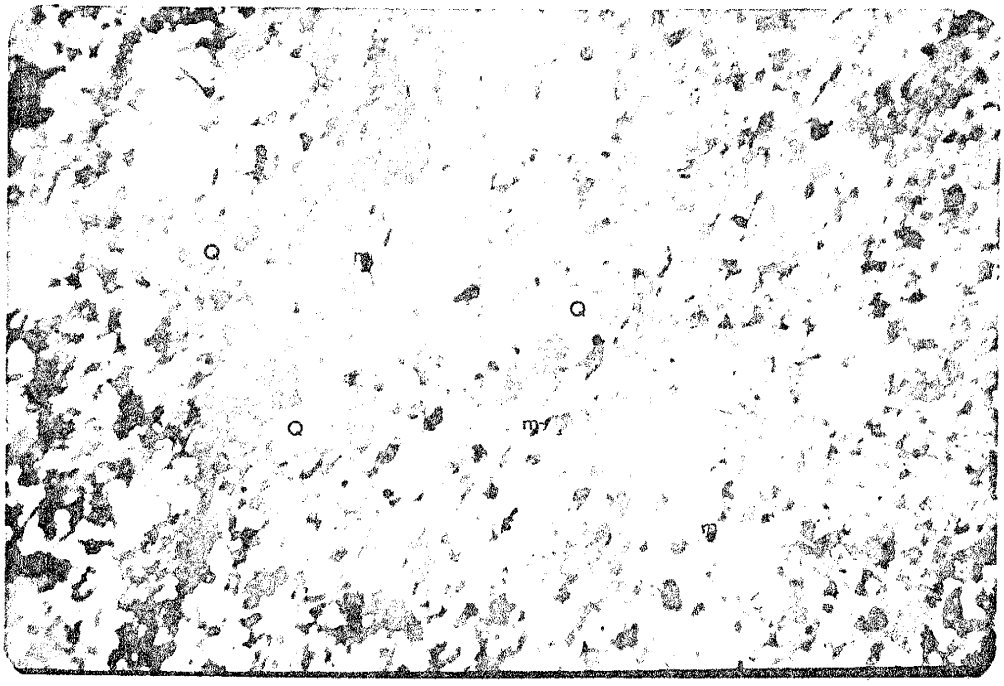

Figure 9 Photomicrograph of quartzite unit with arrested quartz (Q) grains that show dimensional preferred orientation. Minor amounts of magnetite (m) also show a weak lineation. 1.0 mag., x-nicols, sample # 31.

The unit is composed primarily of quartz in a fine grained (less than 0.5mm in diameter) granoblastic texture. Spry (19/6) states, "Recrystallization is a time-dependent process and as the the texture evolves from the original to a final equilibrium texture, various kinds of grain boundary can be recognized: ....(2) Arrested boundaries, if equilibrium is not achieved.....and leave it irregular, sharply curved, dentate or sutured.... ". The Quartz grain boundaries observed are arrested (Fig. 9) and in addition Thomas (1949a) noted elongate quartz bands. Spry (1976) believes the development of granoblastic elongate texture in quartzite is due to nucleation and growth of entirely new quartz crystals at the expense of old quartz grains. Polygonalization has not occurred in the quartzite, but the quartz grains do give slightly biaxial interference figures along with undulatory extinction, which indicates lattice straining. Trace amounts of orthoclase (?), muscovite-sericite, and magnetite occur in the quartzite. Thomas (1949a), noticed biotite up to 1% in some quartzite thin sections, along with andesine and apatite needles. For thin section descriptions of quartzite see appendix I, sample number 31.

Biotite gneiss -- Thomas (1949a) described the biotite gneiss in great detail and called it the "lit-par-lit gneiss", owing to his interpretation of its mode of formation. He mapped it as part of the undifferentiated Archean metamorphic-igneous suite. However, since the biotite gneiss is intimately mixed with the 1.35 b.y. granite gneiss complex, it is believed to be similar in age, or slightly older. Therefore the biotite gneiss is Proterozoic and not Archean in age, as Thomas (1949a) believed it to be.

The biotite gneiss is characteristically very well-foliated, garnetiferous, has quartzo-feldspathic layers and is ptygmatically folded. The biotite gneiss occurs as discontinuous layers and lenses in the granite gneiss complex. It is very difficult to trace on the surface due to its extreme irregularity and represents probably less than 10% of the total rock types in the field area. Contacts of the biotite gneiss with granite gneiss rock type are variable. Occasionally it is gradational, but within a short distance the contact can become very sharp. Outcrops of the biotite gneiss vary in width from less than a meter to greater than 5 meters. The biotite gneiss is dark brown with patches of iron staining, and outcrops are normallly extensively weathered. The light

colored areas within the biotite gneiss are quartzo-feldspathic layers. The lighter bands combined with the dark layers give a definite gneissic texture in the rock type. The width of the quartzo-feldspathic layers varies from less than 1 cm to greater than 20 cm. The light layers pinch and swell and occasionally show boudinage structure (Hobbs, et al. 1976). Outcrops of the biotite gneiss are ptygmatically folded (Fig. 10).

Microscopically the biotite gness displays a very pervasive foliation marked by parallel alignment of biotite flakes (Fig. 11). Light layers of the biotite gneiss are composed chiefly of alkali feldspars 55%, quartz 15-45%, with a trace of oligoclase An28, magnetite and biotite and chlorite. Dark bands of the biotite gneiss are composed mainly of biotite flakes 45%, and subidioblastic grains of brownish garnet (almandite) 30%, feldspars 10%, chlorite 15% and trace amounts of feldspars, magnetite, actinolite-tremolite (?) and augite (?). Overall the dark bands of the biotite gneiss account for greater than 60% of the total rock volume. Thomas (1949a) detected the presence of sillimanite as the fibrolite variety, intergrown with biotite, quartz and feldspar, in the biotite gneiss; however, none was observed in this study. The primary alteration product

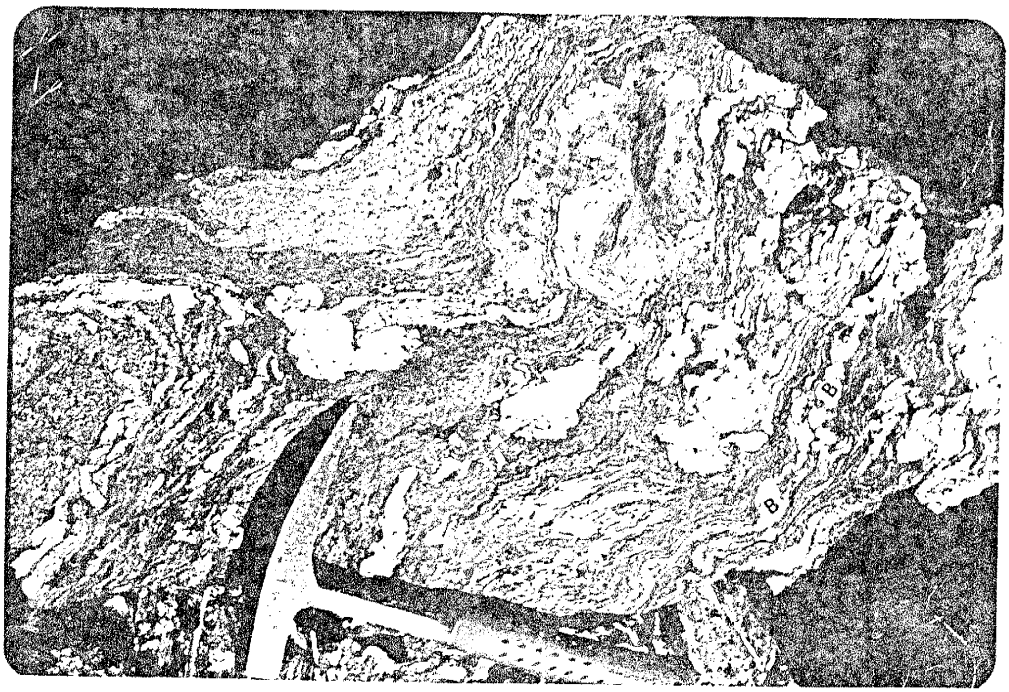

Figure 10 Outcrop of biotite gneiss that is ptygmatically folded and shows well developed boudinage (B) of quartzo-feldspathic fractions. Location section 33, T24N, R18W.

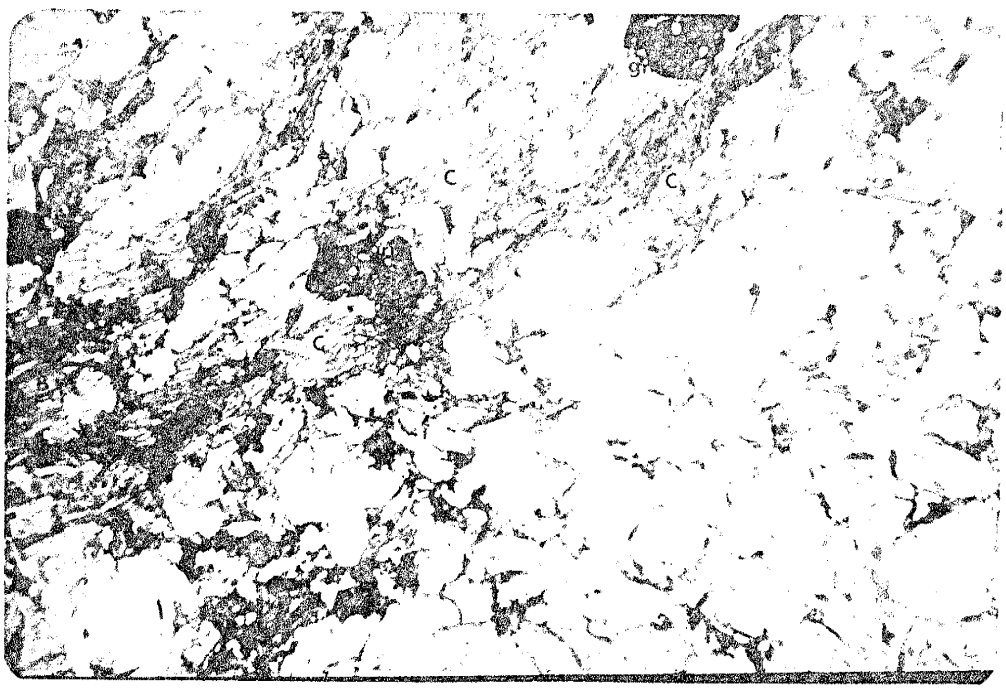

Figure 11 Photomicrograph of biotite gneiss showing a well developed foliation outlined by chlorite (C) and biotite (B). Garnets (grn) are poikilioblastic and are being altered to chlorite. 1.0 mag., uncrossed nicols, sample# 29.

1mm

is sericite, which is ubiquitous in all thin sections of the biotite gneiss.

Most minerals in the biotite gneiss are poikiloblastic especially garnets (Fig. 11), with inclusions of biotite and quartz. The feldspars show exsolution textures and occasionally are graphic. The biotite gneiss shows deformation features such as strain fractures, undulatory extinction and bent twin lamellae. Arrested quartz grain boundaries (Spry, 1976) attest to recrystallization and an overall weak mortar texture is observed in thin section. For thin section description of the biotite gneiss see appendix I, sample numbers 29 and 30.

Granite gneiss -- Granite gneiss was first described in the Chloride district by Lee (1908); a more detailed description is given by Thomas (1949a). Thomas (1949a) separated a coarse grained porphyritic (?) facies of this rock, which he called the Diana granite. He based the separation on the grounds of its inferred igneous origin. However, field evidence is not explicit enough to warrant this separation. Therefore the Diana granite is believed to be a coarser grained facies of the granite gneiss rock type and has been mapped as part of the undifferentiated complex.

Since it was first mapped the granite gneiss has been assigned to the Precambrian. Thomas (1949a) believed the unit to be Archean, but a Rb:Sr date of the Diana granite by Damon and Giletti (1961), gave an age of 1.35 b.y. Therefore the rock is believed to be Proterozoic or slightly older and associated with the Elsonian orogenic event of 1.3 b.y. to 1.4 b.y. (Windley, 1978).

The granite gneiss is fine-to medium-grained, has a gray hue and typically is porphyroblastic. Outcrops of the rock are relatively uniform in composition and normally show some gneissic texture. Some exposures show no obvious metamorphic texture but they are not common (Thomas, 1949). The majority of the unit is exposed in the eastern half of the study area. The total thickness was never measured but is believed to be in excess of 600 meters. Contacts of the granite gneiss with other units are variable. Gradational contacts are present in the southeastern portion of the field area with a similar lithologic unit, however a definite intrusive contact with amphibolite is seen due east of the Schenectady mine in an arroyo (Fig. 2). Outcrops are light to medium gray when fresh and light brown when weathered and tend to form spheroidal masses. Variations from off-white to dark gray occur depending on the amount of mafic

constituents present locally. Porphyroblasts of feldspar are very common and can be several centimeters in diameter. Ptygmatically folded quartzo-feldspathic veins normally less than 3 cm wide occur in almost all outcrops. These veins can be either concordant to the mineral fabric or can crosscut the fabric at oblique angles.

Under the microscope granite gneiss displays a cataclastic texture (Spry, 1976, pp.229) with porphyroblasts (relict phenocrysts ?) surrounded by a fine to microcrystalline crushed matrix (Fig. 12 and Fig. 13). The degree of deformation varies from protoclastic (Spry, 1976, pp.229) to mylonitic (Spry, 1976, pp.229). Foliation in thin section is produced by the alignment of biotite flakes. Most thin sections have arrested grain boundaries (Spry, 1976) and a granoblastic matrix. Together these two features in thin section indicate recrystallization. Porphyroblasts commonly are poikiloblastic and show strain features, such as undulose extinction, strain fractures, deformed twin lamellae and weak pressure shadows (Spry, 1976, pp.246). Myrmekitic and graphic textures are seen in the feldspars, with graphic being the most abundant. In addition, feldspars also show perthitic and antiperthitic textures.

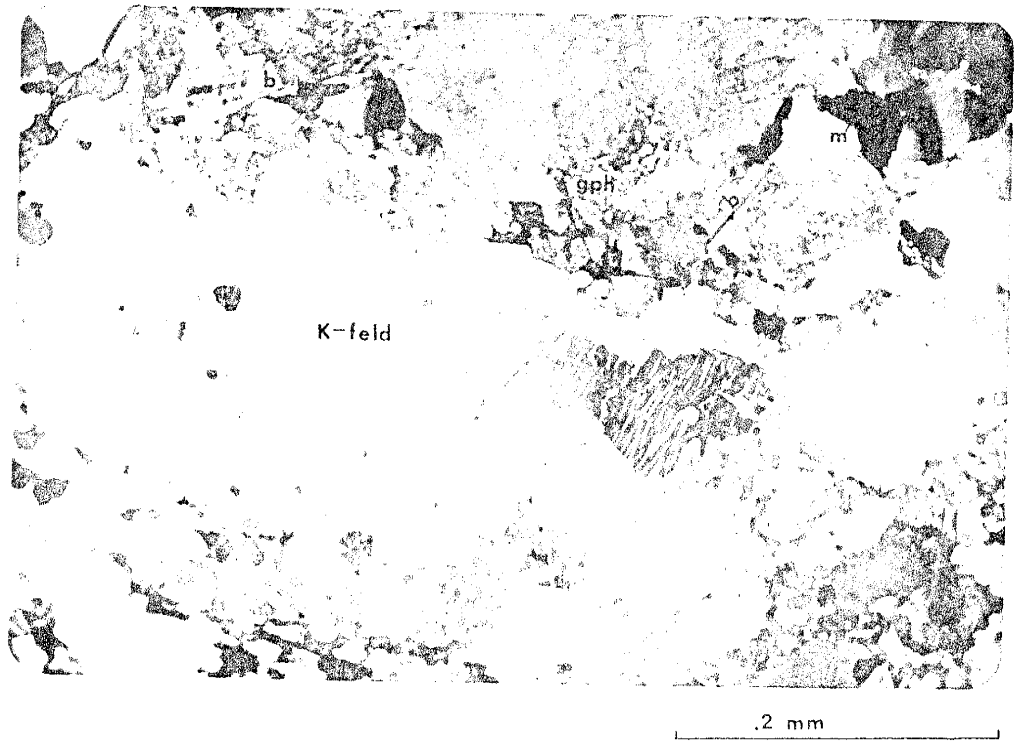

Figure 12 Phogomicrograph of granite gneiss unit with a large potassium feldspar (K-feld) crystal showing exsolution textures and carlsbad twinning. The overall texture is cataclastic. Graphic texture (gph) in feldspar, biotite (b) and magnetite (m). 2.5 mag., x-nicols, sample # 25.

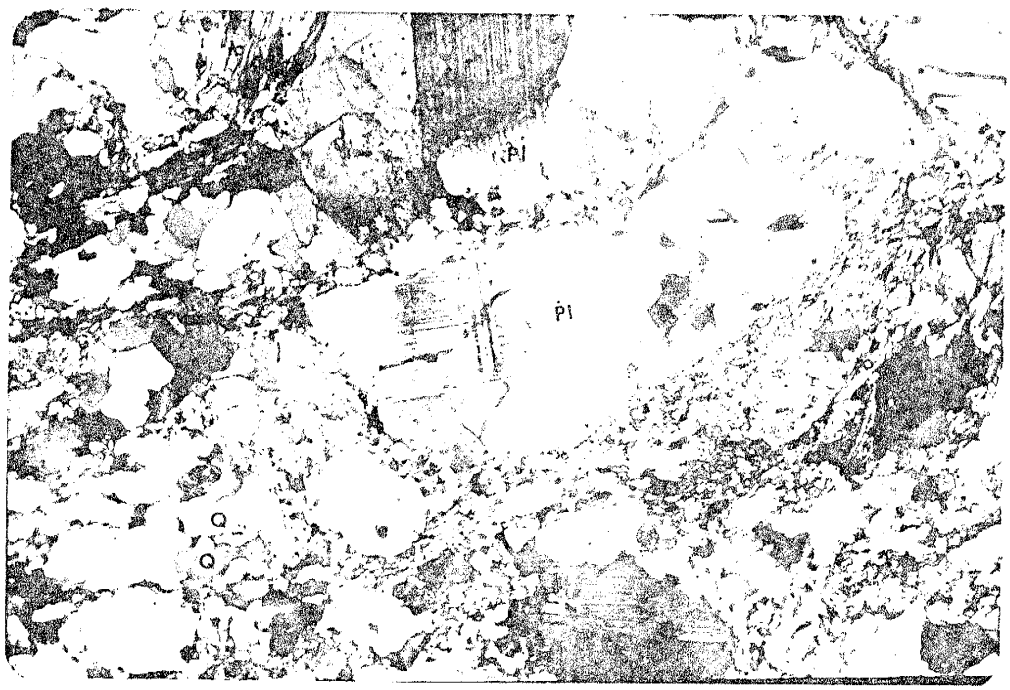

Figure 13 Photomicrograph of granite gneiss with bent twin lamellae in plagioclase (pl) set in a cataclastic matrix. Biotite (b) outlines a foliation, quartz (Q) shows arrested grain boundaries. 2.5 mag., x-nicols, sample # 28.

The principal mineral in thin section is quartz, from 25 to 45% of which shows undulatory extinction. Orthoclase is very common forming 20 to 30% of the rock along with 10 to 25% microcline. The porphyroblasts are commonly poikiloblastic alkali feldspars with inclusions of quartz, biotite and plagioclase. Between 5 and 15% oligoclase, averaging An28, showing well developed polysynthetic twinning is present in thin section. The primary mafic minerals are biotite 10 to 15%, and magnetite with cubic habit. Zircon crystals and sphene are scattered throughout the sections in trace amounts and Thomas (1949a) reports apatite needles. Sericite is common in the granite gneiss, as a late stage hydrothermal product after feldspar. Chlorite has formed after biotite and hematitic staining is seen in thin section. For thin section description of granite gneiss see appendix I, sample numbers 24-28.

Precambrian granite

Precambrian granite was first separated from the undifferentiated granite gneiss complex, in this study, as an apophysis of the Chloride granite. This genetic tie with the Chloride granite was based on its field and petrographic similarities. Geochemical data suggest that the Precambrian granite is distinct, and may not be an apophysis of the Chloride stock; thus it is treated as a separate unit. Since the Precambrian granite appears to have intruded the 1.35 b.y. old undifferentiated complex it is interpreted as younger, but the actual age is indeterminate.

Precambrian granite is a light-gray, medium-grained, weakly-foliated granitic rock, that crops out in the southeast portion of the map area in section 2, T23N, R18W. The rock crops out over a diameter of 1 km or more. Several smaller and less distinct similar lithologic types, crop out throughout the field area. No attempt was made to either genetically tie these smaller outcrops, with the Precambrian granite or differentiate them from the undifferentiated complex. The contact of the Precambrian granite with the undifferentiated complex is extremely irregular and gradational; this is expected because of their mineralogical similarities. The only

definite contact of the Precambrian granite with the undifferentiated complex was observed in the southwest portion of section 2.

In the field Precambrian granite is very similar to the Chloride granite. Precambrian granite is medium grained equigranular and has scattered garnets (almandite ?) throughout. The color of the outcrops is dull white to light brown, with a salt and pepper appearance weathering to light brown friable spheroidal masses. Most outcrops have a weak foliation due to alignment of biotite flakes. The Precambrian granite differs from the granitic fraction of the undifferentiated complex by its lack of feldspar porphyroblasts and ptygmatically folded quartzo-feldspathic veins. In isolated localities within the Precambrian granite the unit is highly altered to an off-white argillized rock. These zones of alteration are occasionally associated with transverse shearing. In addition some areas within the Precambrian granite are silicified and show fractured iron-stained outcrops.

Modal analyses by the author (table 2) indicate that the average composition of the Precambrian granite is quartz monzonite (Fig. 14). The principal mineral is quartz accounting for 30 to 50% of the total volume. Alkali feldspar accounts for 20 to 35% and oligoclase (An28) is between 15 and 25%. Pleochroic dark green to

Table 2 Modal analyses of Precambrian granites in the Chloride district. Chloride granite = 2, 16, 17; Garnetiferous alaskite = 18, 19; Precambrian granite = 1, 20, 21, 22, 23. Trace minerals are zircon, sericite, sphene, apatite; tr = trace amount.

Sample #	K-feldspar	Plagioclase	Quartz	Biotite	Magnetite	Muscovite	Garnet
2	37	24	36	2.8	-	1.0	tr
16	35	18	38	8.6	0.2	-	tr
17	24	21	44	10.6	tr	tr	tr
18	22	27	45	1.8	-	4	0.4
19	28	17	45	0.7	-	1	8.2
1	34	24	31	11	-	-	0.6
20	35	20	37	7.2	-	-	1.6
21	20	21	46	11.8	-	-	1.2
22	21	24	40	14.4	-	-	1
23	22	14	50	14	-	-	tr

Chloride granite – 2, 16, 17
Garnetiferous alaskite – 18, 19
Precambrian granite – 1, 20, 21, 22, 23

After Bateman et.al. 1963

FIG. 14

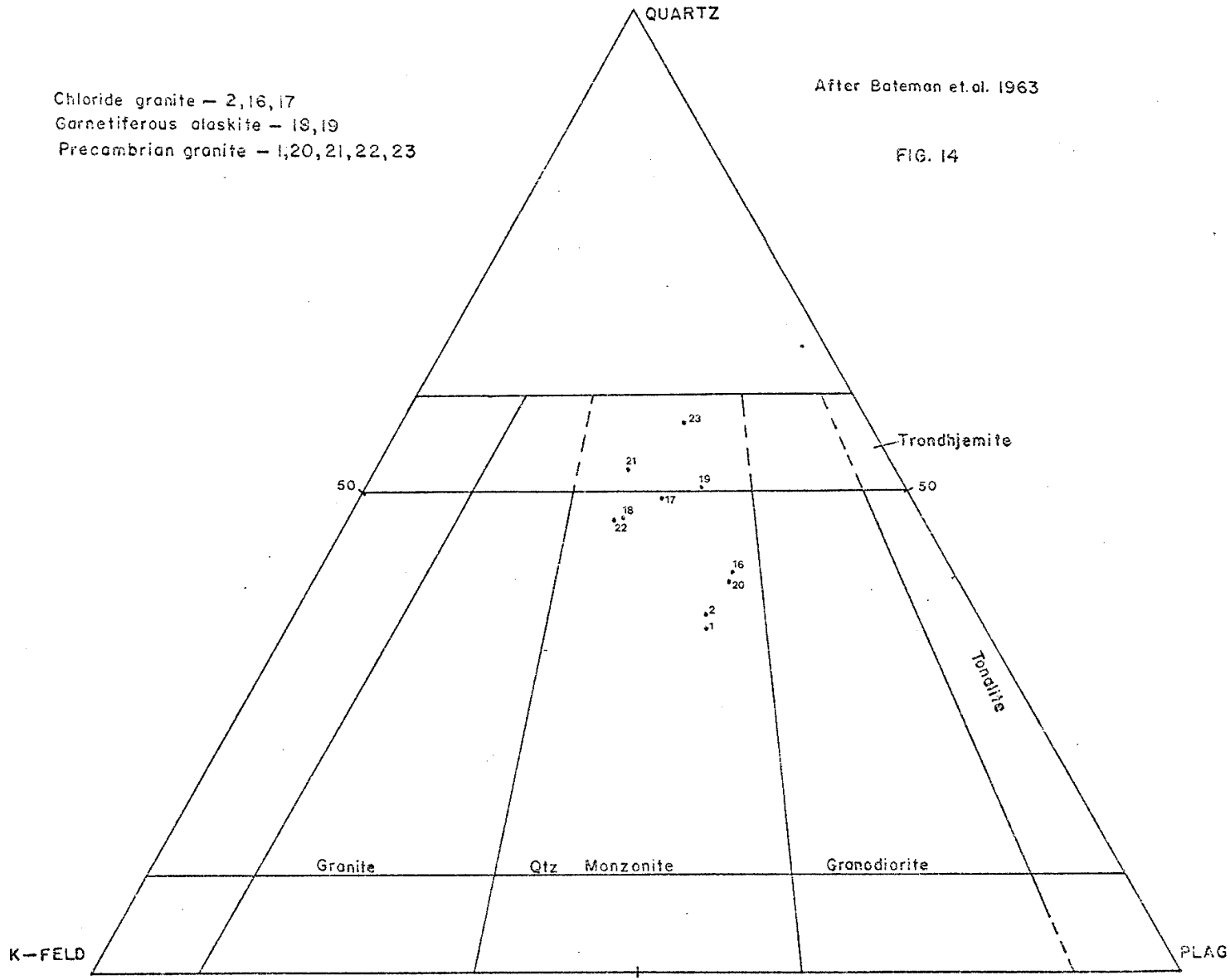

brown biotite comprises, between 6 and 15% and garnet (almandite) is present from .5 to 1.5%. Zircon, apatite and magnetite occur in trace amounts.

The microscopic texture is cataclastic with feldspars up to several millimeters in diameter (Fig. 15) surrounded by a fine-grained crushed matrix. Strain fractures, bent twin lamellae, annealed grain boundaries and poikiloblastic textures are common. The alkali feldspars commonly are perthitic and show graphic textures; they are xenoblastic and contain numerous inclusions, including zircon and apatite. Plagioclase occasionally shows myrmekitic textures, also with inclusions of zircon and apatite. Plagioclase is more intensely sericitized than alkali feldspar and often shows no twinning. Secondary products are biotite after garnet, chlorite after biotite and hematitic staining after magnetite. For thin section description of the non-foliated granite see appendix I, sample numbers 1, 1-a, 20-23.

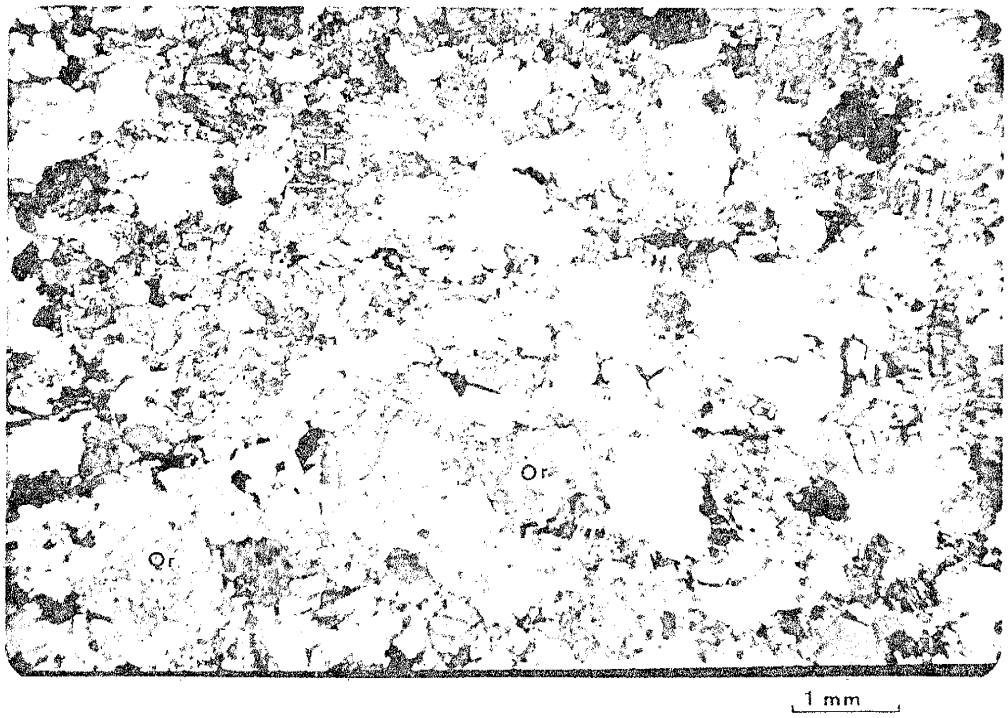

Figure 15 Photomicrograph of the Precambrian granite with a well developed mortar texture. Plagioclase (pl) is being preferentially altered compared to orthoclase (Or). 1.0 mag., x-nicols, sample # 20.

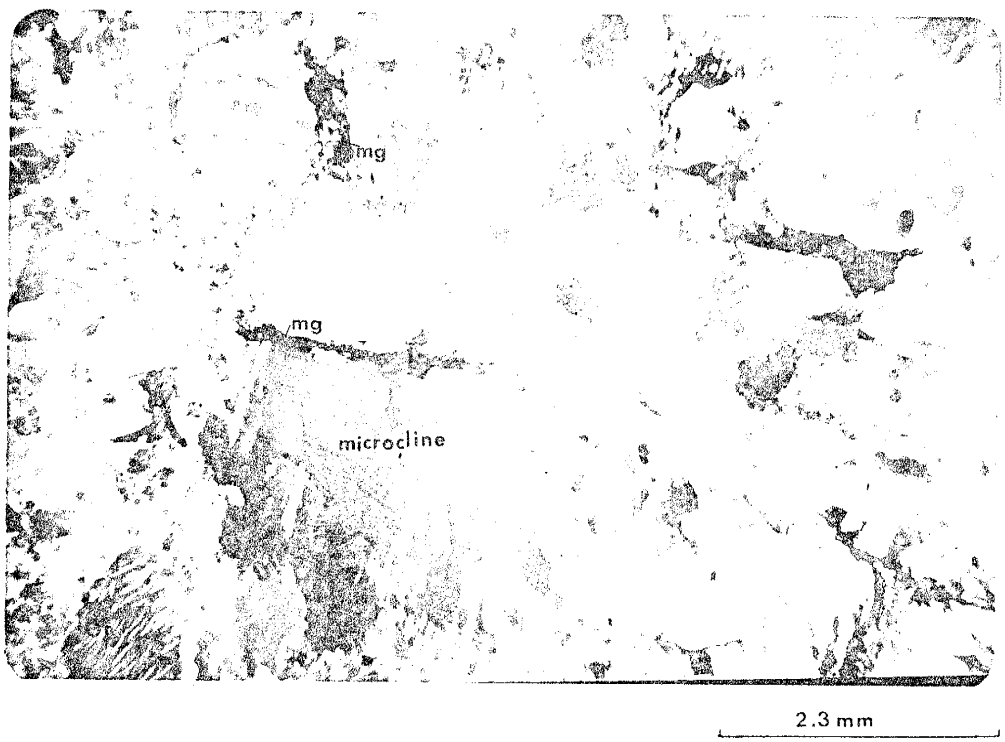

Figure 16 Photomicrograph of the Chloride granite showing mortar texture. Microcline and orthoclase (Or) show exsolution textures; biotite (b), magnetite (mg). 1.0 mag., x-nicols, sample # 16.

Chloride granite and garnetiferous alaskite

In the central part of the map area a large sill-like unit called the Chloride granite has been intruded into the earlier Precambrian rocks. On the western border of the intrusive a more felsic facies of the granite is exposed, the garnetiferous alaskite. Outcrops are limited to a small fraction of the Chloride granite exposures.

Chloride granite

The Chloride granite was first mapped by Schrader (1909) and had been genetically related to an intrusive stock 5 miles south called Ithaca Peak. Not until Dings (1951) mapped the Cerbat Mountains, was the Chloride granite recognized as a separate intrusive. The Rb:Sr age of the intrusive is 1.21 b.y. old (Damon and Giletti, 1961); therefore it is Proterozoic and possibly associated with the final stages of the Elsonian orogenic event (Windley, 1978).

The Chloride granite is a light gray medium-grained, weakly foliated granitic rock. Several workers (Thomas 1949a, Dings 1951) as well as the author have interpreted it as a steeply dipping sill, 600 to 1500

meters thick, tnat has been intruded into the axial region of a complex folded structure. The Chloride granite forms rounded hills that rise 300 meters above the townsite of Chloride. The contacts of the granite with the country rock are normally sharp. No contact metamorphic effects are reported (Thomas, 1953). A gradational contact, however, exists between the Chloride granite and the genetically related garnetiferous alaskite. Several inclusions of biotite schist occur throughout the Chloride granite, reaching a maximum diameter of 5 meters. The granite is medium-grained, equigranular and contains scattered garnets (almandite ?). The fresh color is dull white to light brown, with a salt and pepper appearance weathering to light brown friable spheroidal masses. Most outcrops have a weak foliation due to preferential alignment of biotite flakes. Few if any pegmatitic fractions occur in the intrusive. The Chloride granite is crosscut by a metarhyolite dike and diabase dikes. In isolated localities within the intrusive the rock is intensely altered to an off-white argillized rock along zones of minor transverse shearing.

Modal analyses by the author (table 2) indicate the average composition of the Chloride granite is quartz monzonite (Fig. 14). The principal mineral is quartz

accounting for 35 to 45% of the total volume. Orthoclase and microcline together comprise 25 to 35% of rock. Fifteen to twenty-five percent oligoclase (An25) and 2 to 10% biotite are the remaining minerals which exceed trace amounts. Magnetite, zircon, apatite, and muscovite are present in amounts less than 1%. Garnet (almandite ?) can be found in most hand specimens, but little was seen in thin section.

The microscopic texture is cataclastic with xenoblastic grains of feldspar surrounded by a crushed matrix of quartz, biotite and feldspar (Fig. 16). Strain fractures, and arrested grain boundaries are found as well as bent twin lamellae. The alkali feldspars are commonly perthitic with graphic textures; they are often poikiloblastic with inclusions of quartz, biotite, zircon and apatite. Rarely does the plagioclase show myrmekitic texture, although, inclusions of alkali feldspar, zircon, biotite and apatite do occur. The plagioclase is more intensely sericitized than the alkali feldspars. Albite twinning is common in the plagioclase; combined carlsbad and pericline twinning along with untwinned plagioclase is also present. Secondary products are chlorite after biotite, and hematite after magnetite. Thin sections normally show a pervasive sericitic alteration. For thin section description of the Chloride granite see appendix I, sample numbers 2,16,17.

Garnetiferous alaskite

Dings (1951) was the first to recognize a more felsic facies of the Chloride granite, however, he did not map it as a separate unit. The garnetiferous alaskite is interpreted as a more felsic border facies of the Chloride granite and is believed to be similar in age (i.e. approx. 1.21 b.y.).

The alaskite is off-white, medium-grained with preferentially aligned "pods" of garnets (almandite ?) (Fig. 17). Outcrops of garnetiferous alaskite are mainly located along the western border of the Chloride granite sill-like intrusive. The alaskite interfingers with the undifferentiated complex and several apophyses can be located throughout the field area. No attempt was made to map these apophyses because of their extreme discontinuity and field similarities to pegmatitic and aplitic lenses and dikes. The contact of the garnetiferous alaskite with the Chloride granite is gradational, and shows an increase of mafic constituents toward the intrusive. Elsewhere the garnetiferous alaskite has fairly sharp contacts concordant with other Precambrian units in the field area. Approximately 1/4 mile east of the Juno mine, the garnetiferous alaskite has intruded and partially assimilated, biotite gneiss

Figure 17 Garnetiferous alaskite with monomineralic pods of garnet (almandine). Location section 33 T24N, R18W.

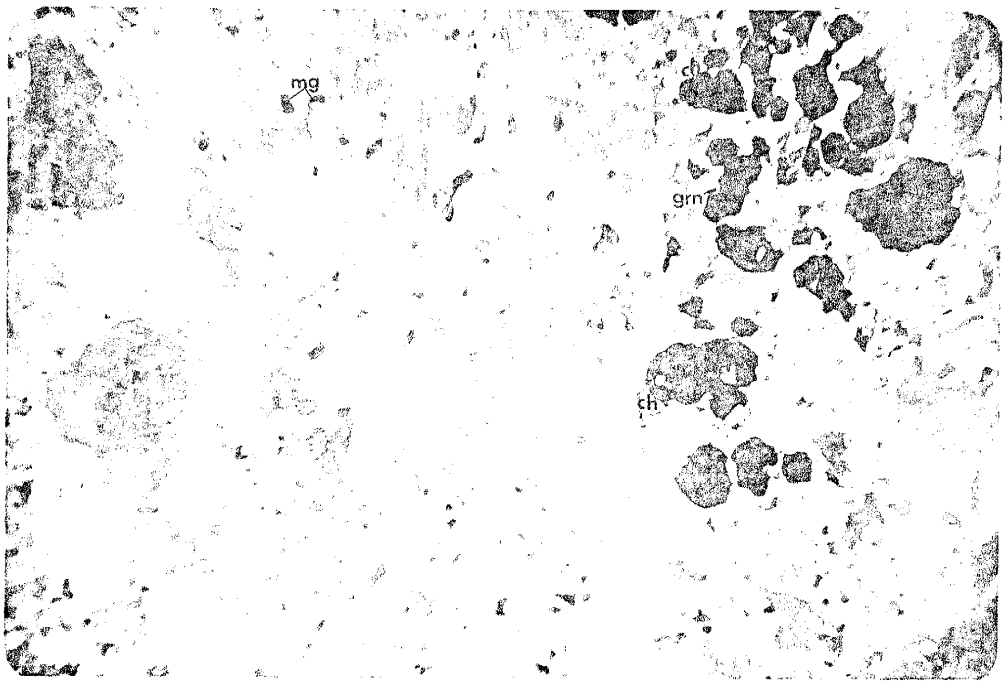

Figure 18 Photomicrograph of garnetiferous alaskite, note the absence of mafic minerals, outside of minor magnetite (mg) and garnet (grn). Garnets are retrograding to chlorite (ch) and the overall texture of the thin section is cataclastic. 1.0 mag., x-nicols, sample # 19.

giving the outcrop a migmatitic appearance. In the field the unit crops out similarly to Chloride granite, except that it has a lighter appearance. The monomineralic lenticular "pods" of garnet (almandite ?) parallel a metamorphic mineral fabric. Most outcrops are medium-grained, however coarse-grained and even pegmatitic fractions do occur. Outcrops of the pegmatitic fraction occur near the Juno mine in section 33.

Modal analyses by the author (table 2) indicate the average composition of the garnetiferous alaskite is quartz monzonite (Fig. 14). The principal mineral is quartz accounting for approximately 45% of the total volume. Oligoclase (An28) accounts for 20 to 25% and alkali feldspar from 20 to 30% of the remainder. Up to 5% muscovite along with as much as 9% garnet (almandite ?) are the varietal minerals. Trace amounts of zircon, apatite and magnetite are present.

The overall microscopic texture is cataclastic with xenoblastic grains of feldspar surrounded by a crushed matrix of quartz, and feldspar. Most grains show strain fractures and the plagioclase may show bent twin lamellae. The quartz shows sutured grain boundaries that tend to be polygonal. Alkali feldspars are commonly perthitic and have graphic textures. Twinning in the plagioclase is according to the albite law, but it can be combined with pericline and carlsbad twinning. Untwinned

plagioclase also occurs in thin section. Sericitic alteration is ubiquitous in thin section, with the plagioclase being preferentially altered. The garnets are being altered to biotite and occur as monomineralic lenticular "pods" in thin section (Fig. 18). For thin section description of the garnetiferous alaskite see appendix I, sample numbers 18,19.

Metarhyolite

Metarhyolite has not been previously mapped as a separate unit. It crops out as a dike-like body and crosscuts most Precambrian units in the map area. No crosscutting relationship was observed between metarhyolite and the Precambrian granite. In turn metarhyolite is transected by diabasic dikes of possible Tertiary age. Metarhyolite has a pervasive metamorphic tabric and has undergone intense shearing. Because of its metamorphic texture and field relationships the unit is assumed to be late Precambrian.

Metarhyolite is dark green, has a phyllitic sheen on its foliation planes, and contains relict feldspar phenocrysts. The metarhyolite dike varies from less than 1 meter to greater than 15 meters wide. Its average trend is northeast, parallel with the axial plane of a

regional Precambrian fold. The contact of the metarhyolite unit with the surrounding Precambrian units is discordant and normally quite sharp. Little, if any, contact metamorphism is present.

The metarhyolite has two facies: a border facies that is fine to medium grained (phaneritic facies) with a strong foliation, and a core facies that is aphanitic, both facies contain relict feldspar phenocrysts (Fig. 19). The boundary between these two facies is very gradational. Most outcrops contain both facies; however, in some places only the coarser grained facies is observed. Outcrops of metarhyolite vary from green to dark gray in color and normally are resistant to weathering compared to the country rock.

Much of the metarhyolite displays a very strong foliation that strikes approximately N30° E and dips approximately 80° to the southeast. The foliation planes nave a phyllitic sheen and parting along these planes is quite common. The phaneritic facies looks like fine-grained granite but its intimate association with the aphanitic facies discriminates it from the country rock. Both facies often have relict feldspar phenocrysts that can occur up to 1 cm or larger in diameter. The relict phenocrysts are normally associated with quartzo-feldspathic veins that display ptygmatic

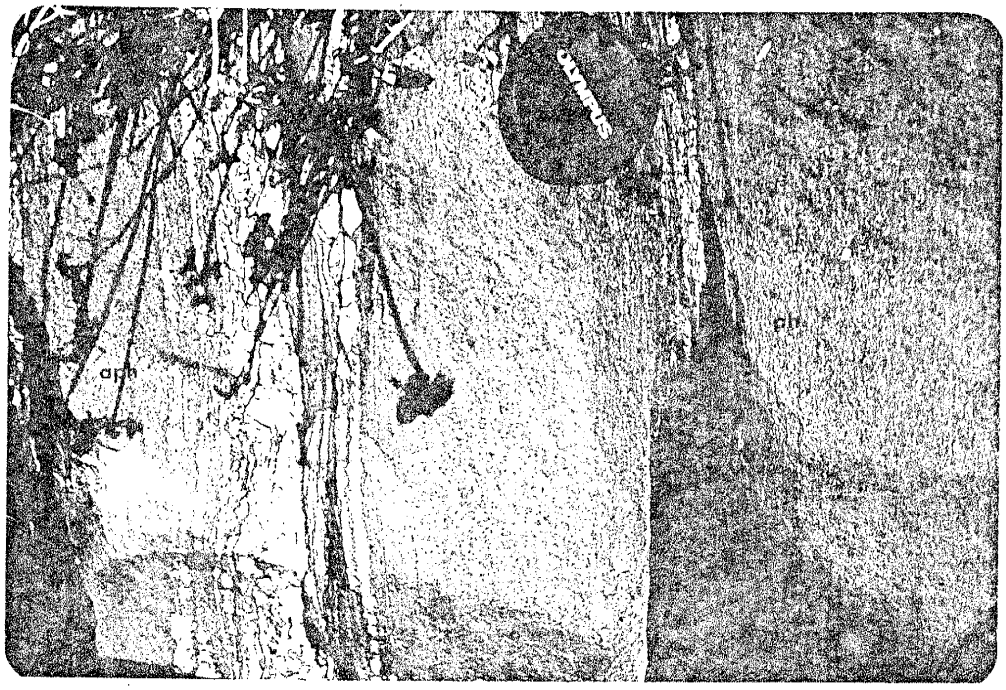

Figure 19 Outcrop of metarhyolite unit showing gradation from the aphanitic facies (aph) to the phaneritic facies (ph). Quartzo-feldspathic band mylonitized within the aphanitic facies. Minor feldspar phenocrysts (f) in the phaneritic facies. Location section 35, T24N, R18W.

patterns, but roughly parallel foliation. The quartzo-feldspathic veins containing relict phenocrysts appear to reflect flow textures, either due to mylonitization or original igneous flowage. In several localities outcrops of the metarhyolite have been altered hydrothermally. This alteration results in a very off-white outcrop, that is silicified, highly fractured and shows iron staining. Traces of precious metals are detected in these outcrops.

Phaneritic facies -- The principal mineral in the phaneritic facies is quartz, accounting for 30 to 40% of the total volume, with the second most abundant species being chlorite. Chlorite is very fine-grained and resolution under the highest power is very difficult; its alignment contributes to the foliation. Chlorite accounts for 15 to 20% of the total volume. Muscovite and sericite are also present and account for 5 to 10% of the rock. Feldspars occur mainly as relict phenocrysts, and can be as large as 1.5 mm across (Fig. 20). Most of the relict phenocrysts are either orthoclase or microcline; however plagioclase (An30) does occur. Feldspars are also in the matrix, and combined with the relict phenocrysts, they account for 35 to 40% of the total volume seen in thin section. The relict

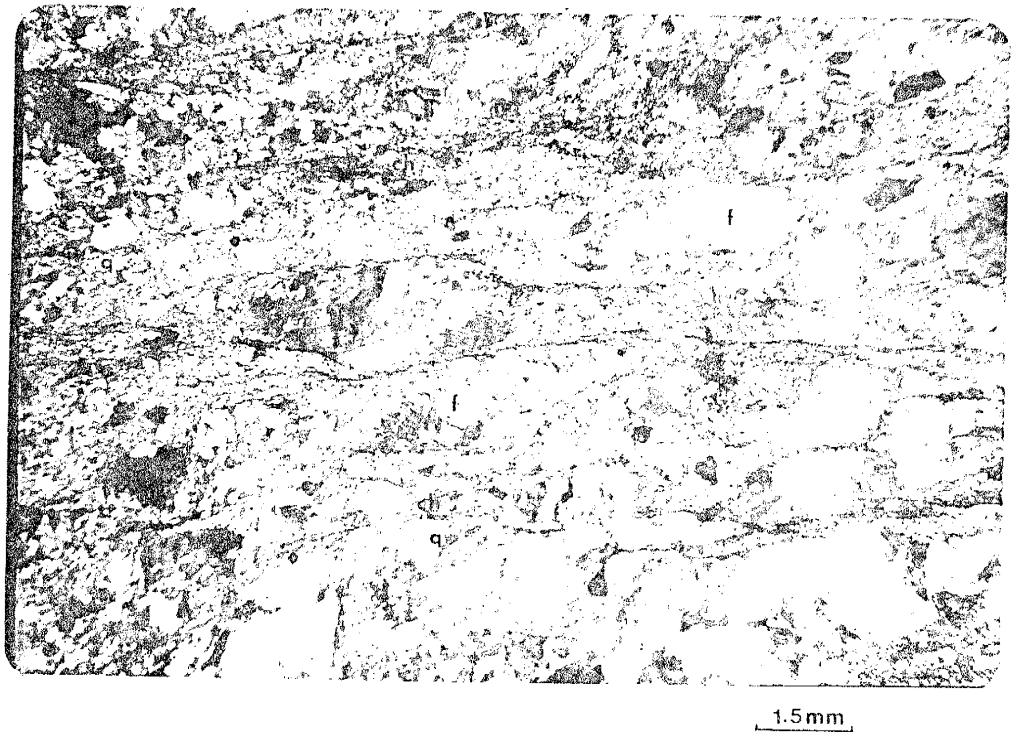

Figure 20 Photomicrograph of the metarhyolite phaneritic facies, showing a strong foliation and relict phenocrysts with pressure shadows (f). The matrix is composed of quartz (q), feldspar, and chlorite (ch). 1.0 mag., x-nicols, sample # 39.

Figure 21 Photomicrograph of the metarhyolite aphanitic facies, with a well developed foliation. Relict phenocrysts of feldspars (f) show excellent pressure shadows. The matrix is mainly chlorite with some quartz and feldspar; minor sphene (sp). 1.0 mag., uncrossed nicols, sample # 40.

phenocrysts are commonly poikilitic (poikiloblastic) and display excellent pressure shadows (Fig. 20), as well as strain fracture. Inclusions in the relict phenocrysts are chlorite and quartz. The relict alkali feldspar phenocrysts commonly show exsolution and graphic textures. The relict plagioclase phenocrysts may show bent twin lamellae. The matrix is recrystallized with undulatory extinction, and occasional aggregates of arrested quartz grains. The main alteration product is sericite, which preferentially alters plagioclase phenocrysts. Trace amounts of sphene, zircon, alunite, apatite and magnetite are present. Overall the rock has mylonitic texture. For thin section description of the phaneritic facies of the metarhyolite see appendix I, sample numbers 32-38.

Aphanitic facies -- Quartz is the principal mineral in the aphanitic facies comprising approximately 30% of the total volume. Chlorite is equally abundant varying from 25 to 35% of the rock. The aphanitic facies contains more chlorite than the phaneritic facies, but it is very fine grained and is difficult to resolve even under the highest power. Muscovite and sericite make up about 15% and in one sample as much as 25% was estimated. The abundance of micaceous minerals accounts for the very

pervasive foliation seen in thin section (Fig. 21). Like the coarser grained facies the aphanitic facies has relict feldspar phenocrysts. The phenocrysts are chiefly alkali feldspar, although plagioclase is is also present. The total volume of relict phenocrysts is 20 to 25%. The relict phenocrysts show well-developed pressure shadows, strain fractures, and they are commonly poikilitic (poikiloblastic). Inclusions are mainly chlorite and quartz. The relict phenocrysts, like the phaneritic facies, can exceed 1.5 mm in diameter (Fig. 21). The few grains of plagioclase were insufficient to determine the An content. Alkali feldspar phenocrysts show exsolution textures but very little graphic texture was observed. Trace amounts of apatite, sphene, zircon, hornblende laths, alunite and magnetite are present. The most abundant alteration product is sericite which preferentially alters plagioclase over alkali feldspar. The matrix is mainly a very fine-grained intergrowth of chlorite and quartz. Quartz is recrystallized displaying sutured grain boundaries and undulatory extinction. Overall the rock has mylonitic textures with a pervasive foliation. For thin section description of the aphanitic facies of the metarhyolite see appendix I, sample numbers 40,41.

PHANEROZOIC ROCKS

Ithaca Peak porphyry, 5 miles south of the study area has been dated by Mauger and Damon (1965) at 72 m.y. by K:Ar method. No apophyses of the Mesozoic stock were seen in the study area, however various dikes possibly related to the intrusive were observed (Thomas, 1953). The dikes crosscut the Precambrian units in the field area, and are either diabasic, pegmatitic, mafic, or aplitic. Because these dikes are later than the known Precambrian units, lack metamorphic textures, and may be related to Ithaca Peak, they are assigned to late Phanerozoic time. No isotopic ages have been recorded from the dikes so they could be late Precambrian in age, similar to the diabase dikes of the Apache group of southeastern Arizona. Diabase, mafic and porphyritic mafic dikes were mapped as separate units; aplites and pegmatitic lenses and dikes, are a more abundant type, but due to their discontinuous nature no attempt was made to distinguish them on the geologic map.

Diabase

Schrader (1909) first described diabase dikes in the district. Dings (1951) mapped diabase dikes and noted they were older than vein mineralization and concluded that their age is Mesozoic.

Diabase dikes occur throughout the study area with random strikes and steep dips. The dikes range in thickness from less than 1 meter to greater than 50 meters (Thomas, 1953), and can be traced for more than 1/2 km. The most prominent outcrops are near the Hercules mine in the southeastern portion of section 35, and near the Payroll mine, in the northeastern portion of section 2. Diabase dikes also intrude the Chloride granite in the northern portion of section 34. Contacts of the diabase dikes with Precambrian country rock are discordant and normally quite sharp. In the northern portion of the Chloride granite, diabasic dikes, trending roughly north- south crosscut an eastward trending metarhyolite dike; the contact at this locality is obscured by intense hydrothermal alteration.

On fresh surface diabase dikes vary from gray to green, weathering to a buff-green to brown. Most outcrops are intensely weathered and often have a pitted appearance due to preferential weathering of plagioclase

laths, magnetite and pyrite (?). In several localities diabase dikes include numerous xenoliths of partially assimilated pegmatitic material (Fig. 22). This mixture was described as hybrid rock by Thomas (1953). The pegmatitic inclusions vary in size from less than 5 mm to greater than 30 cm in diameter. Outcrops of diabase are commonly fractured and the fracture surfaces are coated with secondary euhedral to subeuhedral crystals of epidote.

Microscopic examination shows diabase composed of 30 to 50% plagioclase (An45), 10 to 20% hornblende (after pyroxene), and 10 to 30% augite. Magnetite is present from 5 to 10%, and is commonly poikilitic and subeuhedral. Trace amounts of calcite, natrolite and zircon were observed as well as opaque needles of an unidentified mineral. Thomas (1953) reports trace amounts of apatite and biotite in the diabase. Most specimens have quartz and feldspars as inclusions. The proportion of inclusions varies from less than 1% to greater than 40%. In the sample with the most quartz and feldspar inclusions, the two minerals occur as sutured aggregates with graphic texture (Fig. 23) and undulatory extinction. The plagioclase is intensely sericitized and some of the pyroxene is altered to actinolite- tremolite. Hematite after magnetite is

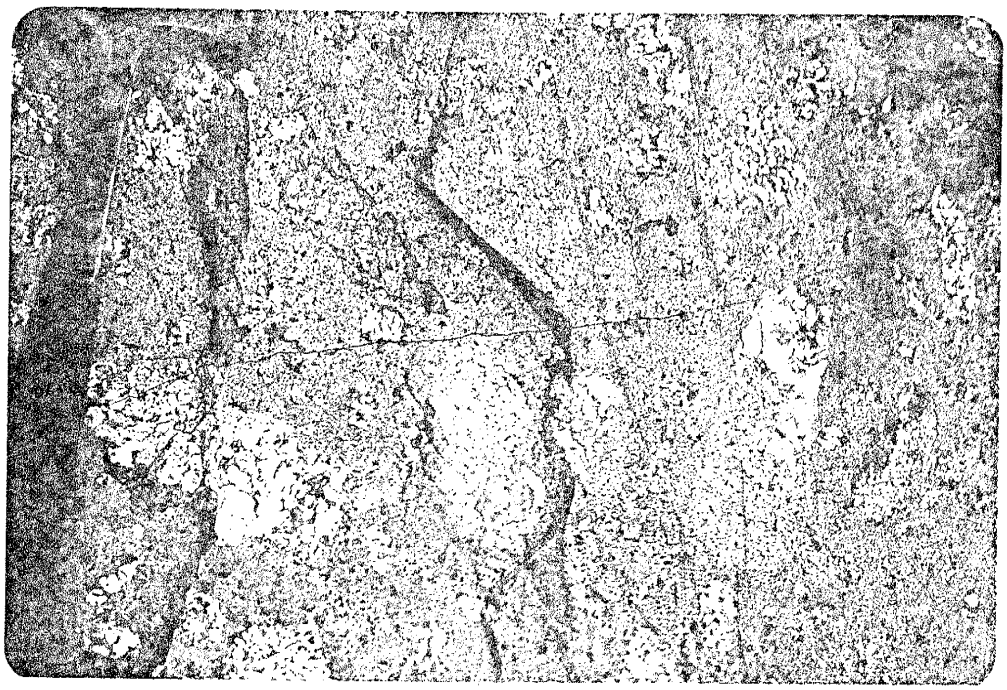

Figure 22 Diabase dike with numerous pegmatitic xenoliths. Location section 35, T24N, R18W.

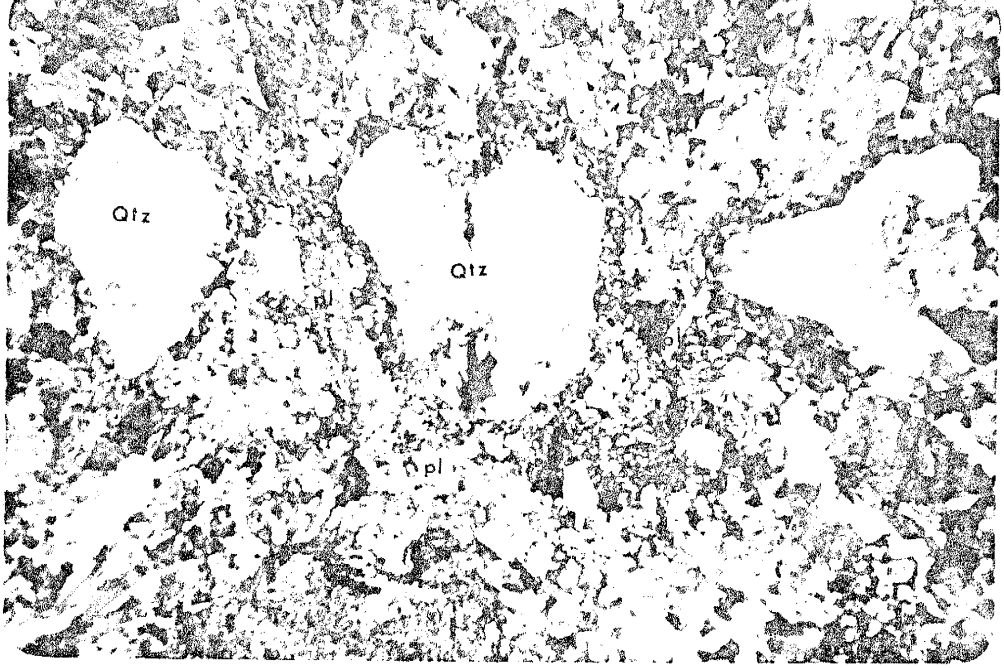

Figure 23 Photomicrograph of diabase with sutured aggregates of quartz (Qtz) set in an ophitic matrix. The matrix is composed mainly of plagioclase (pl) highly altered, and hornblende after pyroxene. 1.0 mag., x-nicols, sample # 44.

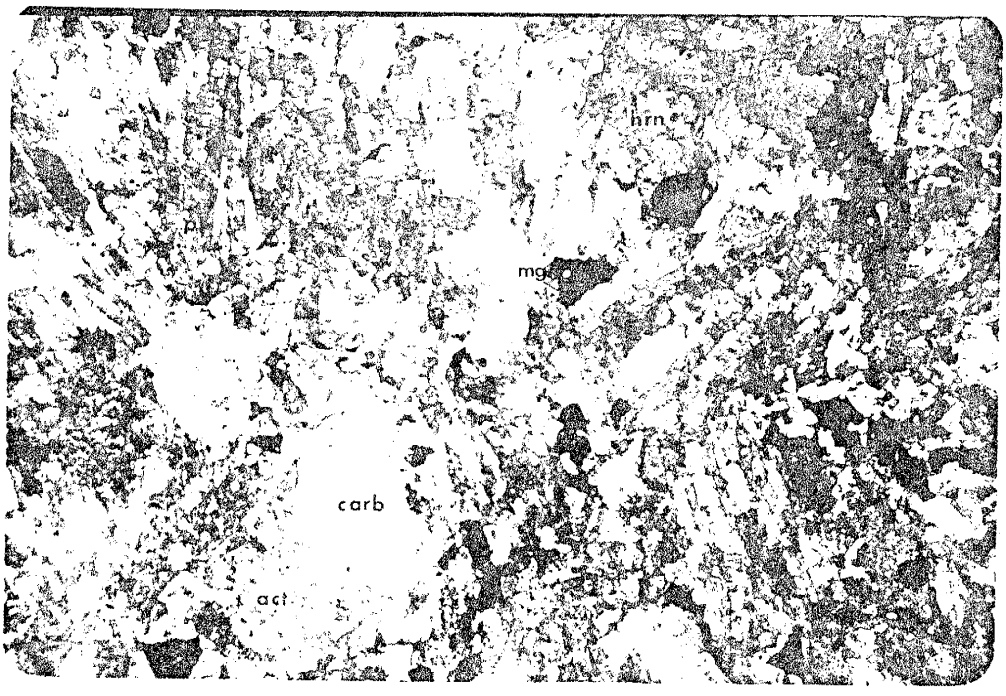

Figure 24 Photomicrograph of diabase showing a well developed ophitic texture. Altered plagioclase (pl), magnetite (mg), actinolite-tremolite (act), hornblende (hrn) and calcite (carb). 1.0 mag., uncrossed nicols, sample #43.

common in hand specimen and thin section. Overall the rock has a strong ophitic texture (Fig. 24). For thin section description of the diabase see appendix I, sample numbers 42,43,44.

Mafic dikes

Thomas (1949a), described a variety of lamprophyre dikes such as vogesite, kersantite and spessartite. To this list Dings (1951) added minette and camptonite. In this report lamprophyre dikes have been grouped with mafic dikes to include porphyritic and non-porphyritic types. The age of the mafic and lamprophyric dikes was assumed by Dings (1951) to be similar to the diabase dikes (i.e. Mesozoic).

The mafic dikes crop out as fine-grained, dark green rocks that commonly are porphyritic. Mafic dikes are limited in occurrence within the study area; however, prominent outcrops are found in section 2. At this location a mafic dike is not off-set by a northeastward trending fault, which does truncate the Payroll vein. The vein parallels the N50°W trend of the mafic dike. Either the fault does not extend far enough to the southwest to off-set the mafic dike, or the dike is post faulting. The thickness of the mafic dikes varies from

less than 1 m to greater than 10 m. Contacts of the mafic dikes with the country rock are discordant and snarp. The mafic dikes vary from light gray to dark green, on fresh surface and weather to a buff-green to brown. Most mafic dikes are porphyritic with feldspar, hornblende, and/or pyroxene phenocrysts. The phenocrysts vary from less than 1 mm to greater than 2 cm in diameter. Most of the phenocrysts are subeuhedral to euhedral and are randomly distributed in an aphanitic to fine-grained greenish groundmass. The groundmass is nornblende- chlorite (?), pyroxene (?), and plagioclase, and often has an ophitic texture. Alteration products are chlorite derived from hornblende and pyroxene, calcite (minor), sericite and possibly epidote (Thomas, 1953).

Pegmatites

Thomas (1949a) reported extensive pegmatites in the district, and recognized at least two generations. The older associated with the Precambrian biotite gneiss and a younger set of pegmatitic dikes which crosscut Precambrian units. However, Dings (1951) believed that most if not all of the pegmatites are genetically related to the 72 m.y. old Ithaca Peak intrusive 5 miles south

of the study area. The author agrees with Thomas (1953) that many of the pegmatites are possibly Precambrian in age representing a final stage of metamorphism. However, the lack of metamorphic textures and compositional similarity to Ithaca Peak, combined with extreme discontinuity and irregular exposures precluded detailed distinctions and all of the pegmatites in this study have been assigned to the Phanerozoic.

Pegmatitic dikes and lenses are coarse-grained, and off-white in color on both fresh and weathered surface. They are composed chiefly of quartz and alkali feldspar (Fig. 25). Outcrops of pegmatite are widespread in the field area, but are most abundant in the undifferentiated complex. Stringers and small veins of pegmatite occur in the amphibolite unit, but only very minor amounts of pegmatitic material invade the Chloride granite and Precambrian granite. The most prominent outcrop of pegmatite trends north-south, in Tennessee Wash, and can be traced for nearly 1/2 km with an average width of 130 meters. Most vein-type pegmatites are complexly folded, displaying ptygmatic patterns. Contacts of the pegmatites with the country rock are both concordant and discordant, and normally are sharp. Gradational contacts are seen with the granite gneiss and the garnetiferous alaskite.

Figure 25 Outcrop of pegmatite with large euhedral cystals of feldspar. Location section 33 T24N R18W.

Gray to milky quartz is the principal mineral in pegmatite (Thomas, 1953) accounting for 30 to 40% of the total volume. The remainder of the rock is orthoclase and minor amounts of bluish-gray microcline (Thomas, 1953). Small amounts of muscovite and biotite as well as black opaques (magnetite and sulfides), are recognized in hand specimen. Some outcrops have very large crystals of orthoclase, up to 5 cm in width and length, which display excellent Manebach twinning. Thomas (1953) recorded a few rare minerals in isolated pegmatites, such as: beryl, gadolinite, tourmaline, and rutile. These rare minerals were not observed in this study.

Aplite

Thomas (1953) made the first record of aplitic dikes in the district. The discussion of age for the pegmatites is applicable to aplites (i.e. Phanerozoic). Aplites occur as both dikes and lenses in the country rock and are less abundant than the pegmatites. Aplites are off-white, fine-grained rocks composed essentially of quartz and feldspar with a saccharoidal texture. Aplite dikes and lenses are mainly observed in the Precambrian granite gneiss and are normally less than 1 m wide. Contacts are both discordant and concordant with the country rock and can be both sharp and gradational.

The composition of the aplites is similar to the pegmatites, except that the alkali feldspars are more abundant than quartz (Thomas, 1953). The rock commonly contains from 1 to 4% small grains of almandine (?) garnet. No other minerals were observed in hand specimen. In the western portion of the field area the aplite resembles the garnetiferous alaskite unit. The alaskite unit has been distinguished because of its spatial association with the Chloride granite and its coarser texture as compared to aplite.

STRUCTURE

The study area is located on the west slope of the Cerbat Mountains, an eastward tilted fault block in the Basin and Range Province. The structure is complex, reflecting remnant Precambrian folding as well as Laramide and Tertiary activity. Foliation is developed to a varying degree in all Precambrian rock types along with a complex pattern of joints. Faulting is evident in numerous mineralized fissures throughout the study area. Only a few transverse faults exist, and these are not mineralized. Cataclastic textures prevail in most Precambrian rocks, testifying to dynamic metamorphism.

Foliation

Foliation within the study area is well developed in the amphibolite unit, biotite gneiss and faintly developed in the granite gneiss. The more massive units such as the Chloride granite and its border facies exhibit a very weak foliation, that is scarcely discernible in the field.

In figure 26 387 poles to foliation have been plotted and contoured by the method outlined in Billings (1972, pp.104). The majority of the measurements are representative of the amphibolite and biotite gneiss units. From the plot the most prominent great circle gives a regional foliation that strikes N44°E and dips 54° SE. This measurement agrees with the average foliation of Thomas (1949a).

Joints

Thomas (1949a) delineated three types of joints in the Cerbat Mountains, which he called "strong", "moderate", and "weak". He classified the "strong" joint on the basis that it extended beyond the area of observation and had numerous parallel joints. In contrast he considered a joint "weak" if it seemed small and had only a few parallel joints. Any joint between these extremes Thomas (1949a) classified as "moderate".

Thomas (1949) plotted poles to joints on an upper-hemisphere equal-area projection. From the work he determined the strongest joints strike approximately northwest and generally have steep dips. The "moderate" joints, Thomas found are less consistent in strike, but prefer a northeast trend with steep eastward dips. Weak

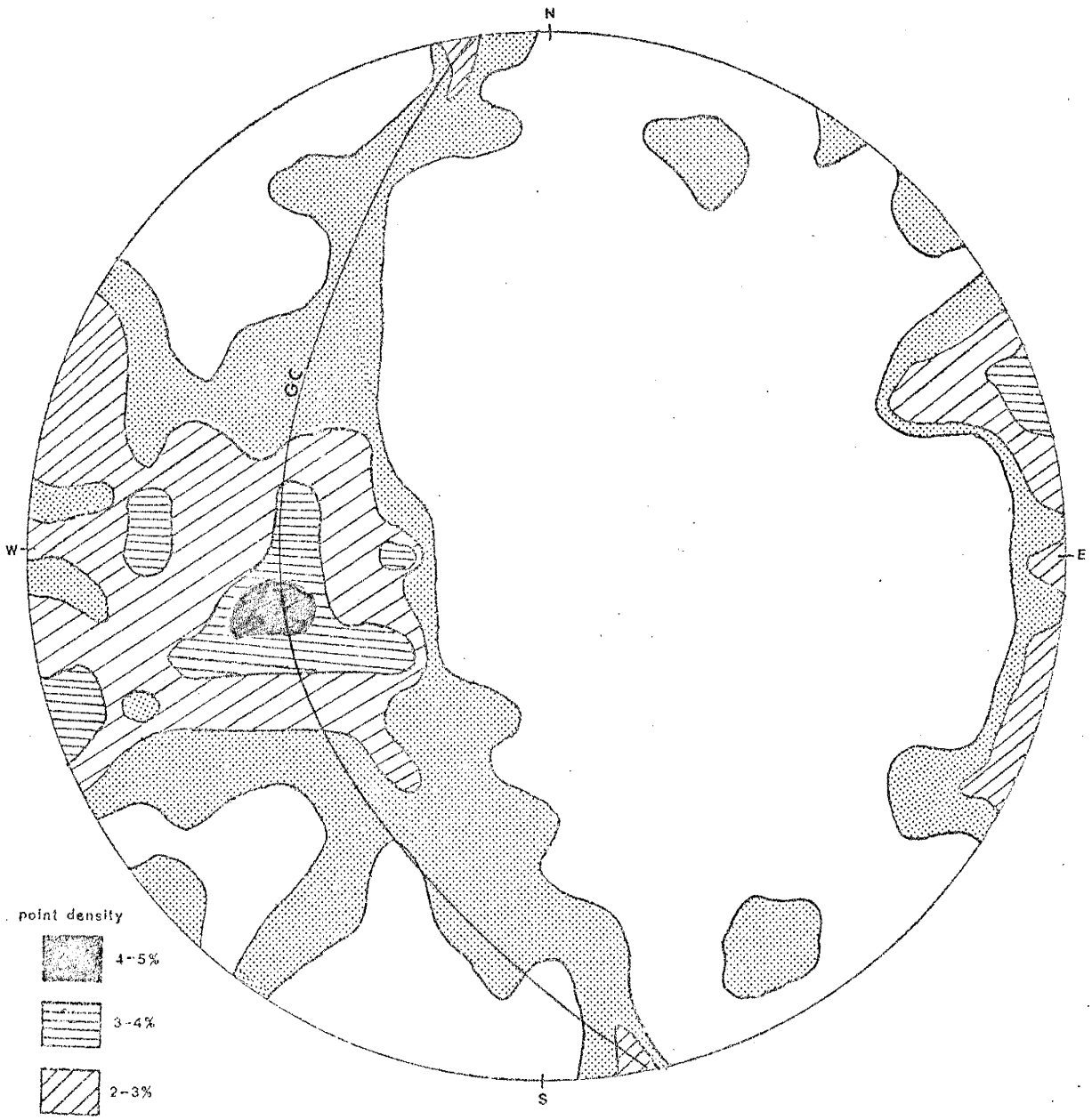

PI DIAGRAM OF 387 POLES
TO FOLIATION

GC: great circle

FIG. 26

joints were too scattered for Thomas (1949a) to determine a strike. However, field observations by Thomas (1949a) show that when all three types of joints occur together the weakest favors a north-south strike, with a steep dip.

In this study no attempt was made to delineate three types of joints as Thomas (1949a) did; however a conjugate set of joints was measured in outcrop. The conjugate set may correspond to Thomas's "strong" and "moderate" joints. A total of 67 sets of conjugate joints were plotted on an equal- area-stereonet (Fig. 27). The poles to these conjugate joints plot randomly, making it impossible to delineate any great circle to determine the average strike and dip of the joint sets.

Faults

The most recognizable faulting in the study area is the fissures along which mineralization has occurred (Thomas, 1949a). These fissures display brecciation, open space filling and gouge, all three attesting to faulting. Thomas (1949a) by detailed mapping of the Cerbat Mountains, found that 80% of these veins strike approximately northwest. This trend agrees with several veins observed in the current area being studied.

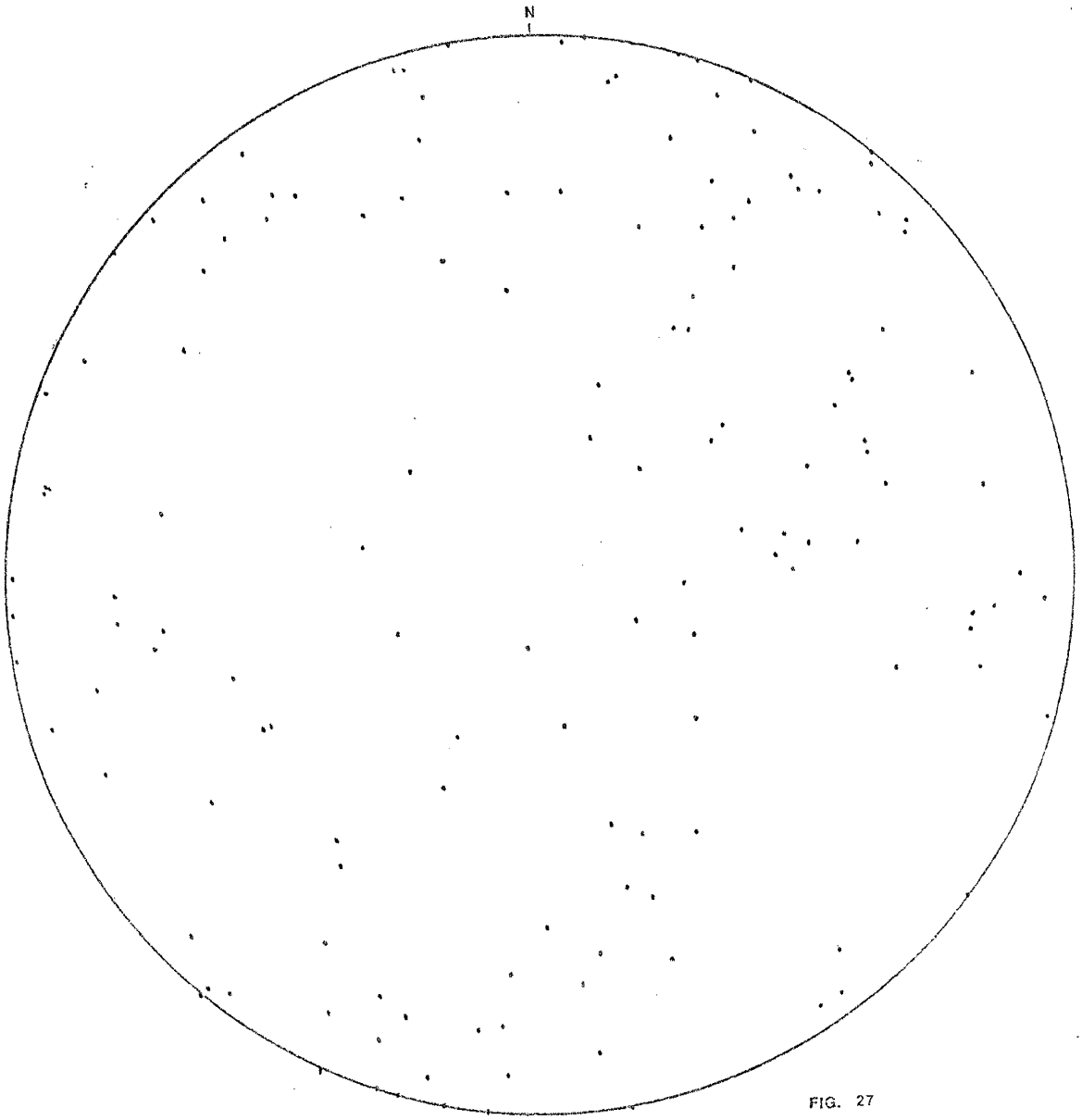

FIG. 27

PI DIAGRAM OF 134
POLES TO JOINTS
"conjugate sets"

However, several veins especially near the Juno Mine, can strike anywhere from north-south to east-west. Most fissures in the study area have steep dips to the northeast, which agrees with observations by Thomas (1949a), and Dings (1951).

Several of the veins show slickensides, with an excellent exposure in the Silver Hill Mine along a northward-trending drift. Thomas (1949a) believed most of these mineralized faults are normal with only a few reverse faults.

The amount of movement along mineralized faults was indeterminate, but several periods of activation are reflected in outcrop. By the use of ore microscopy Thomas (1949b) was able to delineate 5 periods of fault activity in the veins. The first period opened the fissures which was followed by three intra-mineral fracture periods ending in post mineral fracturing.

The exact age of fracturing to produce the fissures in the Chloride district is not known. Thomas (1949a) believes that faulting and mineralization are contemporaneous and both are younger than rhyolite and andesite dikes of Tertiary age. Dings (1951) observed siliceous dikes related to Ithaca Peak porphyry (72 m.y.) (Mauger and Damon, 1965), filling fractures making them pre-intrusive. In contrast Drake (1972) noticed a

mineralized fault clearly crosscutting the Mineral Park intrusive, thus making the fault post-intrusive. The author believes that the initial development of the fractures was pre-intrusive and possibly Precambrian in age, then a later event reactivated the faults and allowed mineralizing fluids of Mesozoic age or Tertiary (?) to be injected along them.

Minor transverse faulting has occurred in the study area with the exact age of activation indeterminate. The most controversial transverse fault is located in section 2 near the Payroll mine. Dings (1951) states the vein has been off-set approximately 600 feet, by a northeastward trending fault with supposedly the South Georgia mine the off-set extension, however; Dings (1951) also reports that the Payroll vein follows the transverse fault, thus making the fault pre-mineralization. A second transverse fault is located on the southern extremity of Silver Hill, where the fault strikes approximately N50° W and and appears to be pre-mineralization.

About 2 miles west of Chloride Thomas (1949a) proposed a normal fault which he called the Sacramento fault. The Sacramento fault is beyond the boundary of the current map area. It strikes N48°W, dips 60°S and brings volcanic rocks of assumed Tertiary age on the

southwest side in fault contact with Precambrian rocks on the northeast side (Thomas, 1949a). Thomas (1949a) traced the fault for 2 1/4 miles to the northwest, and to the southeast he projects it beneath the alluvium for almost 4 miles. Thomas (1949a) believes the northerly truncation of the Cerbat Mountains is evidence for the faults continuation, thus he believes the Sacramento fault is responsible for the formation of the eastward tilted Cerbat Mountains. Thomas (1949a) estimated the movement of the Sacramento fault, assuming only dip-slip motion to be: 3165 feet of net vertical displacement and 1830 feet of net horizontal separation.

Since the Sacramento fault cuts Tertiary (?) lavas, it is assumed to be one of the youngest events in the district and may have initiated in late Tertiary time (Thomas, 1949a). Thomas (1949a) mapped a similar fault on the east side of the Cerbat Range, which he called the "Neal Ranch Fault". In addition Thomas (1949a) delineated auxiliary faults and other smaller normal faults in the Cerbat Mountains.

rolding

Folding is seen throughout the study area on both a small scale and a large scale. The small scale folding is best seen in the ptygmatic patterns of the quartzo-feldspathic veins, which occur in most rock types (Fig. 10). Thomas (1949a) believes the ptygmatic folds have formed under conditions of active major folding, since the axial planes of the small folds are roughly parallel to the foliation of the enclosing rock. Field evidence during this study supports Thomas' (1949a) observations.

The largest fold (Fig. 28) which is outlined in the outcrop pattern of the amphibolite, was originally interpreted as a large anticlinal structure by Thomas (1949a). He determined the axis of the anticline to trend northeast and plunge 80°.

From the additional detail of this report the amphibolite unit appears to outline a more complex structure than Thomas' (1949) interpretation (Fig. 28). The overlay on figure 28 shows the possible continuation of the amphibolite unit, which may reflect three periods of Precambrian folding.

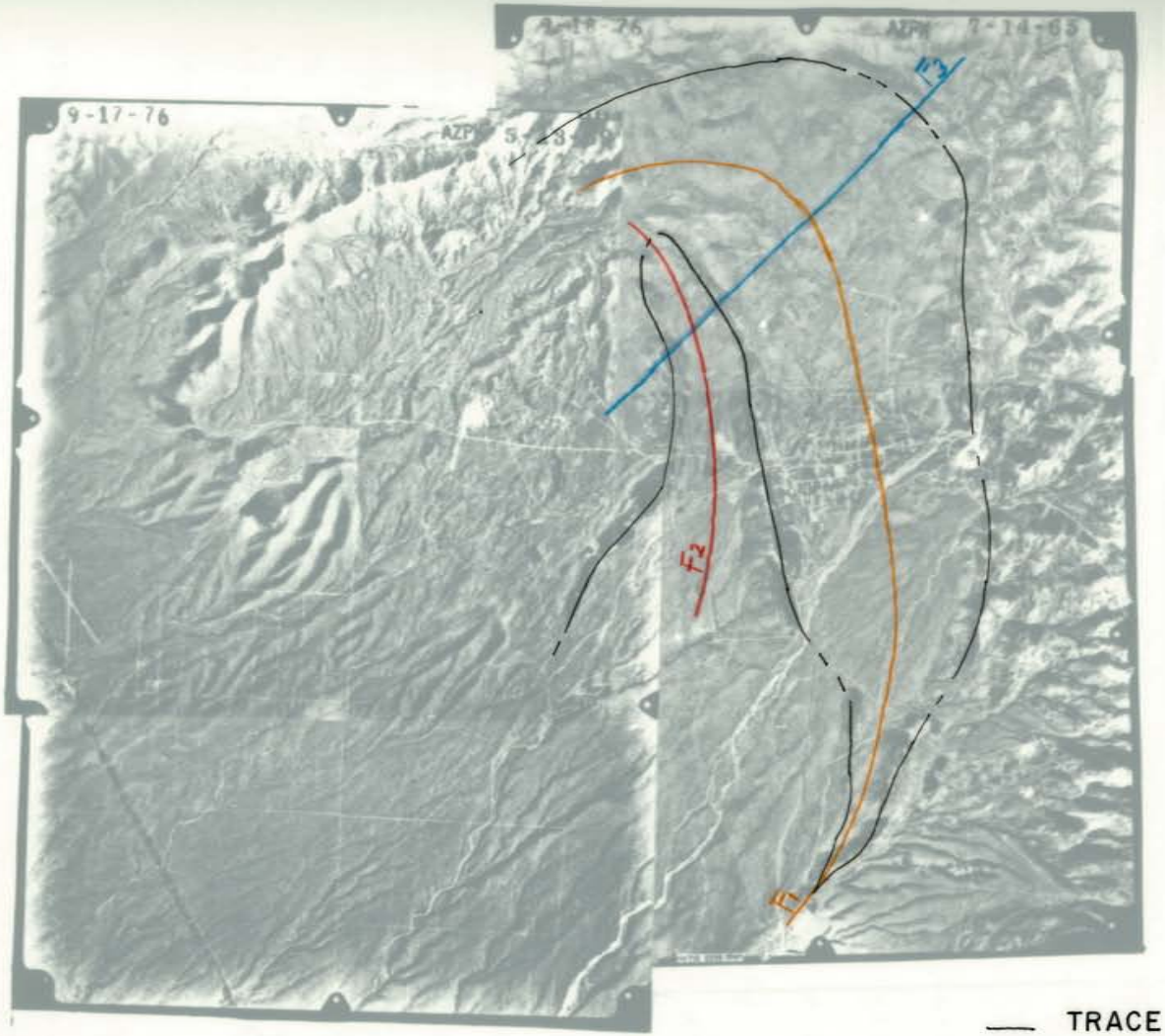

TRACE OF AMPHIBOLITE UNIT
FOLD AXIS 1
FOLD AXIS 2
FOLD AXIS 3 the axis of the anticlinal structure interpreted by Thomas (1949a)

FIG. 28

Figure 29 is the plot of 387 poles to foliation, used to help interpret the Precambrian folding history. Most of the measurements are from the amphibolite and biotite gneiss units. From the pi-diagram the attitude of 3 great circles (GC) can be delineated: GC1, 286° and dips 66° SW, GC2, 74° and dips 84° NW and GC3 170° and dips 50° SW. The attitude of the axial planes for the folds, was determined by drawing a line that passes through the axis (pole to GC) and between the maximum point cluster and minimum point cluster for the corresponding great circle. The attitudes of the axial planes (AP) are: AP1, 5° and dips 64° SE, AP2 165° and dips 70° NE and AP3 44° and dips 54° SE. Each axial plane (AP1, AP2, AP3) corresponds to each great circle (GC1, GC2, GC3) respectively. The last attitude for the axial plane is reflective of the last episode of folding and it represents the attitude of the most pervasive foliation in the field area (i.e. 44° and dips 54° SE). This measurement for the foliation agrees with observations by Thomas (1949a).

Contained within each axial plane is the attitude of the fold axis (FA), they are: FA1 trends 16° and plunges 24°, FA2 trends 162° and plunges 6°, and FA3 trends 80° and plunges 40°. Each fold axis corresponds to each axial plane similar to the above. (i.e. FA1 corresponds to

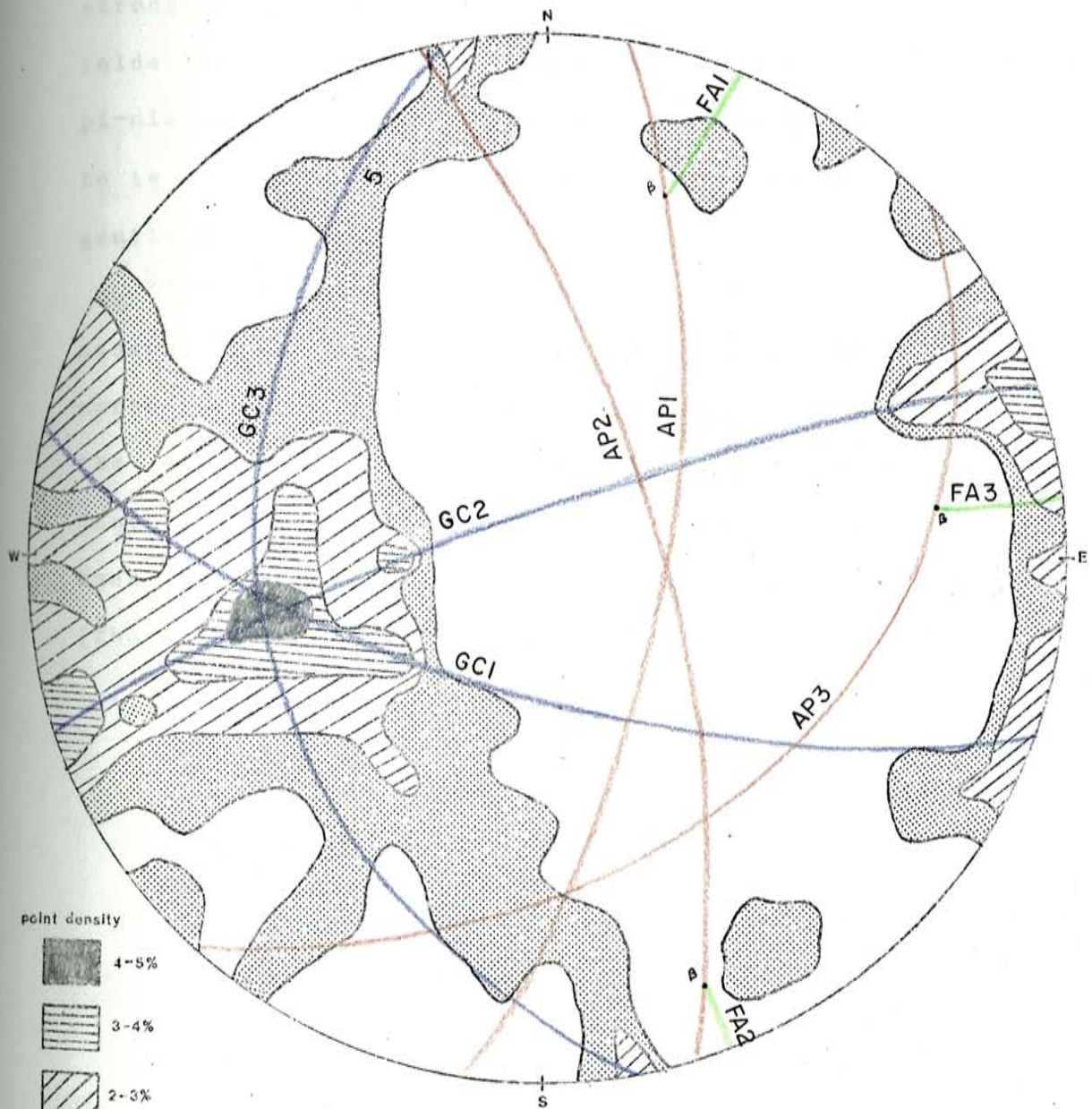

PI DIAGRAM OF 387 POLES TO FOLIATION

GC : great circle
AP : axial plane
FA : fold axis

FIG. 29

APl). The data indicate three distinct periods of folding with the last period (FA3) reflecting the strongest pattern in the pi-diagram. The shapes of the folds based on interlimb angles as determined from the pi-diagram are: fold 1 (corresponding to FA1) is tight to isoclinal, fold 2 is tight to isoclinal and fold 3 is gentle to open.

Thomas (1949a) also delineated another fold near Mineral Park, with a fold axis that trends north-northeast and plunges 75° to the northeast. Only the northwest limb of this fold is exposed in outcrop. Many of the folds developed during Precambrian time have been obliterated by intrusive action and granitization (Thomas, 1949a).

GEOCHEMISTRY

The purpose of the geochemical study is to: 1) determine if the amphibolite unit in the field area represents a single unit and thus outlines a refolded fold, 2) determine if the Precambrian granite in the southeast portion of the field area is chemically similar to the Chloride granite, and thus possibly genetically related, and 3) to give a bulk chemical composition of the amphibolite, Chloride granite and Precambrian granite, to aid in classification.

It must be noted that the units analyzed in this section have undergone medium to high-grade regional metamorphism (amphibolite facies) and hydrothermal alteration; both of these factors will influence the chemical data.

Method

Since the amphibolite unit reflects the proposed pattern of refolding in the study area, it has been used as a marker horizon and samples of amphibolite were collected at various locations along the fold (see appendix II). Representive samples were collected of the

Chloride stock and homogenized before analysis; the same was done for the Precambrian granite. All samples were analyzed for major elements by nondestructive X-ray fluorescence using U.S.G.S. rock standards (see appendix IV). Cu, Co, Ni, Zn, Pb, and loss on ignition (LOI), were determined by atomic absorption at New Mexico Bureau of Mines, Socorro, New Mexico. Raw data from the XRF for each sample, was calculated by computer into oxide percentages, for 17 elements (see appendix VI)

Amphibolite

Chemical compositions for the amphibolites are given in table 3, with 7-a a duplicate run of 7. The major chemical data indicate the amphibolites are tholeiitic in composition (see Fig. 30 and Fig. 31) but have a slight enrichment of Ca (table 3) compared to average basalts. Figure 30, an AFM plot (Irvine and Baragar, 1971) shows a tight cluster of sample points. Samples 8 and 9 are enriched slightly in iron. Sample 8 is located along the east exposure of the amphibolite unit, approximately 600 feet due west of the Elkhart mine, section 34 T24N, R18W. Sample 9 is located approximately 600 feet due north of the Silver Age mine, section 2 T23N, R18W. Both samples (i.e. 8 and 9) are believed to

Table 3 Average compositions of Amphibolite sample from the Chloride district. Sample 7-A, is a duplicate run of number 7.

Sample No.	3	4	5	6	7	7-A	8	9	10
SiO_2	47.300	47.846	47.984	47.713	45.747	45.808	46.444	46.490	46.954
TiO_2	0.914	1.080	0.981	1.390	1.188	1.171	1.378	1.307	0.935
Al_2O_3	13.457	13.240	13.034	14.191	13.498	13.407	12.282	12.562	13.202
Fe_2O_3	2.41	2.58	2.48	2.89	2.69	2.67	2.88	2.81	2.44
FeO	8.21	7.98	8.34	6.70	8.24	8.25	10.02	9.22	7.81
total iron as Fe_2O_3	11.536	11.450	11.753	10.331	11.844	11.835	14.015	13.054	11.118
MgO	9.232	9.251	9.138	8.200	8.942	8.931	8.218	8.622	9.798
CaO	14.031	14.029	13.002	13.363	14.727	14.760	12.916	13.048	15.127
Na_2O	2.248	2.006	2.201	2.481	1.719	1.634	2.351	2.396	1.791
K_2O	0.213	0.228	0.004	0.273	0.481	0.450	0.499	0.204	0.187
CO_2									
loss on ignition	1.18	0.89	0.97	0.82	0.80	.80	0.65	0.38	1.08
MnO	0.214	0.239	0.240	0.230	0.101	0.109	0.053	0.222	0.018
P_2O_5									
Total	99.15	99.37	98.34	98.17	98.25	98.17	98.16	98.01	99.13
Total w/% LOI	100.33	100.26	99.31	98.99	99.05	98.971	98.81	98.39	100.21
Cu ppm	68	90	74	95	60	73	115	52	120
Co	93	98	92	120	102	103	113	113	103
Ni	123	123	110	125	123	138	108	110	143
Zn	140	190	140	170	120	150	220	100	120
Pb	29	35	31	20	25	37	26	27	37

After Irvine and Baragar 1971

$A = Na_2O + K_2O$

$F = FeO + 0.8998\ Fe_2O_3$

$M = MgO$

FIG. 30

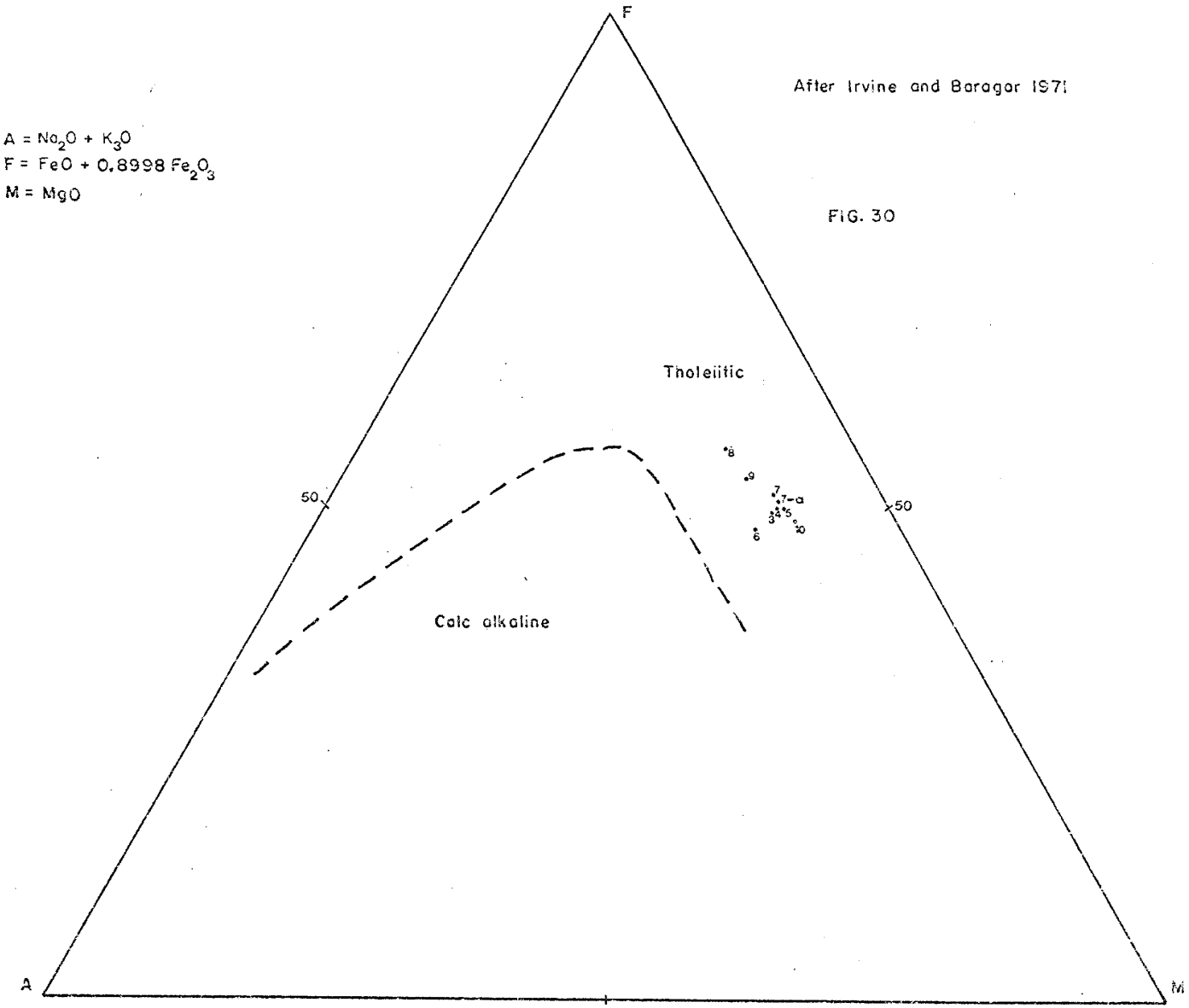

belong to the same continuous unit (see appendix II). The higher iron content in both of them, may be explained by their spatial association near a large hydrothermal vein system (i.e. Tennessee-Schuylkill and Silver Age) and by the mobility of iron (Davies et. al, 1979). Similarly sample 6 may be enriched slightly in Na2O and K2O caused by metamorphism and contamination by the Silver Hill hydrothermal vein. Both Na2O and K2O are relatively mobile elements (Davies et. al, 1979). Despite these variations and the mobility of certain elements, the AFM plot is fairly tight, for all amphibolite samples and they fall within the tholeiitic field. Figure 31 is a binary plot after Irvine and Baragar (1971), used to distinguish between alkaline and subalkaline fields. All amphibolite samples fall within the subalkaline field. The slight scatter for the plot, may be due to the high mobility of Na2O and K2O (Davies et. al, 1979).

Figure 32 is a Jensen Cation plot (1976) proposed for classifying subalkalic volcanic rocks. The cation plot relates the cation percentages of Al2O3, FeO + Fe2O3 + TiO2 and MgO and allows discrimination between differentiation trends of komatiitic, tholeiitic and calc-alkalic suites of volcanic rocks (Jensen, 1976). All of the amphibolite samples fall within the high- Mg

FIG. 31

After Irvine and Baragar 1971

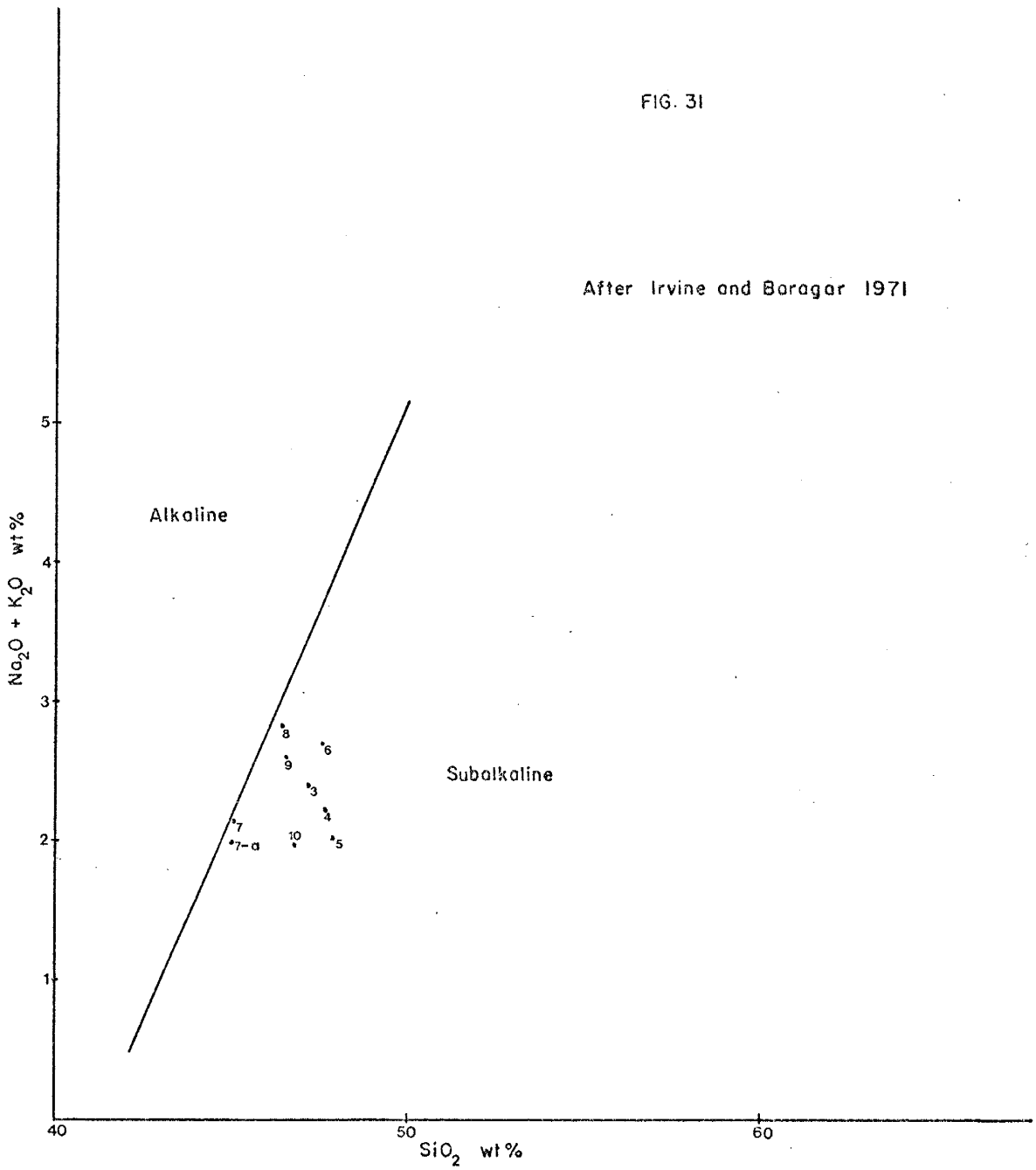

JENSEN CATION PLOT 1976

FIG. 32

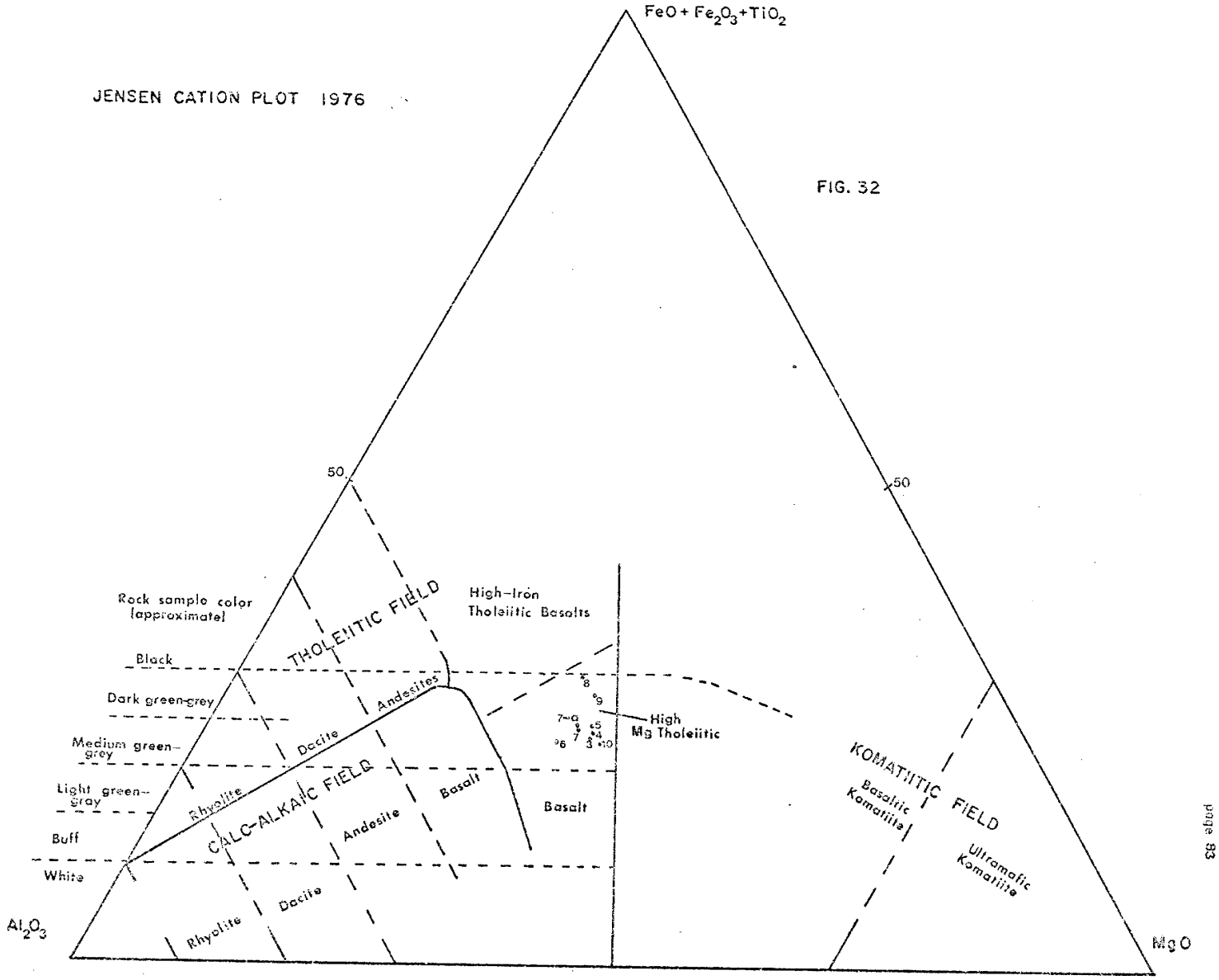

tholeiitic basalt field and also fall within a fairly tight cluster, similar to the AFM plot (Fig. 30). Again samples 8 and 9 are slightly enriched in iron and deviate slightly from the rest of the samples.

Davies et. al (1979) in a study of Archean volcanic rocks of the Timmins area of northeastern Ontario, used certain immobile trace elements (i.e. TiO2, Y, Zr, and Cr) to distinguish between different lithostratigraphic units and to aid in deciphering volcanic structure. Employing the same idea to the current study area, relatively immobile trace elements of amphibolite samples were plotted together, to see if the amphibolite is a single lithogeochemical unit, and thus one continuous norizon. Figure 33 A gives the tightest plot, which is in agreement with the immobility of TiO2 and Co (Davies et. al 1979). The slight scatter in figure 33 B and C, is possibly due to the moderate mobility of Ni (Davies et.al, 1979). Despite the mobility of certain elements and the effects of alteration all three plots give a rairly tight cluster, similar to the AFM diagram and Jensen Cation plot. Therefore the geochemical data for the amphibolite unit is consistent with the thesis that the amphibolite is a single continuous lithologic unit and thus outlines a complex structural refolding history.

FIG. 33

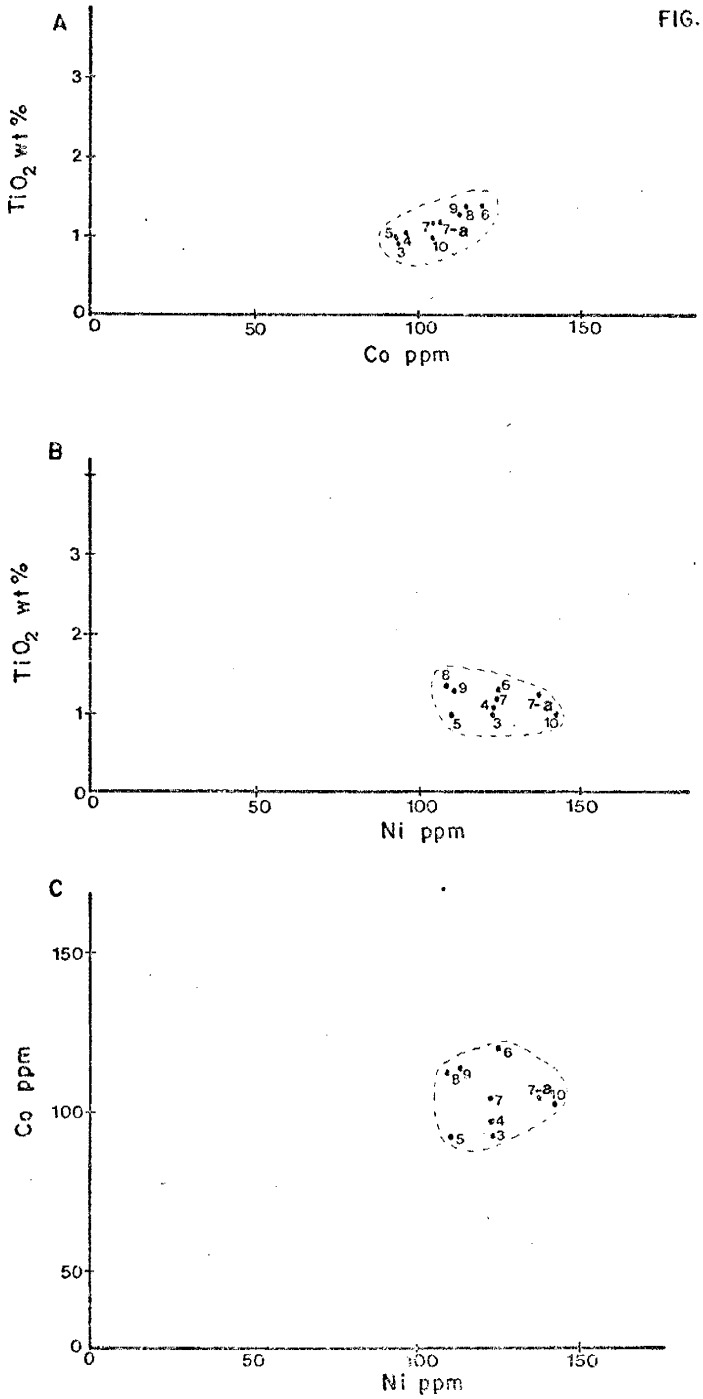
A
TiO_2 wt %
3
2
1
0
0
50
100
150
Co ppm
B
TiO_2 wt %
3
2
1
0
0
50
100
150
Ni ppm
C
Co ppm
150
100
50
0
0
50
100
150
Ni ppm

CIPW normative calculations were performed on the amphibolite samples, with the results tabulated in appendix IV. The norm calculations for volcanic rocks give a fair approximation of the mineralogic and modal composition of the sample as crystallized at low pressure and under relatively anhydrous conditions (Irvine and Baragar 1971). The total iron from the whole rock analysis has been converted to Fe2O3 and FeO prior to norm calculations as outlined by Irvine and Baragar (1971, p.526). The norm calculations, were performed by computer (see appendix V).

The estimated original mineralogy for the amphibolites shows clinopyroxene predominant, followed by plagioclase and olivine. In thin section most of the clinopyroxene has been converted to hornblende and biotite (see table 1). Normative plagioclase compositions (100 An/(An+Ab+5/3Ne) are between 52 to 67%. Olivine is present in normative values but none was observed in thin section.

Following the chemical classification scheme proposed by Irvine and Baragar (1971), all of the amphibolites fall within the basalt field (Fig. 34).

After Irvine and Baragar 1971

FIG. 34

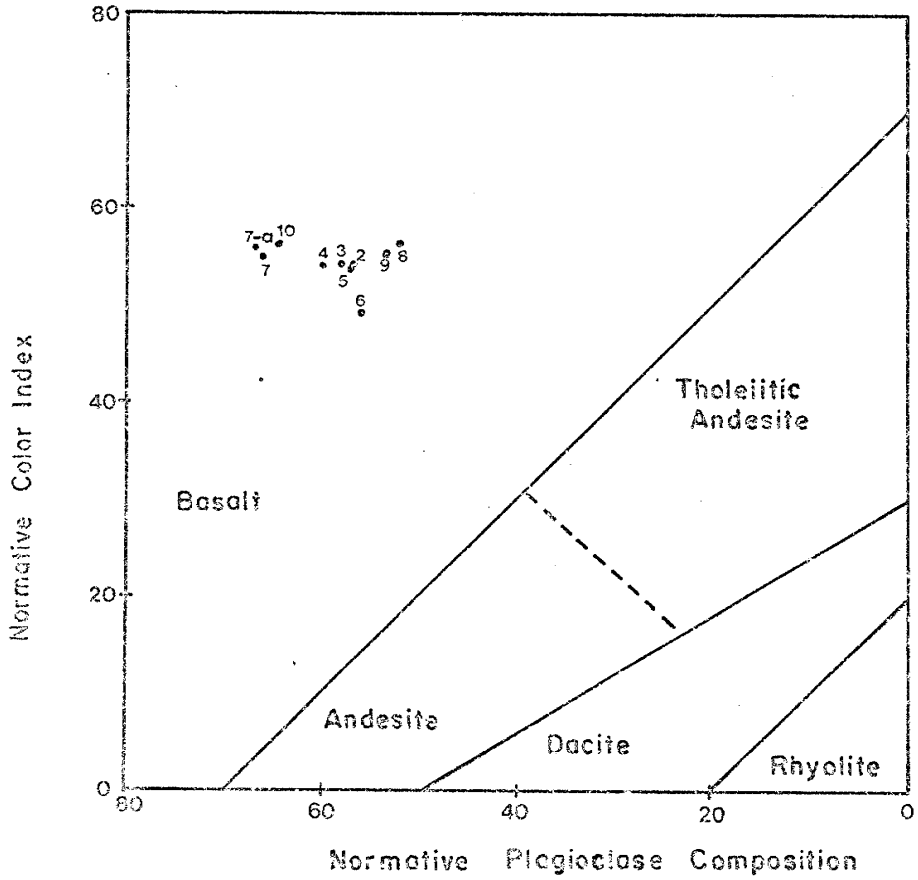

Granites

Chemical compositions for the granites are given in table 4 . Sample 1 and 1-a are duplicate runs of the precambrian granite and sample 2 represents the Chloride granite. For sample locations and preparations see appendix II and III respectively

Condie and Budding (1978) used a three fold subdivision to distinguish between Precambrian rocks in New Mexico. Using the same subdivision the Precambrian granite falls within the high-Ca group and the Chloride granite falls within the high-K+ group (Fig. 35). The high-Ca group is represented by high Ca (2-3.5%), intermediate K2O (3-4.5%), SiO2 at (60-70%) and a K2O/Na2O ratio from 1 to 1.5 (Condie and Budding 1978). The high-K group is represented by K2O values between 4.5-6% and a K2O/Na2O ratio between 1.3-2 (Condie and Budding 1978).

Normative feldspar compositions for the granites (see appendix V), show the Precambrian granite (1, 1-a) falls within the granodioritic field and the Chloride granite (2) lies in the granite field (Fig. 36). Modal analyses (table 2 and Fig. 14), indicate however, a quartz monzonite composition for both granites.

Table 4 Average compositions of Precambrian granites from the Chloride district. Precambrian granite = 1 and 1-A (duplicate run); Chloride granite = 2.

Sample No.	1	1-A	2
SiO_2	69.064	69.677	74.874
TiO_2	0.366	0.359	0.914
Al_2O_3	15.346	15.339	15.376
Fe_2O_3	1.87	1.86	1.53
FeO	2.03	2.10	0.22
total iron as Fe_2O_3	4.128	4.198	1.774
MgO	2.498	2.423	1.607
CaO	2.984	2.968	1.509
Na_2O	3.185	3.160	2.947
K_2O	3.622	3.615	5.258
CO_2			
loss on ignition	0.98	.66	.84
MnO	0.256	0.228	0.226
P_2O_5			
Total	101.45	101.96	103.60
Total w/% LOI	102.43	102.62	104.44
Cu ppm	35	33	36
Co	47	70	36
Ni	<25	<25	<25
Zn	100	90	90
Pb	47	49	52

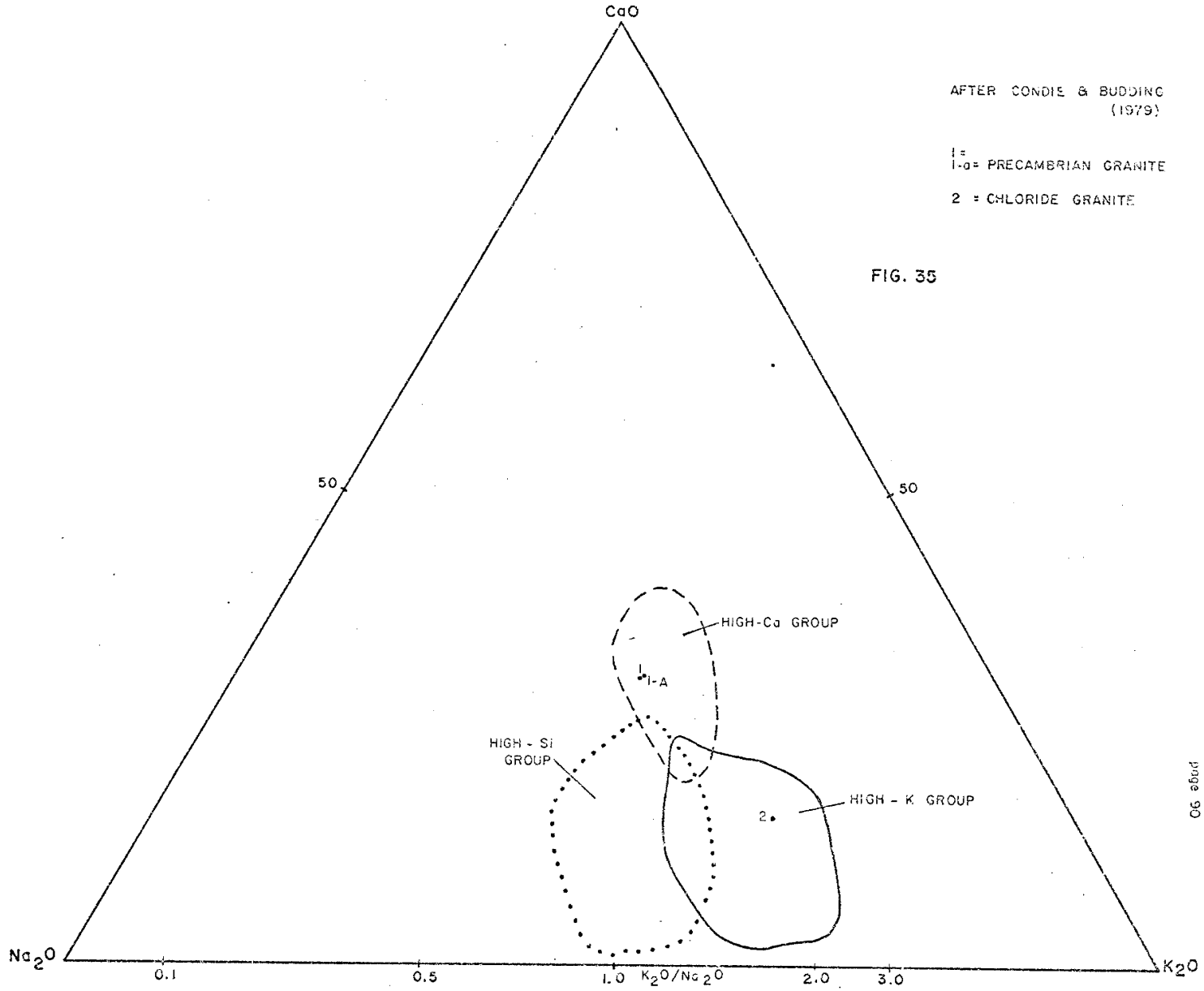

AFTER CONDIE & BUDDING (1979)

1 = 1-a = PRECAMBRIAN GRANITE

2 = CHLORIDE GRANITE

FIG. 35

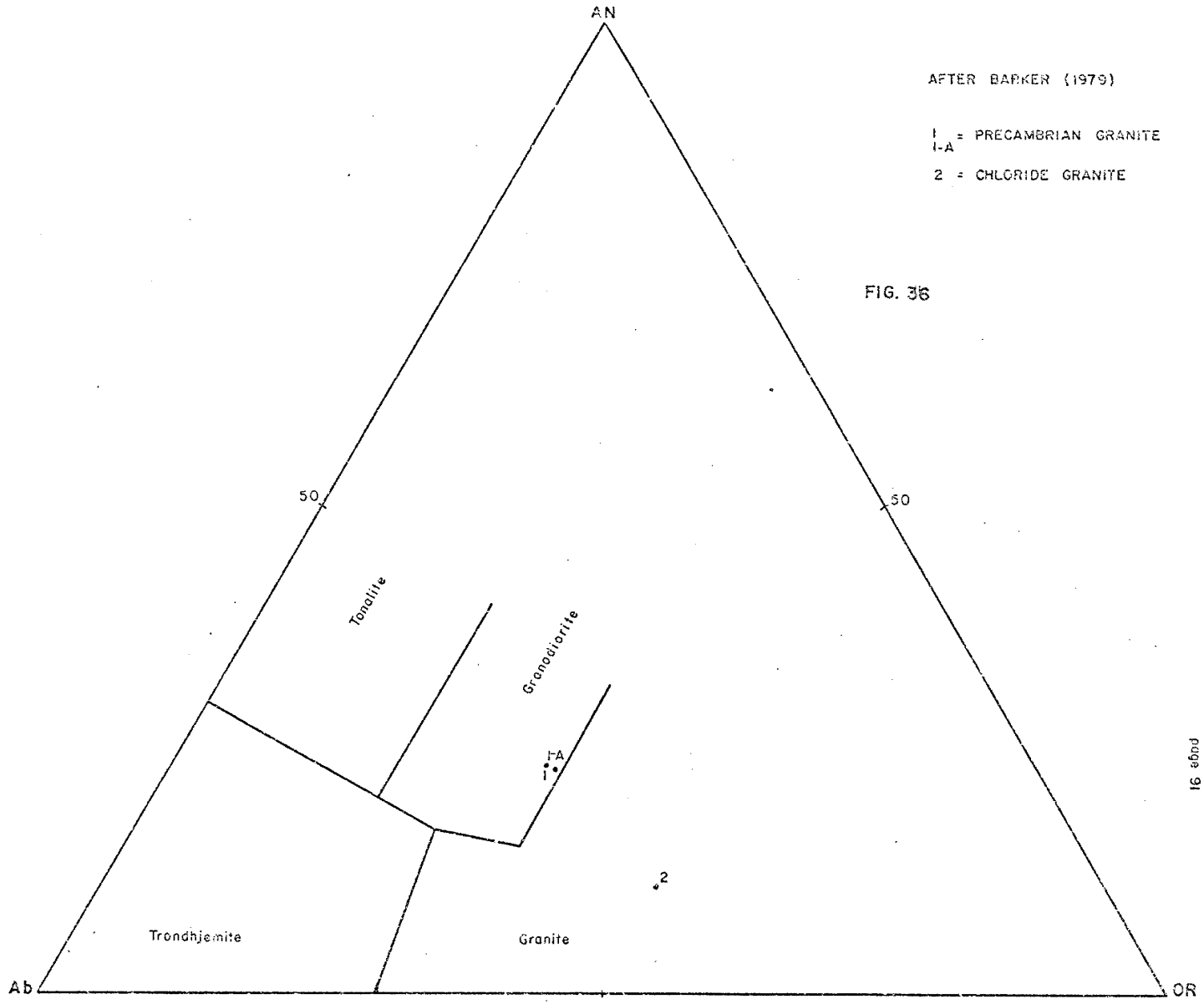

AFTER BARKER (1979)

I / I-A = PRECAMBRIAN GRANITE

2 = CHLORIDE GRANITE

FIG. 36

Figures 35 and 36, indicate that the Precambrian granite and the Chloride granite are chemically distinct. To further compare the granites, immobile elements of the samples were plotted relative to each other (Fig. 37). Ti, Co, and Mn are relatively immobile and SiO2 is slightly mobile (Davies, et.al, 1979). Figure 37 A and B indicate the Precambrian granite (1,1-a) is chemically different from the Chloride granite (2); however figure 37 C, is not quite as conclusive. Normative compositions for the two granites (see appendix V) show that the Chloride granite is richer in quartz and orthoclase as compared to the Precambrian granite. Therefore, despite figure 37 C, an overall comparison between the Precambrian granite and the Chloride granite, indicate the two are chemically distinct. In accordance with this chemical data the two granites have been mapped separately (see plate 1). It must be pointed out that this chemical separation does not totally preclude a genetic tie between the two stocks.

2=Chloride granite
1-a, 1=Precambrian granite

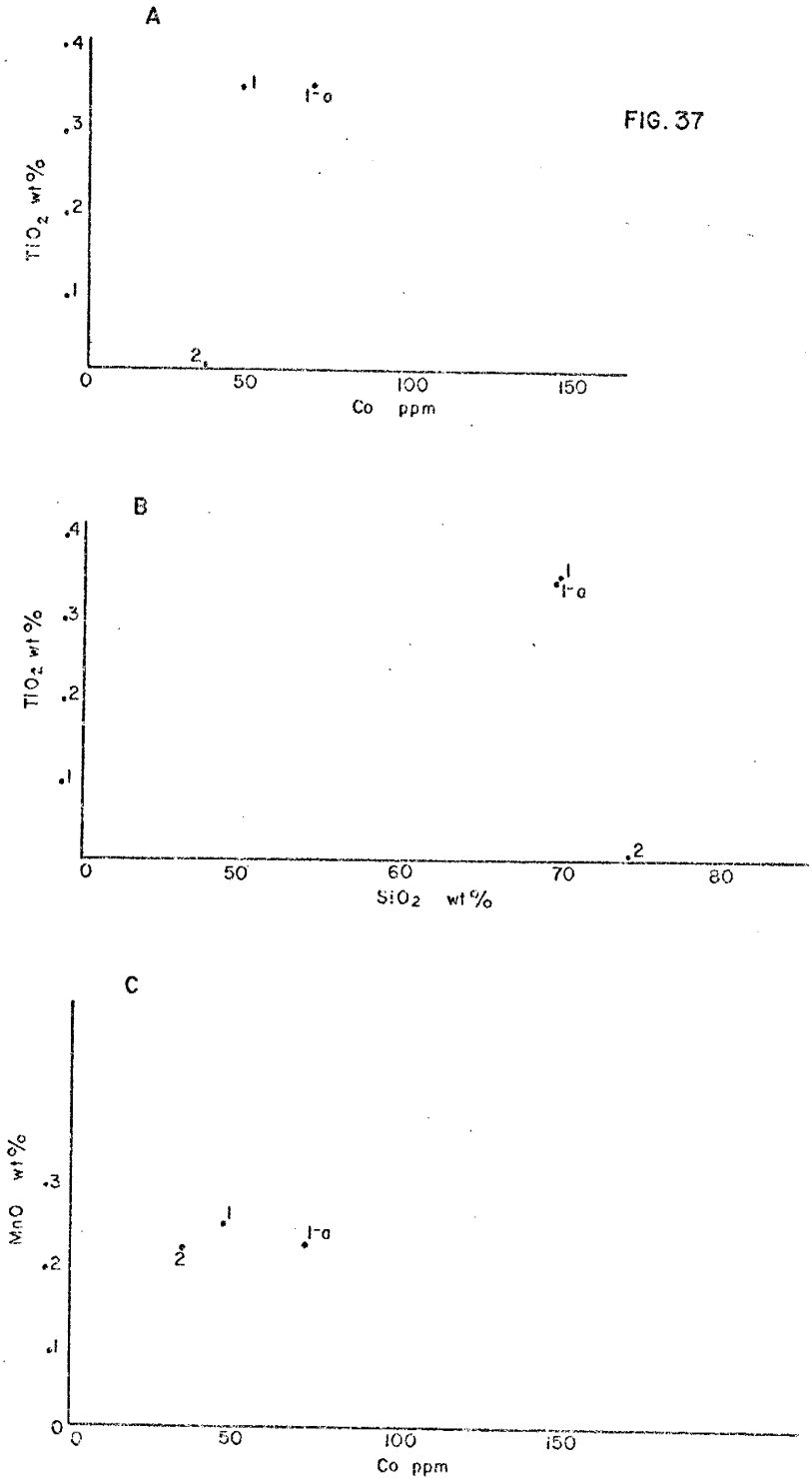

FIG. 37

ORE DEPOSITS

Beginning in the mid 1800's and continuing into the 1940's the most valuable ore deposits in the Wallapai district were the hydrothermal vein deposits. Near surface oxidation zones were mined for silver and gold and as mining continued below the oxidized levels production was chiefly from sulfide ores (Thomas, 1949b).

Two mines have large production records, they are: the Golconda mine in the Cerbat district (approx. 3 km south of Mineral Park), and the Tennessee-Schuylkill mine, located in the eastern portion of the current study area, (Chloride district). The Golconda mine and the Tennessee-Schuylkill mine are two of the deepest mines in the district, with shafts at 1600 and 1400 feet, respectively. In 1948, the total value (dollars) of production for the Wallapai district was $22,472,902 (Dings, 1951). Today the only active mine in the district is Mineral Park a porphyry copper-molybdenum deposit.

Regional distribution

Dings (1951) mapped the Wallapai district at a scale of 1:24,000 and traced numerous mineralized veins (see Dings, 1951). These veins occur as large swarms extending both northwest and southeast from the centrally located Mineral Park porphyry. The veins show a strike length that varies from less than 8 meters to greater than 2 km. The attitude of the veins ranges from N30° W to N60° W and they normally have steep dips to the east (Dings, 1951).

Chloride district distribution

The greatest concentration of veins in the Wallapai district are located within the study area, with more than 100 veins present (Thomas, 1949b). In this study two types of ore deposits have been delineated. First are the hydrothermal veins characterized by brecciation, open-space filling, quartz gangue, gold and silver minerals, and sulfide mineralization with depth. The most complete study of hydrothermal veins was done by Thomas (1949b). The second type is the alteration zones characterized by intense alteration, iron-staining, fractured outcrops, and trace amounts of precious metal

mineralization. For distribution of both types of veins in this study area see plate I.

The hydrothermal veins generally strike from north to northwest and have steep dips to the east, although west dips can be found. The alteration zones are more random compared to the hydrothermal veins and the alteration zones generally trend more east-west. Dips are very difficult to measure on the alteration zones, but available data is from steep to vertical. Numerous alteration zones can be found in section 35, north of the Badger mine.

Hydrothermal veins

Hydrothermal veins crop out as brecciated, iron-stained, quartz ridges, that are relatively easy to trace on the surface. Most outcrops show open-space filling with cockade structure and occasionally symmetrical banding (Fig. 38). Fine-grained quartz grades into coarse-grained, euhedral crystals of quartz in open spaces. This latter texture, is seen in thin section (Fig. 39) where the first quartz crystals to form along the side of a vein crystallized rapidly because of heat loss to wall rocks. In contrast the euhedral crystals in the center of cavities had more time

Figure 38 Hydrothermal vein showing open-space filling, cockade texture, iron-staining and brecciation. Location section 33, T24N, R18W, northwest extension of the Juno vein system.

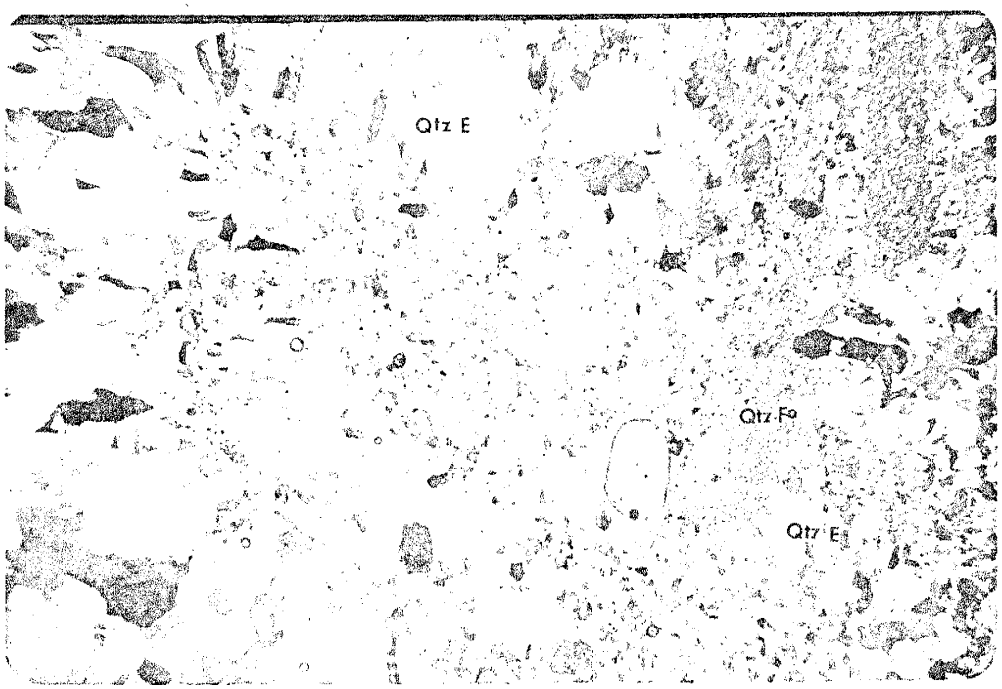

Figure 39 Photomicrograph of a hydrothermal vein. Euhedral quartz crystals (Qtz E) growing into open spaces. The open spaces have been filled with later fine-grained quartz (Qtz F). 1.0 mag., x-nicols sample # 45.

to develop (Park and MacDiarmid, 1975). In addition, the photomicrograph (Fig. 39) shows secondary solutions of quartz filling the veins post-crystallization of the euhedral quartz crystals. This indicates multiple periods of fluid injection to form the hydrothermal veins. No sulfide minerals or free gold were observed in thin section. Hydrothermal veins show striations in the wall rocks, gouge zones between the vein and the wall rock, and rolled and crushed fragments both in the veins and the gouge zones (Fig. 40). All of these characteristics indicate shear stress has occurred along the mineralized veins (Thomas, 1949b). Several hydrothermal veins bifurcate (as seen north of the Juno mine) and/or have small splits branching from the main body.

The hydrothermal veins are oxidized in their upper portions, which can extend to depths of 350 feet, but generally the limit of strong oxidation is the 100 foot level (Thomas, 1949b). Most veins are less than 1 meter wide but some are greater than 10 meters, with the average vein being 1 to 2 meters (Dings, 1951). Mining is difficult because of the pinch and swell nature of the veins which occurs along strike and dip (Dings, 1951).

Figure 40 Gouge zone (rock hammer) between a hydrothermal vein (right side) and wall rock (left side). Location section 35, T24N, R18W.

mineralogy -- The principal gangue minerals of the hydrothermal veins are: quartz (most abundant), calcite (present) and siderite (minor), (Thomas, 1949b). The primary sulfides found are: pyrite, sphalerite, galena, arsenopyrite, chalcopyrite; all very common. The most abundant silver mineral is proustite (Ag_3AsS_3) (Thomas, 1949b). Native gold is found in minor amounts in all veins (Dings, 1951, Thomas, 1959b., Haury, 1947). Bastin (1925) also observed other silver sulfides such as: argentite and pearceite.

Thomas (1959b.) listed a host of seconday minerals found in the oxidized part of the hydrothermal veins, with goethite-limonite as the most abundant species. The oxidation effects are of major economic importance in the veins. In contrast secondary enrichment is of minor economic importance in the veins.

Geochemistry -- Drake (1972) did a complete study of the ore forming fluids of Mineral Park porphyry and several of the hydrothermal veins throughout the Wallapai district, and concluded that genesis of the veins is hydrothermal.

Drake (1972), analyzed 5 specimens from selected mines within the current study area, and a total of 31 specimens from selected mines throughout the Wallapai

district. Fluid inclusion data from quartz for the 5 mines in the current study area are listed in table 5. The Aurora mine is not labeled on the map; it is located approximately 300 meters directly south of the New Tennessee mine. The Clyde mine is located southeast of the New Deal mine in an arroyo on the east edge of the map (the name is not shown).

The 31 samples analyzed over the district, by Drake (1972) gave homogenization temperatures ranging from a low of 160°C to a high of 390°C . The high temperature was estimated since the upper limit of the heating stage was 360° C. All inclusions homogenize at liquid phase and at 25° C all have two phases, liquid and gas (Drake, 1972). The majority of the inclusions homogenize at 275° C to 325° C, and freezing temperatures for 15 samples range from -0.6° to -2.8°C (Drake 1972). Minimum vapor pressures calculated from homogenization temperatures and salinities gave values of 400 to 500 bars (Drake, 1972). In conclusion Drake (1972) felt that there was a subtle trend toward higher temperatures closer to Mineral Park (5 miles south of the Chloride district) for the hydrothermal veins. The thermal difference was not clear enough to draw thermal isotherms; however, Drake (1972) believed the thermal center for all hydrothermal veins is Mineral Park porphyry, and that a genetic relationship exists between Mineral Park and the hydrothermal veins.

Table 5 - Fluid inclusion data from several localities within the Chloride district; from Drake, 1972.

Sample #	Location	Phase	# of inclusions observed	Homog. T°	Phase in which Homog. occurs
V110	Bullion Mine	2	2	160-168°C	Liq.
V115	Dardaneles Mine	2	5	288-290°C	Liq.
V117	Argyle	2	4	250-253°C	Liq.
V122	Aurora	2	8	240-260°C	Liq.
V112	Clyde	2	7	289-300	Liq.

Paragenesis -- Figure 41 is the paragenesis of hypogene minerals from Thomas (1949b). Despite the difficulty of relating mineralization to period of deposition, Thomas (1949b) concluded that quartz was deposited intermittently throughout the period of mineralization, pyrite and arsenopyrite preceded sphalerite and galena, and the majority of the latter two minerals preceded the latest minerals.

As stated earlier secondary enrichment has not been an important factor in the economic potential of the hydrothermal veins (Thomas, 1949b). Zinc was removed in the oxide zone but was not reprecipitated at depth and lead was oxidized but not transported from the original site of deposition (Thomas, 1949b). The same appears to have occurred with the primary silver minerals (Thomas, 1953b).

Alteration -- Wall rock alteration extends only a few meters from the hydrothermal veins. Thomas (1953b.) noticed three types of alteration, they are: " 1) propylitic, characterized by chlorite, pyrite, epidote, sericite, calcite and clay minerals 2) silicification with associated muscovite, 3) intense sericitization with abundant clay minerals and sphene ".

PARAGENESIS OF HYPOGENE MINERALS

(Vertical lines represent periods of fracturing)

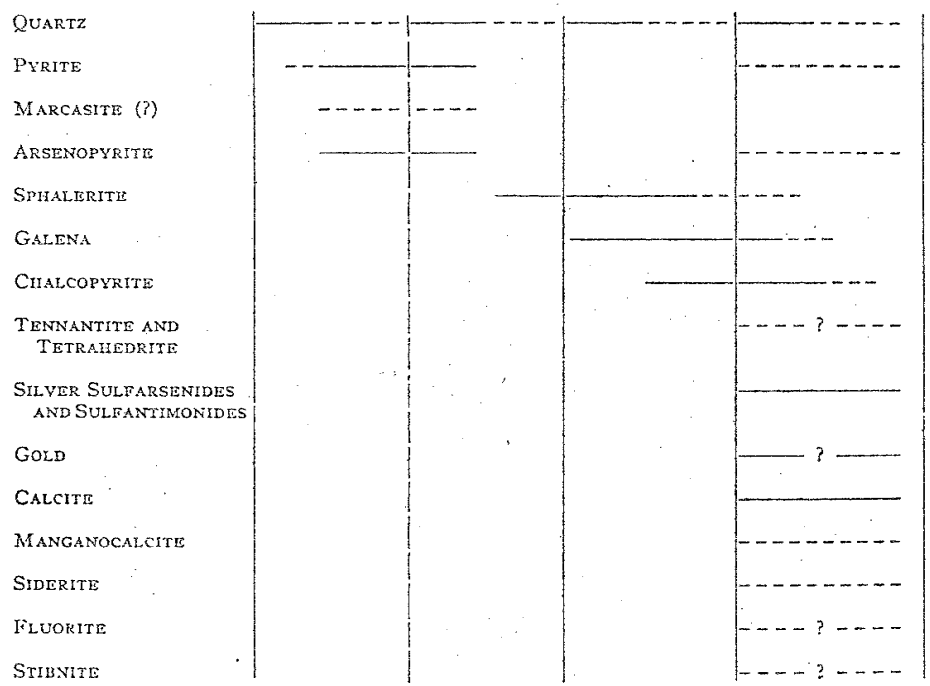

FIG. 41 Paragenesis of vein deposits. Horizontal spacing indicates relative positions of minerals, not time units. Dashed lines indicate minor significance.

from Thomas 1949b

Age -- The De La Fontaine mine, a hydrothermal vein located in the southern portion of the Cerbat Mountains, has a Pb206/Pb207 model age of 195 m.y. (Mauger, Damon and Giletti, 1965). Drake (1972) observed "hydrothermal veins" crosscutting all other generations or mineralization in Mineral Park porphyry. This implies an age of hydrothermal vein mineralization younger than 72 m.y. Drake (1972) also reported that rhyolite dikes which are younger than Ithaca Peak porphyry are themselves cut by hydrothermal type veins. In conclusion the age at which mineralization began cannot be determined but the final stages did continue post consolidation of Mineral Park and could have possibly continued into late Tertiary time as Thomas (1949b) believed. In contrast the initial fracture pattern which the hydrothermal veins follow may have begun as early as Precambrian time.

Alteration zones

Alteration zones crop out as silicified, iron-stained bodies. Open-space filling is minimal if at all present (Fig. 42) and no brecciation was observed. Several alteration zones have higher relief than the surrounding country rock because of silicification. The

Figure 42 Alteration zone, showing minor open-space filling. Intense iron staining along fractures. Location section 35, T24N, R18W.

alteration zones have linear outcrop expressions and previously have been mapped as "hydrothermal veins". Despite the fact they are probably hydrothermal in origin, they are distinct from the hydrothermal veins, by the lack of open-space filling and brecciation. Therefore, in this study they have been mapped as separate zones of mineralization.

Several alteration zones are associated with the metarhyolite unit and they appear to have formed by injection of fluids along the dike. In contrast, alteration zones can be found in section 35 with no apparent lithologic controls. The average trend of the alteration zones ranges from east-west to northwest. Iron oxide staining outlines the intense fracturing seen in outcrop, giving it a pseudo-stockwork appearance. Precious metals occur in trace amounts in the alteration zones.

In thin section, sericite, chlorite and hematite staining are abundant (see appendix I, sample numbers 46,47 and 48). In all thin sections observed the host rock is granitic, belonging to the undifferentiated complex. Therefore the mineralogy is similar to that described for the undifferentiated complex, except for the anomalous amount of alteration minerals. Black opaque minerals (not identified) are present in thin

section along with analcite (?). The latter mineral possibly developed by metasomatic effects in response to the formation of alteration zones (Kerr, 1959). Fluid inclusion work or other geochemical analysis has not been performed on the alteration zones.

METAMORPHISM

The Precambrian rocks of the Chloride district have undergone a major period of dynamothermal metamorphism. After deposition of the supracrustal units (i.e. the present amphibolite, quartzite, biotite gneiss), the rocks were buried and underwent dynamothermal metamorphism in response to orogenic disturbance. This active period during the Precambrian formed regional and small scale folds and a suite of metamorphosed rocks. Toward the end of the orogeny, after folding, the area was intruded by several phases of igneous rocks. Continued stress occurred after the igneous activity, resulted in cataclastic texture in the rocks and some retrograde mineral assemblages.

Metamorphic effects are either a high temperature phase of medium-grade (amphibolite facies) or high-grade (granulite facies), depending on pressure, (Fig. 43), (Winkler, 1976). The ACF values for the amphibolite samples are listed in appendix VII. The initial oxide compositions for the amphibolites are corrected for accessories (magnetite 2-8%, biotite 2-6%), stoichiometrically, as outlined by Winkler (1976, p.37-40). Corrected oxide percentages were then converted

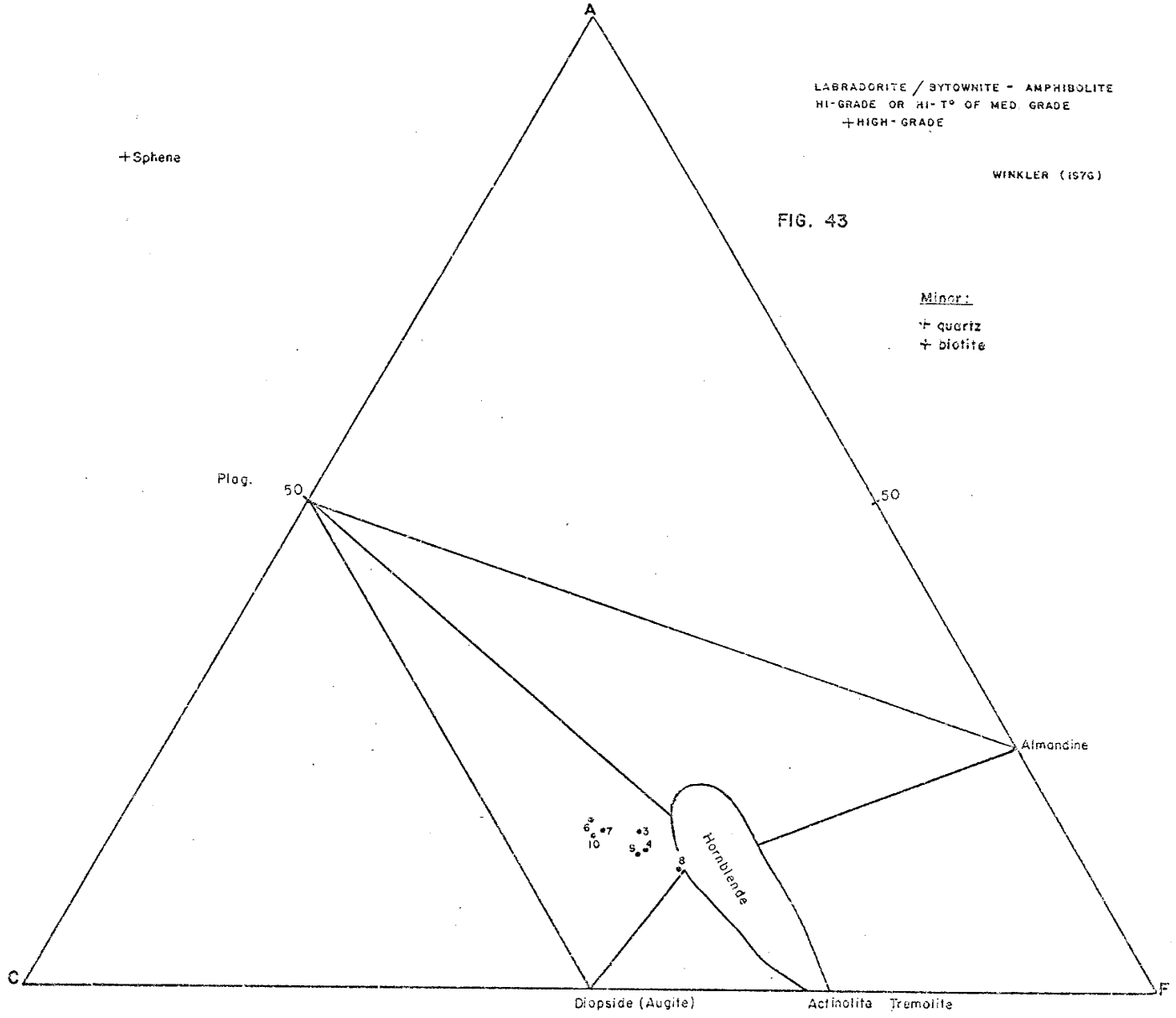

LABRADORITE / BYTOWNITE - AMPHIBOLITE
HI-GRADE OR HI-T° OF MED. GRADE
+HIGH-GRADE

WINKLER (1976)

+Sphene

FIG. 43

Minor:

+ quartz
+ biotite

to molecular proportions and plotted on the ACF diagram. All amphibolite samples fall within the subtriangle diopside-hornblende-plagioclase, which agrees fairly closely with observed mineralogy in thin section; however the plagioclase composition is more sodic than expected (An35).

Winkler (1976, p.166) and Miyashiro (1973, p.211) have stated that An content in plagioclase increases with increasing temperature of metamorphism; however both agree that this is not universally true. Therefore the more Na-rich plagioclase observed in thin section is not rare. In conclusion, the close agreement between predicted and observed assemblages for the amphibolite suggest that equilibrium was attained in this district during dynamothermal metamorphism.

In contrast Condie and Budding (1978, p.35), proposed a facies series which implies a geothermal gradient of about 40° C per Km depth, which is in accordance with Precambrian time. Using their plot (Fig. 44) the amphibolite samples fall within the greenschist facies and therefore the observed mineral assemblage does not agree with the predicted assemblage. This implies that equilibrium was not attained during dynamothermal metamorphism of this district and retrograde metamorphism has occurred in response to falling temperature.

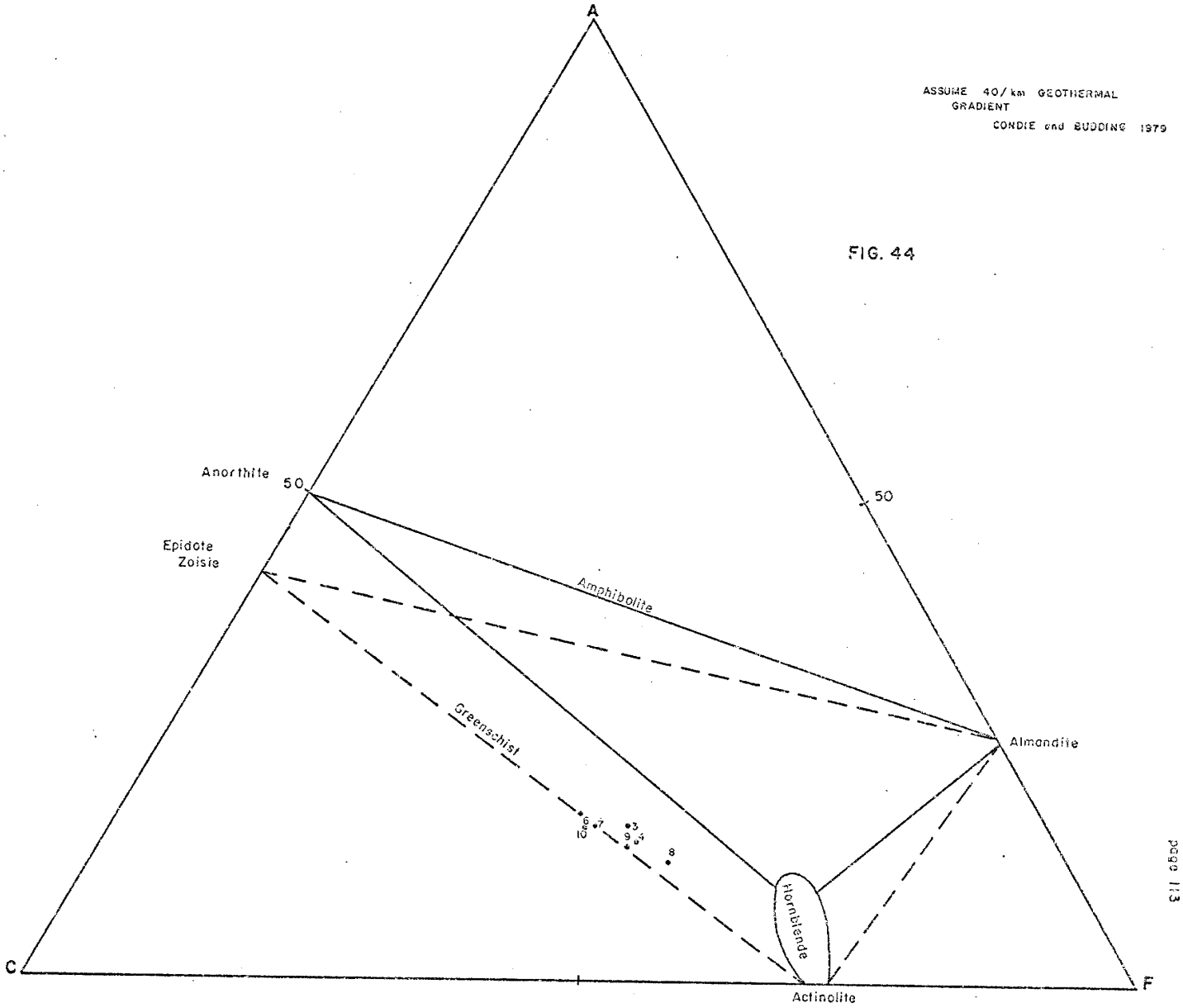
A
ASSUME 40/km GEOTHERMAL GRADIENT
CONDIE and BUDDING 1979
FIG. 44
Anorthite
50
50
Epidote
Zoisie
Amphibolite
Greenschist
Almandite
Hornblende
C
F
Actinolite

The primary mineral assemblages present in the metamorphosed units are: amphibolite unit-hornblende, biotite, plagioclase (An35); biotite gneiss unit-hornblende, plagioclase, K-feldspar, almandine, quartz, chlorite; quartzite unit-quartz, muscovite.

The lack of muscovite when quartz and plagioclase are present is used to define the change from medium to high-grade metamorphism (Winkler, 1976, p.82). The only unit which shows muscovite is the quartzite unit; however Winkler, (1976, p.83), states that quartz and muscovite can persist to very high temperatures in quartzite so long as plagioclase is absent. Therefore despite the presence of muscovite in quartzite, the suggested mineral assemblages indicate temperatures from 500° C to 600° C, reaching the high-grade metamorphic facies. The temperature could exceed these values as suggested by the migmatitic appearance of the undifferentiated complex (anatexis); however lack of diagnostic minerals precludes such a conclusion.

The regional folding and pervasive foliation in the area imply a certain degree of hydrostatic pressure. The range of the pressure could vary from a low of 2 Kb to a high of 10 Kb. The observed mineral assemblage would not change under this wide range of pressure since the minerals are more temperature dependent than pressure

dependent. The original host rocks were too low in Al content to develop any pressure sensitive minerals, such as: kyanite, sillimanite, and andalusite. Thomas (1949a) did record some sillimanite in the biotite gneiss unit, but none was observed in this study to help define pressure ranges.

The deformation accompanying the dynamothermal metamorphism was fairly intense as suggested by the lack of definite relict primary textures, the pervasive foliation, cataclastic textures and the regional and ptygmatic folding.

Evidence for contact metamorphism accompanying intrusion of the Chloride granite and Precambrian granite is lacking in both thin section and outcrop. This is not uncommon since contact metamorphic aureoles around granitic intrusions need not develop in medium-grade metamorphic terrains. For example, most granitic bodies intrude at 700°C and if they solidify at a depth of 5 to 6 Km the country rock will be heated to approximately 550° C (Winkler, 1976). This temperature of 550°C corresponds to medium-grade metamorphism and if the country rock had a mineral assemblage already in equilibrium with this regime, the intrusion would not cause contact metamorphism. In addition the lack of pegmatitic dikes in the Chloride and Precambrian granites indicates a

paucity of volatile constituents, which would hinder metamorphic reactions and limit the development of contact metamorphic aureoles (Beers, 1976).

The final process of dynamothermal metamorphism is cataclasis. This event is post intrusive, since thin sections of both the Precambrian and Chloride granite display cataclastic textures such as: mortar textures, bent lamellae strain fractures and exsolution of feldspar (Spry, 1976) (see appendix I).

As stated by Winkler (1976) and Miyashiro (1973) cataclastic metamorphism has little or no heat associated with it and this limits recrystallization. However, secondary retrograde metamorphism is common with cataclastic metamorphism, since fluids can easily enter the rock through fracture systems (Winkler, 1976).

The most extensive retrograde metamorphism has occurred in the metarhyolite unit with chlorite after biotite and sericite after potassium feldspar. The metarhyolite also displays excellent pressure shadows and fractured relict phenocrysts, both attesting to cataclastic metamorphism. Similarly, the biotite gneiss unit has fractured garnets, and a weak mortar texture juxtaposed to hornblende retrograding to chlorite (see appendix I sample numbers 29 and 30). The garnetiferous alaskite also has garnets retrograding to chlorite set in a cataclastic matrix.

The majority of the greenschist minerals seen in thin section (excluding hydrothermal products such as sericite), are apparently a product of retrograde metamorphism in direct response to cataclastic (dynamic) metamorphism. However, some of the greenschist minerals could be in response to falling temperature as suggested by figure 44 after Condie and Budding (1978).

DISCUSSION

Geologic history

The geologic history of the Chloride district and Cerbat Mountains is long and complex. The oldest units exposed are older than 1.35 b.y. and the youngest are olivine basalts of Recent age (Thomas, 1949a). The geologic history is outlined below:

1) The oldest observable event in the district is deposition of supracrustal rocks (i.e. sediments and mafic igneous rocks (?)). The depositional environment may have been troughs on a Precambrian craton (Stewart, 1976). The thickness of the supracrustal section is hard to determine due to intense folding and intrusive activity.

2) After deposition of the supracrustal rocks orogenic events were imposed on the district, possibly associated with the Hudsonian orogeny (1.6 b.y. to 1.8 b.y.) and the Elsonian orogeny (1.5 b.y. to 1.3 b.y.) (Windley, 1978). The sedimentary and mafic igneous units (?), were intensely folded through two major periods (F1, F2) and underwent dynamothermal metamorphism to the

high-temperature part of the medium grade facies (500°C to 600° C) (amphibolite facies). A third period of folding was imposed on the area (F3), reflecting a different stress field. This last period of folding (F3) is believed to be Precambrian in age but the exact age is not known. Temperatures of metamorphism may have exceeded the limits set for the medium-grade facies (amphibolite facies), allowing anatexis to occur, and thus forming local pegmatites and migmatites.

3) Toward the end of the orogeny, after the folding episode (F1, F2, F3(?)), igneous intrusions were widespread in the district. Contact metamorphic aureoles near the intrusive activity were not formed. The igneous activity produced the Chloride granite and the Precambrian granite. A genetic tie between these two intrusions cannot be demonstrated from field observations, geochemical analysis or thin section data.

Dynamothermal metamorphism continued after crystallization of the intrusions, since both complexes have a metamorphic fabric that passes into the host rocks.

4) After the intrusive activity, a rhyolite dike which crosscuts the Chloride granite was injected along the axial plane cleavage of the last period of folding (F3). Dynamothermal metamorphism was active at this

time, producing a foliation in the rhyolite unit (metarhyolite), but not totally destroying all primary textures. During the multiple orogenic events in the Precambrian cataclastic textures were also developed in the units, possibly caused by regional folding and shear stress. The metarhyolite unit represents the last evidence of Precambrian activity.

5) A long hiatus exists in the geologic record, since no Paleozoic units are exposed in the district. Thomas (1949a) recorded Paleozoic units near the Cerbats, suggesting that they once may have covered the entire district.

6) Beginning possibly in the Sevier-Columbian orogeny (80-130 m.y.) and continuing through the Laramide orogeny (40-80 m.y.) (Windley, 1978), the district had orogenic disturbance. Renewed stress related to the orogenies reactivated fractures parallel to axial plane cleavages and also formed new faults (i.e. Sacramento fault). The fractures were initially developed during the three periods of Precambrian folding (F1, F2, F3). Extrusive volcanism (pyroclastic and lava flows) of Tertiary age in and around the Cerbat Mountains attest to regional stress needed to reactivate the fractures. These fractures made the area more permeable which allowed increased fluid circulation that resulted in retrograde metamorphism of some units

Ithaca peak granite intruded the Cerbat Mountains around 72 m.y. (Mauger and Damon, 1965) ago, along with diabase, mafic and pegmatitic dikes. Some if not all of the dikes may be related to the Ithaca Peak granite. Concomitant with this intrusion, multiple injections of metal-bearing hydrothermal fluids occurred along the reactivated fractures. The fluids may be genetically related to the Ithaca Peak granite, although other deep seated magma sources are possible. The hydrothermal activity continued post-crystallization of the Ithaca Peak granite and may have persisted into Tertiary time (Thomas, 1949a).

7) During the final period of the Laramide orogeny and into the Recent, the Cerbat Mountains have been continuously uplifted. As a result, large quantities of erosional debris have been and are now being shed off of the uplifted block into the valley floor. The last geologic event in Recent time is extrusion of olivine basalts which overlie and interfinger with alluvium. (Thomas, 1949a).

precursor of Precambrian rocks

The units exposed in the field area have undergone intense dynamothermal metamorphism in response to multiple orogenic events. In addition, igneous activity nas also been imposed on the district. These events have recrystallized the units and destroyed most primary textures making it difficult to assess the original rock type. Nonetheless, field observations, petrographic studies and limited geochemical data allow interpretation of original rock types.

The quartzite unit has relict bedding (Fig. 8) which indicates a sedimentary origin, probably a quartz sandstone (Spry, 1976). The small amount of muscovite found in the quartzite may represent sparse remnants of feldspars or clay minerals from the original quartz sandstone. Cross-bedding and gradational bedding are absent in the quartzite but planar bedding is outlined by magnetite crystals, which may have originally been deposited as hematite grains.

In outcrop the biotite gneiss shows fine continuous laminations of felsic material alternating with mafic layers. The laminations are also seen in thin section which possibly suggests that the biotite gneiss may have a sedimentary precursor. If the original rock type is

sedimentary, it could either have been a pelitic sediment or a graywacke, since metamorphism of either could produce a quartzo-feldspathic gneiss similar to the biotite gneiss. In contrast the alternating laminations seen in the biotite gneiss could be the product of either, metamorphic differentiation, differential melting or introduction of hydrothermal fluids concordant with foliation. These multiple explanations for the formation of the biotite gneiss, make it relatively impossible to define an unique precursor for the unit.

The granite gneiss has igneous textures (i.e. porphyroblasts) both microscopically and megascopically and displays igneous contacts with the older amphibolite unit (Fig. 2). On the other hand certain parts of the granite gneiss are highly foliated, gneissic and lack any igneous characteristics. However, since a large majority of the granite gneiss unit appears granitic, the precursor to this unit is interpreted to be intrusive. Partial assimilation of country rock during intrusive activity developed the migmatitic appearance of granite gneiss.

The quartzo-feldspathic veins seen in the granite gneiss unit can be either a product of "sweating-out" due to dynamothermal metamorphism or they may represent hydrothermal fluids injected during igneous activity. It is hypothesized that both types occur in the granite gneiss unit.

The amphibolite unit is a high-Mg tholeiite (Fig. 32), composed of hornblende, plagioclase and various proportions of pyroxene in a granoblastic matrix. Relict textures in the amphibolite are lacking, making it difficult to define a parent rock type.

Chemically the amphibolite in this study is similar to the chemistry of ortho-amphibolites in the literature (see Herze and Banerjee, 1973), with high contents of Ti, Ni and low Niggli k (k=K/Na+K) values (see appendix V). However, the amphibolites have higher contents of CaO (12 to 14%) compared to average ortho-amphibolites (basalts). This higher CaO content could be the product of Ca being introduced during dynamothermal metamorphism and/or nydrothermal activity, since CaO is a highly mobile element (Davies, et al. 1979).

Miyashiro (1973), states that amphibolites can be derived from impure limestones as well as mafic igneous rocks with the latter the most common precursor. Since amphibolites are more commonly derived from igneous rocks and amphibolites in the study area are similar in chemistry to ortho-amphibolites, (except for the CaO content) the amphibolites of the study area are interpreted as ortho-amphibolites. In support of this interpretation, no calcite or wollastonite was observed in thin section, to suggest a para-amphibolite. In

addition, the absence of calcite and wollastonite indicates that calcium must be tied up in hornblende, pyroxene and plagioclase.

To determine if the original mafic igneous rock for the amphibolite was either extrusive or sill-like cannot be determined from existing data. Thomas (1949a) correlated the amphibolite of the Chloride district with pillowed amphibolites of the Grand Canyon series, suggesting the former had an extrusive basalt parent. This correlation by Thomas (1949a) is very speculative and unsupported.

The outcrop pattern of the Chloride granite and its felsic border facies (i.e. garnetiferous alaskite) suggests it originated as an igneous intrusion. The western border of the Chloride granite, where the majority of the garnetiferous alaskite is exposed, shows definite igneous contacts with the biotite gneiss. The intrusive is believed to be sill- like and was intruded into the core of the Precambrian fold (F1).

The Precambrian granite is porphyroblastic and has a weak foliation both in thin section and in outcrop expression. Therefore the origin of this unit is interpreted to be an intrusive igneous body. The gradational contact of the Precambrian granite with the country rock (i.e. undifferentiated complex) can be explained because both have similar lithologies.

The metarhyolite has well defined relict phenocrysts, crops out like a dike, and appears to have intruded along an old fracture line developed during F3. The relict phenocrysts and the dike- like structure suggest an igneous precursor for the metarhyolite.

Contacts of the metarhyolite with the Chloride granite are sharp, but there is a gradation within the dike from an aphanitic core to a medium- grained border facies. The aphanitic core as well as the medium grained facies have relict phenocrysts. This reversed cooling sequence seen in the metarhyolite cannot be explained with present field data and petrographic studies.

Controls on mineralization

The amphibolite unit has been shown to outline three generations of Precambrian folding (F1, F2, F3) in the study area (see pages 64-76). This interpretation was derived from structural data taken in the field and by showing that the amphibolite is geochemically similar and thus one continuous unit. The geochemical method used in the structural interpretation indicates a potential tool to unravel structurally complex areas, so long as a marker horizon can be delineated.

If the structural interpretation is correct (i.e. three periods of folding, F1, F2, F3), complex patterns of fractures parallel to the axial planes would be imposed on the area during folding. The strongest set of fractures trend northwest in direct response to the isoclinal folds of F1 and F2. Another set of weaker fractures trend northeast related to the gentle fold F3. In the hinge zones of the folds, complex patterns of fractures are present. Fractures would be minimal in the Chloride granite and the Precambrian granite since they were intruded post F1 and F2.

From field mapping, hydrothermal veins and alteration zones correspond roughly to the fracture lines developed during the folding of F1, F2 and F3. (see plate 1). Therefore it is suggested that the Precambrian folding episode initially prepared the ground, then later stress associated with orogenies reactivated the fractures allowing metal-bearing hydrothermal fluids to be injected along them.

REFERENCES

Barker, F., 1979, Trondhjemite: definition, environment, and hypothesis of origin, Chapt. 1, Trondhjemite, dacite and refolded rocks, Elsevier Science Pub., p. 1-12.

Bastin, E.S., 1925, Origin of certain rich silver ore near Chloride and Kingman, Arizona: United States Geological Survey Bull. 750, p. 17-39.

Bateman, P.C., Clark, L.D., Huber, N.K., Moore, J.G., and Rinehart, C.D., 1963, The Sierra Nevada batholith a synthesis of recent work across the central part: United States Geological Survey, Prof. Paper 414-D, 46 p.

Beers, C.A., 1976, Geology of the Precambrian rocks of the southern Los Pinos Mountains, Socorro County, New Mexico: M.S. thesis, New Mexico Institute of Mining and Technology, 238 p.

Billings, M.P., 1972, Structural geology: Prentice-Hall Englewood Cliffs, New Jersey, 3rd ed., 606 p.

Boone, G.P., 1967, Visitor's information pamphlet: Duval Corporation, Mineral Park porphyry, Mining Dept., Company report, 11 p.

Condie, K.C., and Budding, A.J., 1979, Geology and geochemistry of Precambrian rocks, central and south-central New Mexico: New Mexico Bureau of Mines and Mineral Resource, Mem. 35, 58 p.

Damon, P.E., and Giletti, B.J., 1961, The age of the basement rocks of the Colorado Plateau and adjacent areas: New York Acad. Sci. Annals, v. 91, art. 2, p. 443-453.

Damon, P.E., Giletti, B.J., and Mauger, R.L., 1965, Isotopic dates of Arizona ore deposits: A.I.M.E., Trans., v. 232, p. 81-87.

Davies, J.F., Grant, R.W.E, and Whitehead, R.E.S., 1979, Immobile trace elements and Archean volcanic

stratigraphy in the Timmins mining area, Ontario: Canadian Jour. of Earth Sci., v. 16, p. 305-311.

Dings, M., 1951, The Wallapai Mining district Cerbat Mountains Mohave County, Arizona: United States Geological Survey Bull. 978-E, p. 123-163.

Drake, W., 1972, A study of the ore forming fluids at Mineral Park porphyry copper deposit, Kingman, Arizona: Ph.D thesis, Columbia University, 226 p.

Haury, P.S., 1947, Examination of zinc-lead mines in the Wallapai mining district, Mohave County, Arizona: United States Dept. of Interior, Bureau of Mines, RI 4101, 43 p.

Hernon, R.M., 1938, Cerbat Mountains: Arizona Bureau of Mines, Bull. 145, Geol. Series, No. 12, p. 110-117.

Herz, N., and Banerjee, S., 1973, Amphibolites of the Lafaiete, Minas Gerais, and the Serra Do Navio manganese deposits, Brazil: Econ. Geol., v. 68, p. 1289-1296.

Hobbs, B.E., Winthrop, D.M., and Williams, P.F., 1976, An outline of structural geology: John Wiley and Sons, Inc. 571 p.

Irvine, T.N., and Baragar, W.R.A., 1971, A guide to the chemical classification of the common volcanic rocks: Canadian Jour. of Earth Sci., v. 8, p. 523-548.

Jensen, L.S., 1976, A new cation plot for classifying subalkalic volcanic rocks: Ministry of Natural Resources, Ontario Division of Mines, Misc. paper 66, 42 p.

Kerr, P.F., 1959, Optical mineralogy: McGraw-Hill Book Co., 3rd ed., 442 p.

Lee, W.T., 1908, Geologic reconnaissance of a part of western Arizona: United States Geological Survey Bull. 352, 96 p.

Mauger, R.L., and Damon, P.E., 1965, K-Ar ages of Laramide magmatism and copper mineralization in the southwest: Atomic Energy Comm. Annual Progress Report No. C00-689-50, p. A-II-1-A-II-8.

Miyashiro, A., 1973, Metamorphism and metamorphic belts: George Allen and Unwin LTD, 2nd ed. 492 p.

Park, C.F., and MacDiarmid, R.A., 1975, Ore deposits: W.H. Freeman and Company, 3rd ed., 530 p.

Schrader, F.C., 1909, Mineral deposits of the Cerbat Range, Black Mountains and Grand Wash Cliffs: United States Geological Survey Bull. 397, 226 p.

Spry, A., 1976, Metamorphic textures: Pergamon Press, 3rd ed., 350 p.

Stewart, J.H., 1976, Late Precambrian evolution of north America: plate tectonics implication: Geology 4, p. 11-15.

Thomas, B.E., 1949a, Geology of the Chloride quadrangle, Arizona: Ph.D thesis, California Institute of Technology, 162 p.

---------- 1949b, Ore deposits of the Wallapai district: Econ. Geol. v.44, No. 8, p. 663-705.

---------- 1953, Geology of the Chloride quadrangle Arizona: Bull. of the Geological Society of America, v. 64, p. 390-420.

Windley, B.F., 1978, The evolving continents: John Wiley and Sons, 385 p.

Winkler, H.G.F., 1976, Petrogenesis of metamorphic rocks: New York, Springer-Verlag, 320 p.

Appendix I
Petrographic Descriptions

Petrographic Description

DATE:

Sample #: 1

Essential Minerals	%
Quartz	30
Plagioclase	25
Orthoclase	30

Varietal Minerals	%
Microcline	5
Biotite	7

Accessory Minerals	%
Zircon	tr
Garnet	tr

Secondary or Alteration products	%
Sericite	3
Magnetite	tr
Biotite	

Plagioclase composition (Michel-Levy)

An 27 Oligioclase

Metamorphic grade

Amphibolite

Textures

Petrotexture is weakly cataclastic with porphyroblasts of feldspar in a medium-grained matrix (<2mm) of quartz and feldspar. Strain fractures, sutured grain boundaries exsolution textures are common.

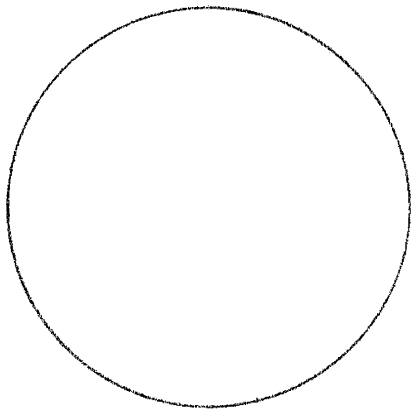

Mineralization

Rock Classification Cataclastic Granite

Possible Parentage Granite

Discussion Mapped as pEg in southeast portion of the field area. Similar to the chloride granite, stained section.

Petrographic Description

DATE:

Sample #: 2

Essential Minerals	%
Orthoclase	35
Plagioclase	25
Quartz	35

Varietal Minerals	%
Biotite	3

Accessory Minerals	%
Zircon	tr
Muscovite	tr

Secondary or Alteration products	%
Sericite	2
Magnetite	tr

Plagioclase composition (Michel-Levy)

An 26 Oligioclase

Metamorphic grade

Amphibolite

Textures

Petrotexture is mortar with large grains of feldspar in a fine-grained cataclastic matrix of quartz and feldspar. Exsolution textures are common.

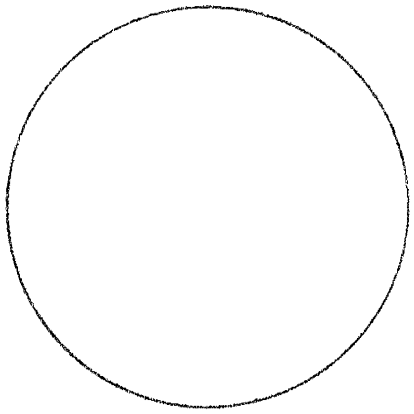

Mineralization

Rock Classification Cataclastic granite

Possible Parentage Granite

Discussion Some quartz grains are strained with small 2V figures

Petrographic Description

DATE: 3-26-80

Sample #: 3

Essential Minerals	%
Hornblende	26
Pryoxene (Augite?)	30
Plagioclase	32

Secondary or Alteration products	%
Sericite	3
Magnetite	5
Hornblende	

Varietal Minerals	%
Biotite	4

Plagioclase composition (Michel-Levy)

Andesine An 32

Metamorphic grade

Amphibolite

Accessory Minerals	%
Zircon	tr
Apatite	tr
Quartz	?

Textures

Petrographic texture is granoblastic to decussate.

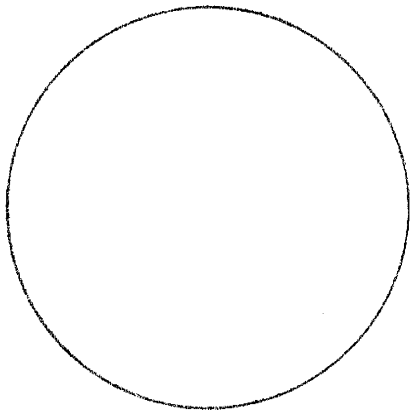

Mineralization

Rock Classification Amphibolite

Possible Parentage Basalt flow or mafic sill

Discussion Geochemically the amphibolite is a high-Mg tholeiite. Hornblende and magnetite have formed at the expense of pyroxene. Some plagioclase is untwinned. Hornblende pleochroic brown to green.

Petrographic Description

DATE:

Sample #: 4

Essential Minerals	%
Hornblende	44
Plagioclase	28
Pyroxene (Augite?)	20

Secondary or Alteration products	%
Magnetite	4
Sericite	1
Hornblende	

Varietal Minerals	%
Biotite	3

Plagioclase composition (Michel-Levy)

Andesine An 34

Metamorphic grade

Amphibolite

Accessory Minerals	%
Zircon	tr

Textures

Petrographic texture is granoblastic to decussate

Veins of pyroxene - altering to hornblende a few mm wide

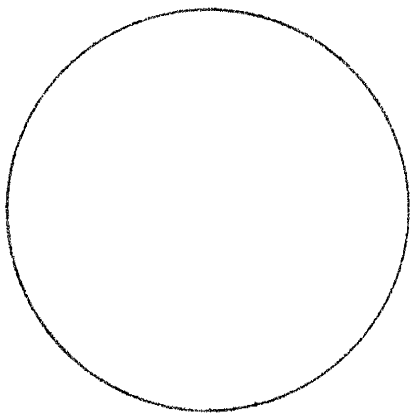

Mineralization

Rock Classification Amphibolite

Possible Parentage Basalt flow or mafic sill

Discussion Chemically the unit is a high-Mg tholeiite. Hornblende and magnetite have formed at the expense of pyroxene. Some plagioclase is untwinned. Hornblende is pleochroic brown to green.

Petrographic Description

DATE:

Sample #: 6

Essential Minerals	%
Hornblende	20
Pyroxene (Augite)	31
Plagioclase	35

Secondary or Alteration products	%
Sericite	5
Magnetite	5
Hornblende	

Varietal Minerals	%
Quartz	?
Biotite	4

Plagioclase composition (Michel-Levy)

An 36 Andesine

Metamorphic grade

Amphibolite

Accessory Minerals	%
Zircon	tr
Apatite	tr

Textures

Overall the petrotexture is granoblastic to decussate with subidioblastic laths of hornblende.

Pericline and albite twinning in plagioclase

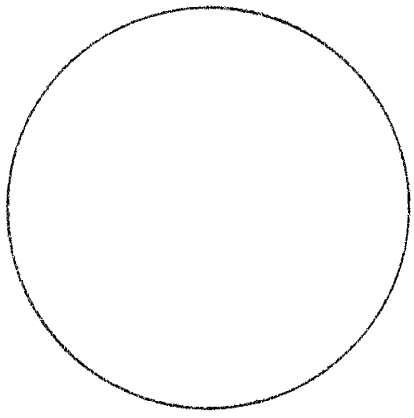

Mineralization

Rock Classification Amphibolite

Possible Parentage Basalt flow or mafic sill

Discussion Chemically the unit is a high-Mg tholeiite. Hornblende and magnetite have formed at the expense of pyroxene. Some plagioclase is untwinned. Hornblende is pleochroic brown to green.

Petrographic Description

DATE: 3-26-80

Sample #: 7

Essential Minerals	%
Hornblende	42
Plagioclase	31

Secondary or Alteration products	%
Sericite	2
Magnetite	7
Hornblende	

Varietal Minerals	%
Pyroxene (Augite)	14
Biotite	4

Plagioclase composition (Michel-Levy)

An 32 Andesine

Metamorphic grade

Amphibolite

Accessory Minerals	%
Zircon	tr

Textures

Petrographic texture is granoblastic to decussate. Many crystals are poikilobastic.

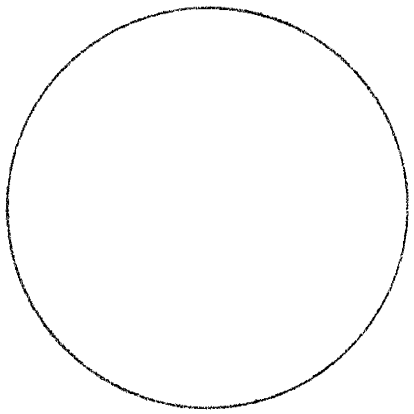

Mineralization

Rock Classification Amphibolite

Possible Parentage Basalt flow or mafic sill

Discussion Chemically the unit is a high-Mg tholeiite. Hornblende and magnetite have formed at the expense of pyroxene. Hornblende is pleochroic brown to green.

Petrographic Description

DATE:

Sample #: 8

Essential Minerals	%
Hornblende	49
Plagioclase	20
Pyroxene (Augite)	21

Secondary or Alteration products	%
Sericite	1
Magnetite	5
Hornblende	

Varietal Minerals	%
Biotite	4

Plagioclase composition (Michel-Levy)

Andesine An 36

Accessory Minerals	%
Zircon	tr

Metamorphic grade

Amphibolite

Textures

Petrotexture is decussate to granoblastic with a weak preferred mineral orientation to produce a foliation.

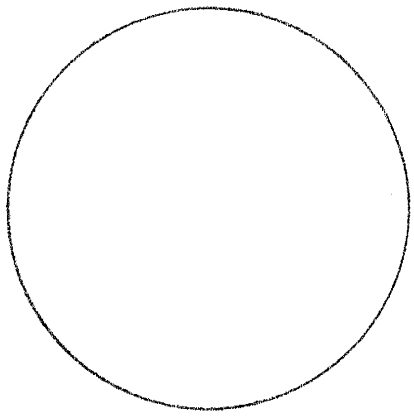

Mineralization

Rock Classification Amphibolite

Possible Parentage Basalt flow or mafic sill

Discussion Chemically the unit is a high-Mg tholeiite. Hornblende and magnetite have formed at the expense of pyroxene. Hornblende is pleochroic brown to green.

Petrographic Description

DATE:

Sample #: 9

Essential Minerals	%
Hornblende	33
Pyroxene (Augite)	31
Plagioclase	22

Varietal Minerals	%
Biotite	6

Accessory Minerals	%
Zircon	tr

Secondary or Alteration products	%
Sericite	1
Magnetite	7
Hornblende	

Plagioclase composition (Michel-Levy)

Andesine An 38

Metamorphic grade

Amphibolite

Textures

Petrotexture is granoblastic to decussate. Many grains are poikiloblastic.

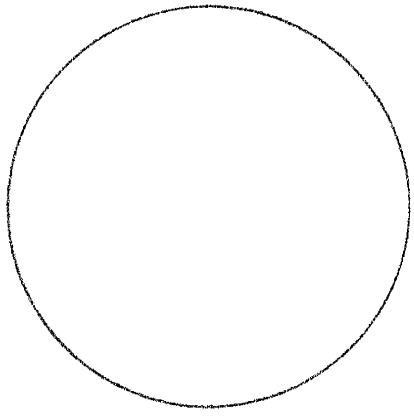

Mineralization

Rock Classification Amphibolite

Possible Parentage Basalt flow or mafic sill

Discussion Chemically the unit is a high-Mg tholeiite. Hornblende and magnetite have formed at the expense of pyroxene. Hornblende is pleochroic brown to green.

Petrographic Description

DATE:

Sample #: 10

Essential Minerals	%
Hornblende	36
Pyroxene (Augite)	40
Plagioclase	17

Secondary or Alteration products	%
Sericite	
Magnetite	5
Hornblende	

Varietal Minerals	%
Biotite	2

Plagioclase composition (Michel-Levy)

Andesine An 31

Metamorphic grade

Amphibolite

Accessory Minerals	%
Zircon	tr

Textures

Petrotexture is granoblastic to decussate.

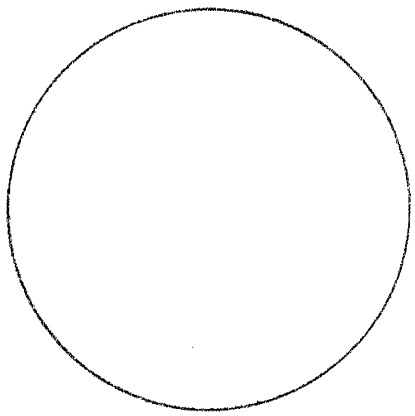

Mineralization

Rock Classification Amphibolite

Possible Parentage Basalt flow or mafic sill

Discussion Chemically the unit is a high-Mg tholeiite. Hornblende and magnetite have formed at the expense of pyroxene. Hornblende is pleochroic brown.

Petrographic Description

DATE: 1-25-80

Sample #: 11

Essential Minerals	%
Hornblende	48
Plagioclase	28
Augite	18

Secondary or Alteration products	%
Sericite	1
Magnetite	3
Hornblende	

Varietal Minerals	%
Biotite	2

Plagioclase composition (Michel-Levy)

An 35 Andesine

Metamorphic grade

Amphibolite

Accessory Minerals	%
Zircon	tr
Orthoclase	tr

Textures

Petrofabric is granoblastic to decussate with minor mortar texture. Plagioclase twins are commonly bent, and some show strain fractures. There is a weak preferred alignment of crystal fabric (i.e. foliation).

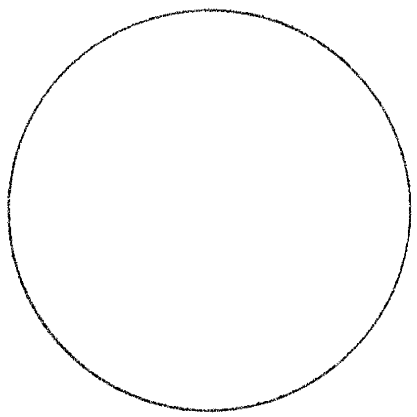

Mineralization: Black opaque magnetite (?)

Rock Classification: Amphibolite

Possible Parentage: Basalt flow or mafic sill

Discussion: Hornblende and magnetite have formed at the expense of pyroxene. Some untwinned plagioclase. Hornblende is pleochroic brown to green.

Petrographic Description

DATE: 1-25-80

Sample #: 12

Essential Minerals	%
Hornblende	40
Plagioclase (alt)	25
Pyroxene (Augite)	20

Secondary or Alteration products	%
Sericite & Muscovite	5
Magnetite	5

Varietal Minerals	%
Biotite	5

Plagioclase composition (Michel-Levy)

An 33 Andesine; by the Carlsbad Albite method

Metamorphic grade

Amphibolite

Accessory Minerals	%
Zircon	tr

Textures

Granoblastic texture of hornblende and plagioclase with preferential alteration of the feldspars by sericitization. Many of the hornblendes are poikiloblastic with inclusions of magnetite and feldspars.

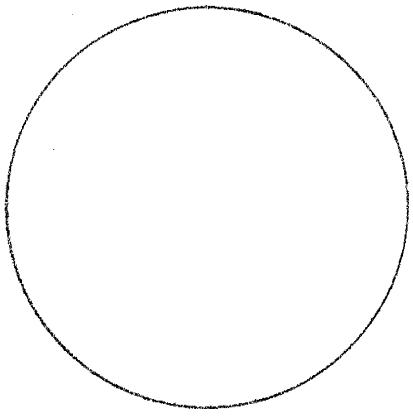

Mineralization

Rock Classification: Amphibolite

Possible Parentage: Basalt flow or mafic sill

Discussion: No quartz detected in this section, and the plagioclase has distinctly altered before the hornblendes. Sample was collected on the Dardanelles dump, where it's assumed from depth indicating alteration is very pervasive in the district. Hornblende and magnetite have formed at the expense of pyroxene. Hornblende is pleochroic brown to green.

Petrographic Description

DATE: 1-19-80

Sample #: 13

Essential Minerals	%
Hornblende	20
Pyroxene (Augite)	30
Plagioclase	30

Secondary or Alteration products	%
Sericite	6
Magnetite	4

Varietal Minerals	%
Quartz(?)	5
Biotite	5

Plagioclase composition (Michel-Levy)

An 40 Andesine; optically-negative? with large 2V

Metamorphic grade

Lower amphibolite

Accessory Minerals	%

Textures

Albite has perthitic texture. Overall-granoblastic texture. Banding present with a band composed predominantly of pyroxene, with crystals. At least 10x larger than the adjacent band. The latter composed of pyroxene, hornblende and feldspars.

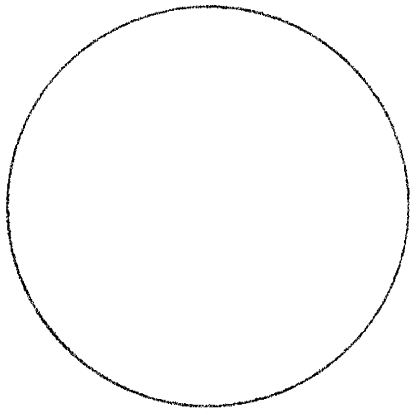

Mineralization

Rock Classification Hornblende-gneiss (Amphibolite)

Possible Parentage Pelitic sediment or graywacke

Discussion The continuous banding of quartzo-feldspathic bands, alternating with more mafic bands suggest a sedimentary precursor. Garnets are present in hand specimen along with a strong pervasive foliation and intense ptygmatic folding. Hornblende and magnetite have formed at the expense of pyroxene. Hornblende is pleochroic brown to green.

Petrographic Description

DATE: 1-22-80

Sample #: 14

Essential Minerals	%
Hornblende	40
Plagioclase	30
Pyroxene (Augite)	20

Secondary or Alteration products	%
Sericite	5
Magnetite	
Hornblende	

Varietal Minerals	%
Biotite	5

Plagioclase composition (Michel-Levy)

An 43 Andesine

Metamorphic grade

Amphibolite

Accessory Minerals	%
Orthoclase	tr

Textures

Granoblastic polygonal aggregates of plagioclase and hornblende. Small quartzo-feldspathic vein that is in the form of a fold, however mineral fabric suggests it was injected and not folded. The vein has poikiloblastic feldspar in a granoblastic texture with quartz, sericitization is intense. Plagioclase show bent twin lamellae and there are stress fractures in the hornblendes. Grain boundaries are sutured.

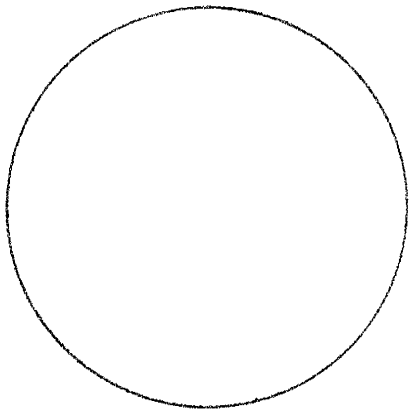

Mineralization

Rock Classification: Amphibolite

Possible Parentage: Basalt flow or mafic sill

Discussion: Hornblende and magnetite have formed at the expense of pyroxene. Quartzo-feldspathic vein is hydrothermal. Hornblende is pleochroic brown to green.

Petrographic Description

DATE: 1-24-80

Sample #: 15

Essential Minerals	%
Hornblende	10
Pyroxene (Augite)	10
Plagioclase	40
Quartz	30

Varietal Minerals	%
Biotite	2
Orthoclase	5

Accessory Minerals	%
Zircon	tr

Secondary or Alteration products	%
Sericite	tr
Magnetite	3

Plagioclase composition (Michel-Levy)

Andesine-oligoclase An 30

Metamorphic grade

Amphibolite

Textures

Petrotexture is granoblastic to decussate. Quartz vein in thin section with hornblende crystals aligning the edge of the vein. Some crenulation of the quartz vein. Sutured grain boundaries and many feldspars have inclusions of magnetite.

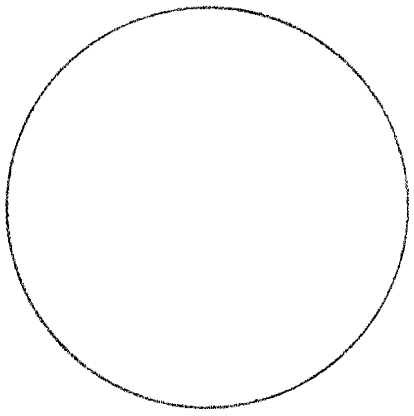

Mineralization

Rock Classification Amphibolite

Possible Parentage Basalt flow or mafic sill

Discussion Arsenopyrite(?) occurs in handspecimen. Outcrop is 30 feet wide with numerous quartz veins. Hornblende is pleochroic brown to green.

Petrographic Description

DATE: 1-19-80

Sample #: 16

Essential Minerals	%
Plagioclase	15
Quartz	36
Orthoclase 2V ≈90°	29

Secondary or Alteration products	%
Sericite	8

Varietal Minerals	%
Biotite	3
Microcline	5

Plagioclase composition (Michel-Levy)

≈ An 25 (4 samples, optically-negative) Oligioclase

Metamorphic grade ≈ Lower amphibolite

Accessory Minerals	%
Magnetite	3
Possible Apatite	<1

Textures

Graphic texture of quartz in plagioclase. Poikiloblastic texture in feldspar. Overall the section displays a mortar texture with porphyroblasts of feldspar in a cataclastic matrix of quartz, feldspar and biotite.

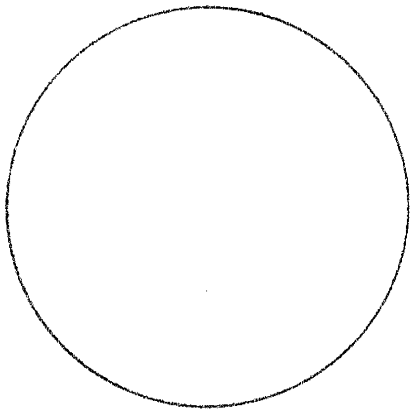

Mineralization

Rock Classification Cataclastic-Granite

Possible Parentage Porphyritic Granite

Discussion Quartz grains may be strained and thus display a biaxial interference figure. Geochemically and by modal analysis the unit is granitic.

Petrographic Description

DATE: 1-20-80

Sample #: 17

Essential Minerals	%
Plagioclase	21
Quartz	44
Orthoclase	15

Varietal Minerals	%
Biotite	10
Microcline	5

Accessory Minerals	%
Zircon	tr
Apatite	tr

Secondary or Alteration products	%
Sericitization	5

Plagioclase composition (Michel-Levy)

An 28 Oligoclase

Metamorphic grade

Amphibolite(?)

Textures

Two directions of micro-fractures are found in some porphyroblasts of feldspar. Albite(?) is intergrown with microcline resulting in a perthitic texture. The section displays a mortar texture with porphyroblasts of feldspar in a fine to medium grained cataclastic matrix of quartz and feldspar. Exsoln. textures are graphic and myrmekitic.

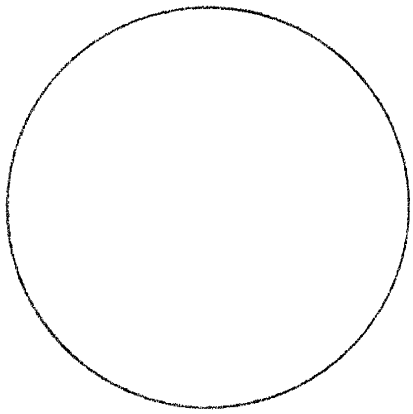

Mineralization

Rock Classification Cataclastic-Granite

Possible Parentage Granite

Discussion Some of the quartz grains show minor straining resulting in a low 2V biaxial figure. Undulatory extinction is common in both quartz and feldspar crystals.

Petrographic Description

DATE: 2-1-80

Sample #: 18

Essential Minerals	%
Quartz	30
Orthoclase	17
Plagioclase	25

Varietal Minerals	%
Microcline	8

Accessory Minerals	%
Garnet (Almandine)	2
Muscovite	2
Zircon	

Secondary or Alteration products	%
Biotite (after garnet)	3
Sericite	13
Magnetite	tr

Plagioclase composition (Michel-Levy)

An 28 Oligioclase

Metamorphic grade

Amphibolite

Textures

Petrofabric is granoblastic aggregate of quartz and feldspar. Preferential alteration (sericitization) of feldspars in section, (plag. over ortho). Recrystallization is pervasive with sutured grain boundaries. Feldspars are poikiloblastic, exsolution textures in feldspars.

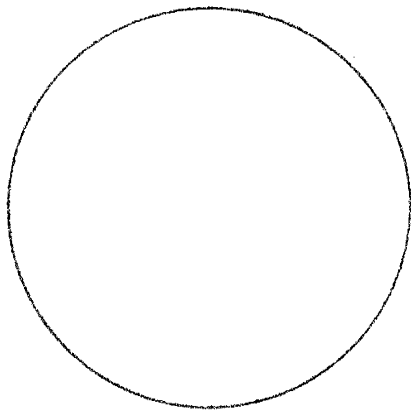

Mineralization

Rock Classification Garnetiferous Alaskite

Possible Parentage Leuco-Granite

Discussion (Kerr 1942, p. 265) Rock subject to hydrothermal alteration orthoclase is ordinarily more resistant then plagioclase. Plagioclase hard to distinguish from ortho. due to alteration - (i.e. twins are mashed).

Petrographic Description

DATE: 1-19-80

Sample #: 19

Essential Minerals	%
Orthoclase	15
Plagioclase	25
Quartz	38
Garnet	5

Secondary or Alteration products	%
Sericite	10
Biotite/Chlorite	2

Varietal Minerals	%
Microcline	5

Plagioclase composition (Michel-Levy)

An 28 Oligoclase

Metamorphic grade

Amphibolite (exsolution text.)

Accessory Minerals	%
Zircon	tr

Textures

Graphic texture displayed in some feldspars, they also display a poikilitic texture. Overall the section displays a mortar texture with strained porphyroclasts of feldspar and quartz. Garnets are fractured poikiloblastic altering to biotite.

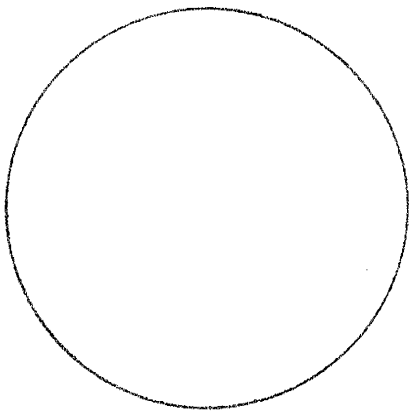

Mineralization

Rock Classification: Cataclastic garnetiferous alaskite

Possible Parentage: Leuco-Granite

Discussion: Garnets occur is monomineralic pods that are often lenticular. In thin section garnets are retrograding to biotite and or chlorite.

Petrographic Description

DATE: 2-2-80

Sample #: 20

Essential Minerals	%
Quartz	35
Microcline	15
Orthoclase	20
Plagioclase	20

Secondary or Alteration products	%
Sericite	5
Muscovite	tr

Varietal Minerals	%
Biotite	5

Plagioclase composition (Michel-Levy)

Not enough to determine composition

Metamorphic grade

Amphibolite

Accessory Minerals	%
Zircon	tr
Apatite(?)	

Textures

Petrofabric is cataclastic with a well developed mortar texture. Porphyroblasts are mainly microcline and orthoclase with some plagioclase. The section is medium grained <1mm and the matrix is granoblastic composed of feldspar and quartz. Porphyroblasts are poikilitic, and show graphic textures, strain fractures and sutured grain boundaries. The matrix is also recrystallized, displayed by sutured grain boundaries.

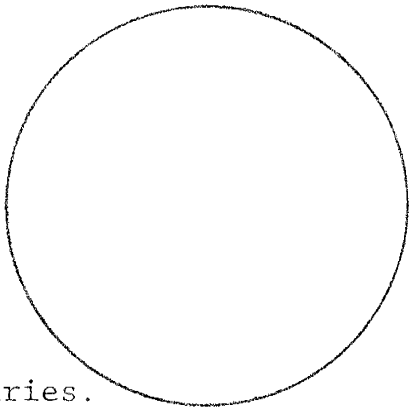

Mineralization

Rock Classification Cataclastic-Granite

Possible Parentage Granite

Discussion The unit is part of pεg mapped in the eastern section of the field area. It is very similar microscopically to section pεcg, 16

Petrographic Description

DATE: 2-2-80

Sample #: 21

Essential Minerals	%
Quartz	35
Orthoclase	30
Plagioclase	20

Varietal Minerals	%
Biotite	5
Microcline	5

Accessory Minerals	%
Garnet	tr

Secondary or Alteration products	%
Sericite	5
Secondary Biotite(?)	
Chlorite	tr

Plagioclase composition (Michel-Levy)

An 27 Oligoclase (8 samples)

Metamorphic grade

Amphibolite (graphic texture)

Textures

Petrofabric is weakly cataclastic with porphyroblasts up to 1.5mm of orthoclase, plagioclase and some microcline. The matrix is fine-to medium-grained (<1.5mm) granoblastic and composed of quartz and feldspar. Strain fractures, graphic texture, bent twin lamellae, sutured grain boundaries are present. Some porphyroclasts are poikilitic. No foliation present

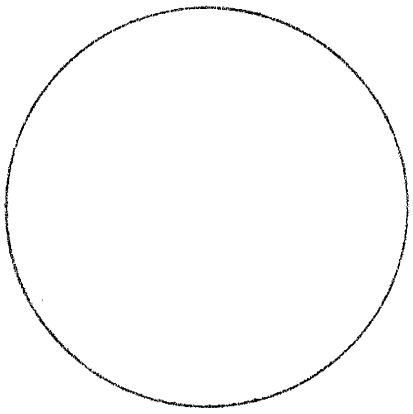

Mineralization

Rock Classification: Cataclastic-Granite (weakly)

Possible Parentage: Granite

Discussion: Mapped as $p\epsilon_g$ in the eastern section of the map area.

Petrographic Description

DATE: 2-1-80

Sample #: 22

Essential Minerals	%
Quartz	30
Orthoclase	26
Plagioclase	28

Secondary or Alteration products	%
Sericite	3
Biotite	
Magnetite	tr

Varietal Minerals	%
Biotite	7
Microcline	5

Plagioclase composition (Michel-Levy)

An 29 Oligoclase optically-negative (8 samples)

Accessory Minerals	%
Garnet	1
Zircon	

Metamorphic grade

Amphibolite

Textures

Petrofabric is weakly cataclastic with large (>2mm) porphyroblasts of microcline orthoclase and occasionally plagioclase in a granoblastic medium-grained (<2mm) matrix of quartz and feldspar. Strain features, sutured grain boundaries and graphic texture are displayed in the section along with a poikilitic texture.

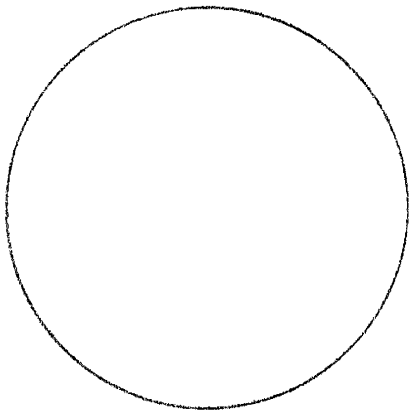

Mineralization

Rock Classification Cataclastic Granite (weakly)

Possible Parentage Granite

Discussion The thin section is very similar compositionally to pecg and texturally - however, it is not as cataclastic (mortar texture is weak). The unit is mapped as pεg in the SE section of the field area.

Petrographic Description

DATE: 2-2-80

Sample #: 23

Essential Minerals	%
Quartz	45
Orthoclase	20
Plagioclase	15

Secondary or Alteration products	%
Sericite	5
Magnetite	tr

Varietal Minerals	%
Biotite	10
Microcline	5
Unknown (thick qtz?)	tr

Plagioclase composition (Michel-Levy)

Not enough to determine composition.

Metamorphic grade

Amphibolite

Accessory Minerals	%
Zircon	tr
Apatite	tr

Textures

Petrofabric is cataclastic with a mortar texture. Porphyroblasts are mainly orthoclase, microcline and occasionally plagioclase. Thin section is medium-grained <1mm and the matrix is granoblastic composed of feldspar or recrystallized quartz. Porphyroblasts are poikilitic and show graphic texture, strain features and sutured grain boundaries.

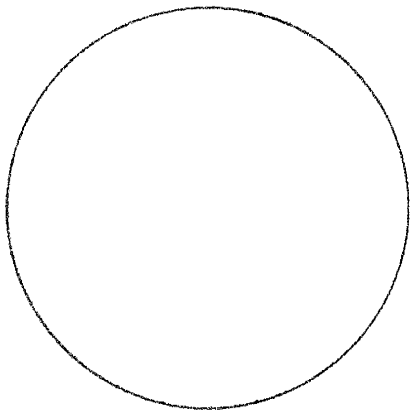

Mineralization

Rock Classification Cataclastic-Granite

Possible Parentage Granite

Discussion The unit is mapped as pεg in the eastern end of the map area.

Petrographic Description

DATE: 1-30-80

Sample #: 24

Essential Minerals	%
Plagioclase	15
Quartz	45
Orthoclase	20

Secondary or Alteration products	%
Sericite	3
Magnetite	tr

Varietal Minerals	%
Biotite	10
Enstatite	2
Microcline	5

Plagioclase composition (Michel-Levy)

An 10 (Abite)

Metamorphic grade

Mid. Amphibolite

Accessory Minerals	%
Zircon	tr
Nepheline	tr

Textures

Petrofabric is mylonitic with porphyroblasts of microcline, orthoclase, plagioclase in a foliated matrix accented by alignment of mica flakes. Porphyroblasts show pressure shadows, strain fractures, bent lamellae, undulose extinction. In addition they are helictitic and occasionally show graphic texture. The matrix is granoblastic and occasionally polygonal and composed chiefly of quartz and feldspar.

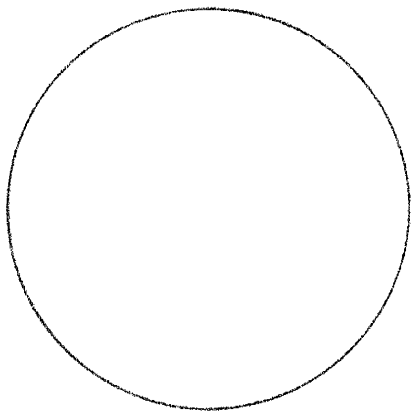

Mineralization

Rock Classification Mylonitized-Granite

Possible Parentage Porphyritic Granite

Discussion The rock unit is the granitic facies of the pɛu unit and is located in the eastern portion of the field area. The unit is mylonitic as compared to the cataclastic texture of pɛcg. Compositionally the two units pɛu and pɛcg are very similar, which may give a clue to the precursor of the granitic facies of pɛu.

Petrographic Description

DATE: 1-26-80

Sample #: 25

Essential Minerals	%
Orthoclase	28
Microcline	25
Quartz	30

Secondary or Alteration products	%
Sericite	5
Magnetite	tr

Varietal Minerals	%
Plagioclase	5
Biotite	7

Plagioclase composition (Michel-Levy)

An 27 Oligoclase (optically-negative)

Metamorphic grade Amphibolite to Upper Amphibolite

Accessory Minerals	%
Zircon Needles	tr
Sphene	tr
Apatite(?)	

Textures

Petrofabric is mylonitic with porphyroblasts of microcline and feldspar in a weak foliation, accented by alignment of mica flakes. Porphyroblasts are, poikilitic, graphitic, and show pressure shadows, strain fractures, bent twin lamellae. Recrystallization is abundant, with suture texture.

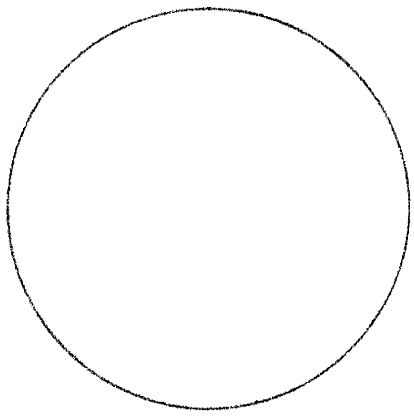

Mineralization

Rock Classification Mylonitic-Granite (pɛu)

Possible Parentage Porphyritic Granite

Discussion The rock unit is very granitic in composition but displays a high-degree of metamorphism (graphic texture and mylonitization). The unit is part of undifferentiated complex. Orthoclase is going to microcline!

Petrographic Description

DATE: 1-20-80

Sample #: 26

Essential Minerals	%
Quartz	25
Microcline	16
Biotite	10
Plagioclase negative	10
Orthoclase	23

Secondary or Alteration products	%
Sericite	10
Magnetite	5
Chlorite	

Varietal Minerals	%
Augite	1

Plagioclase composition (Michel-Levy)

An 28 Oligoclase (optically-negative)

Metamorphic grade High-grade

≈ Amphibolite Facies

Accessory Minerals	%
Chlorite(?)	tr

Textures

Biotite laths are occasionally bent and numerous feldspars are poikilitic with inclusions of quartz and biotite. Strain fractures along with graphic texture is also observed in some feldspar. The quartz crystals display recrystallization, sutured boundaries and undulatory extinction. The overall petro-fabric displays a preferred lineation due to alignment of elongate quartz crystals and microbands of biotite flakes. Weak pressure shadows are noted on some porphyroblasts of feldspar.

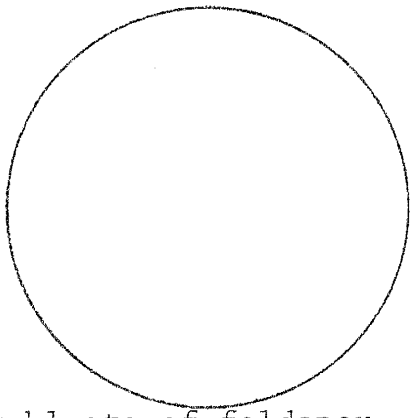

Mineralization

Rock Classification Granitic-Gneiss or Augen-Gneiss

Possible Parentage Granite

Discussion In microscopic examination the unit displays an "Augen" texture and ptygmatic folding of quartzo-feldspathic veins. Part of (pЄu) unit.

Petrographic Description

DATE: 1-31-80

Sample #: 27

Essential Minerals	%
Orthoclase	25
Microcline	15
Quartz	30
Biotite	13

Secondary or Alteration products	%
Sericite	5
Biotite	2

Varietal Minerals	%
Plagioclase	10

Plagioclase composition (Michel-Levy)

An 32 Andesine (4 samples)

Accessory Minerals	%
Zircon	tr

Metamorphic grade

Amphibolite

Textures

Petrofabric is cataclastic with porphyroblasts of orthoclase, microcline and occasionally plagioclase. Porphyroblasts are poikilitic, coarse-grained (up to 8mm), sericitized and display strain fractures and exsolution features (i.e. graphic). Clusters of quartz grains (med.-grained 2-3mm) show sutured boundaries. Matrix is fine-grained <1mm and recrystallized.

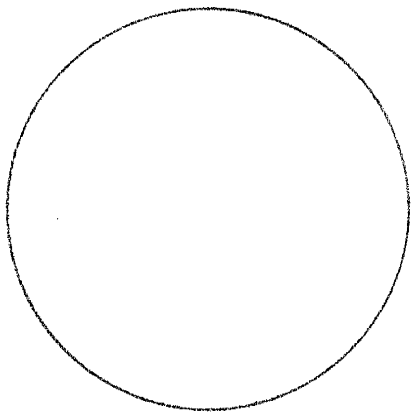

Mineralization

Rock Classification: Cataclastic-Granite

Possible Parentage: Porphyritic Granite

Discussion: The rock is coarse-grained facies of pEu.

Petrographic Description

DATE: 1-26-80

Sample #: 28

Essential Minerals	%
Biotite	10
Quartz	40
Microcline	20
Orthoclase	23

Secondary or Alteration products	%
Sericite	2
Magnetite	tr

Varietal Minerals	%
Plagioclase	5

Plagioclase composition (Michel-Levy)

An 28 (Oligoclase)

Metamorphic grade

Amphibolite Facies

Accessory Minerals	%
Sphene	tr

Textures

Petrofabric is mylonitic with porphyroblasts of microcline, orthoclase and occasionally plagioclase; in a weak foliation accented by alignment of mica flakes. Porphyroblasts are poikilitic, graphic and show pressure shadows, strain fractures, bent twin lamallae, undulose extinction and sutured grain boundaries. The matrix between the porphyroblasts is fine-grained granoblastic and composed chiefly of feldspar and quartz.

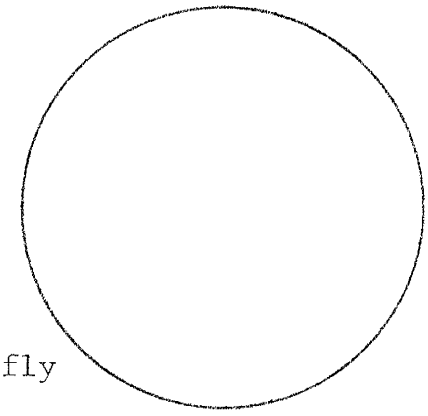

Mineralization

Rock Classification Mylonitic-Granite

Possible Parentage Porphyritic Granite

Discussion The rock occurs within the peu unit, but definitely does not belong to the metarhyolite group.

Petrographic Description

DATE: 3-18-80

Sample #: 29

Essential Minerals	%
Biotite	15
Orthoclase	20
Quartz	15

Varietal Minerals	%
Hornblende	10
Garnet	10
Plagioclase	5
Microcline	5

Accessory Minerals	%
Magnetite	2
Zircon	2
Sphene(?)	1
Sillimanite(?)	tr

Secondary or Alteration products	%
Sericite	5
Chlorite	10
Magnetite	

Plagioclase composition (Michel-Levy)

Oligioclase(?) An 28

Metamorphic grade

Middle Amphibolite

Textures

Petrotexture is banded well-foliated marked by parallel alignment of biotite flakes. Very weak mortar texture. Quartz shows arrested grain boundaries. Feldspars are poikiloblastic, sericitized, and have graphic textures. Plagioclase shows bent twin lamellae. Strain fractures in most crystals (esp. qtz.) Plag = pericline and albite twinning.

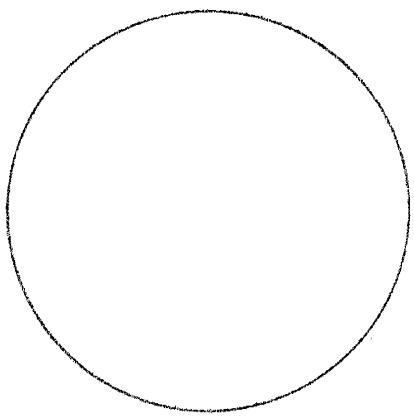

Mineralization

Rock Classification Biotite Gneiss

Possible Parentage Sediment(?) Pelitic or Graywacke

Discussion Well banded ptygmatically folded biotite gneiss, Thomas' Lit-par Lit unit. Hornblende is retrograding to chlorite; loss of pleochroism. Biotite is also going to chlorite.

Petrographic Description

DATE: 1-25-80

Sample #: 30

Essential Minerals	%
Garnet	20
Biotite	20
Microcline	20

Secondary or Alteration products	%
Sericite	5
Chlorite	10

Varietal Minerals	%
Plagioclase	5
Quartz	5
Orthoclase(?)	5
Hornblende	10

Plagioclase composition (Michel-Levy)

An 28 Oligoclase

Accessory Minerals	%
Zircon	tr
Silimanite(?)	(?)

Metamorphic grade Upper Greenschist - Lower Amphibolite

Textures

Petrofabric displays a pervasive foliation with layers of feldspar-quartz alternating with more mafic layers (garnets, biotite). Many of the crystals are poikiloblastic with inclusions of biotite and/or quartz, in addition some feldspars display a graphic feature. Recrystallization is ubiquitous, evidenced by the arrested grain boundaries.

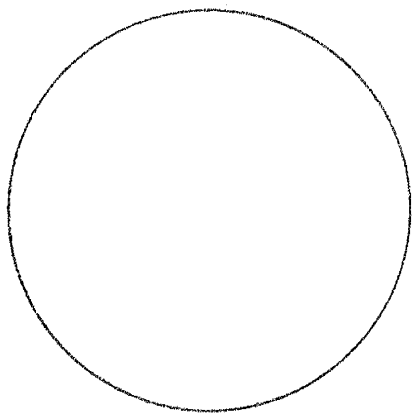

Mineralization Trace of black opaque (magnetite)

Rock Classification Garnet-Gneiss

Possible Parentage Sed.

Discussion The outcrop is very dark and shows a strong gneissic (layering) texture and ptygmatic folding. Hornblende retrograding to chlorite same for biotite.

Petrographic Description

DATE: 1-25-80

Sample #: 31

Essential Minerals	%
Quartz	97

Secondary or Alteration products	%
Sericite	1
Hematite staining	
Magnetite	

Varietal Minerals	%

Plagioclase composition (Michel-Levy)

Accessory Minerals	%
Muscovite	1
Orthoclase	1

Metamorphic grade Upper Greenschist or Lower Amphibolite

Textures

Petrofabric - annealed texture, where recrystallization of a regionally metamorphosed quartzite has occurred. This has tended to produce a granoblastic texture however no polygonalization appears to have occurred yet.

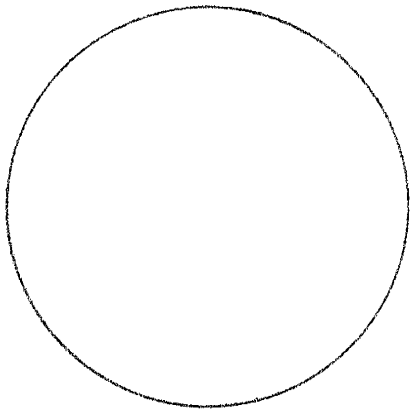

Mineralization Black-Opaque Needles(?), with a rough texture

Rock Classification Quartzite

Possible Parentage Quartz Sandstone or Quartz-Rich Arkose

Discussion Uniaxial figure shows slight separation, which indicates straining of quartz crystals. The micas, and the trace of altered feldspar may indicate an arkosic precursor, or a quartz sandstone with pelitic?

Petrographic Description

DATE: 1-23-80

Sample #: 32

Essential Minerals	%
Orthoclase	20
Biotite and/or Chlorite	10
Quartz	40

Secondary or Alteration products	%
Sericite	5
Alunite(?) Unixial	tr
Chlorite	10
Magnetite	

Varietal Minerals	%
Microcline	15

Plagioclase composition (Michel-Levy)

Not enough to determine composition

Accessory Minerals	%
Zircon	tr
Plagioclase	tr

Metamorphic grade Upper Greenschist Lower Amphibolite Retrograde(?)

Textures

Petrofabric is mylonitic with a foliation that wraps around porphyroblasts of feldspar (microcline and orthoclase) Porphyroblasts as large as 2mm, are helicitic to poikiloblastic, they also show pressure shadows strain features "Pods' and lenticular aggregates of recrystallized quartz form "Augen" and stringers parallel with foliation

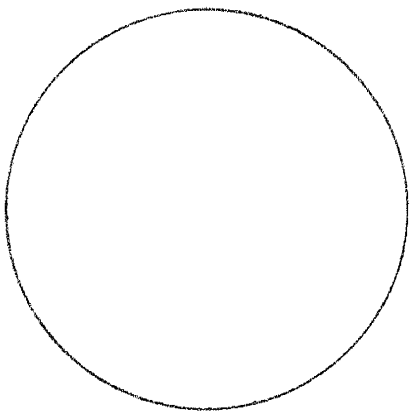

Mineralization

Rock Classification Mylonitic-Quartz-Rhyolite

Possible Parentage Porphyritic Quartz Rhyolite

Discussion The unit crops out near the Schuylkill Mine with the amphibolite unit. It is parallel with the foliation of the amphibolite.

Petrographic Description

DATE: 1-26-80

Sample #: 33

Essential Minerals	%
Quartz	35
Chlorite and/or Biotite	15
Microcline	30

Secondary or Alteration products	%
Sericite	5
Magnetite	

Varietal Minerals	%
Orthoclase	10
Plagioclase	5

Plagioclase composition (Michel-Levy)

An 28 very rough only 3 samples, very altered!

Accessory Minerals	%
Zircon	tr

Metamorphic grade Upper Greenschist or Lower Amphibolite

Retrograde?

Textures

Petrofabric is mylonitic with a pervasive foliation accented by mica flakes and alignment of porphyroblasts, matrix is fine grained (hornfelsic). Porphyroblasts are poikiloblastic - helicitic and they display pressure shadows, strain features and exsolution textures (perthite, graphic). Recrystallization is extensive, with sutured grain boundaries.

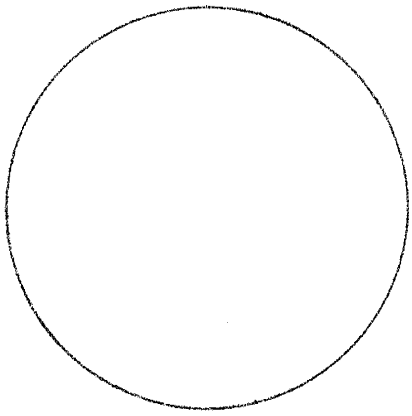

Mineralization

Rock Classification Mylonitic-Rhyolite

Possible Parentage Porphyritic-Rhyolite

Discussion The unit cross-cuts the amphibolite foliation, which is at a high angle to metarhyolitic foliation. Again the unit indicates shearing (mylonitization) which could be past the development of the amphibolite foliation.

Petrographic Description

DATE: 1-22-80

Sample #: 34

Essential Minerals	%
Quartz	25
Biotite and/or Chlorite	27
Orthoclase (hi-2V)	25

Secondary or Alteration products	%
Sericite	3
Chlorite	

Varietal Minerals	%
Microcline	10
Plagioclase	10

Plagioclase composition (Michel-Levy)

An 28 Oligoclase (optically - negative)

Accessory Minerals	%

Metamorphic grade Upper Greenschist to Lower Amphibolite Retrograde?

Textures

Petrofabric is mylonitic with a streaky foliation produced by alignment of grains. Porphyroclasts up to 2mm. are helicitic to poikilobastic. In addition they show pressure shadows, strain fractures and occasionally graphic texture. Recrystallization is ubiquitous, evidenced by the arrested grain boundaries.

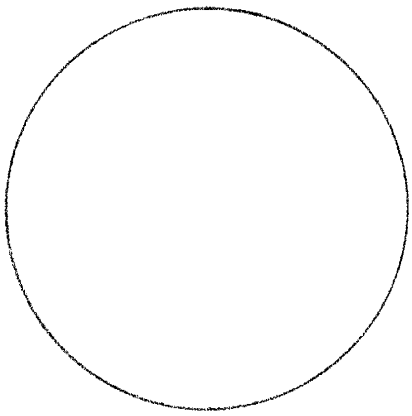

Mineralization

Rock Classification Mylonitic-Rhyolite

Possible Parentage Porphyritic Rhyolite

Discussion See description #35

Petrographic Description

DATE: 1-20-80

Sample #: 35

Essential Minerals	%
Quartz	35
Orthoclase	20
Biotite and/or Chlorite	15

Secondary or Alteration products	%
Sericitization	10
Magnetite	tr

Varietal Minerals	%
Plagioclase	10
Microcline	10

Plagioclase composition (Michel-Levy)

$\sim$ An 30 Andesine/Oligoclase
optically negative

Accessory Minerals	%
Hornblende	tr

Metamorphic grade Upper Greenschist Lower Amphibolite

Retrograde

Textures

Overall texture of the section is mylonitic with a pervasive foliation displayed by alignment of porphyroblasts and biotite crystals. Pressure shadows are commonly observed as ellipsoidal envelopes around porphyroblasts of feldspar. In addition the porphyroblasts display strain fractures, rotations, poikiloblastic textures, undulose extinction and suturing with surrounding grains.

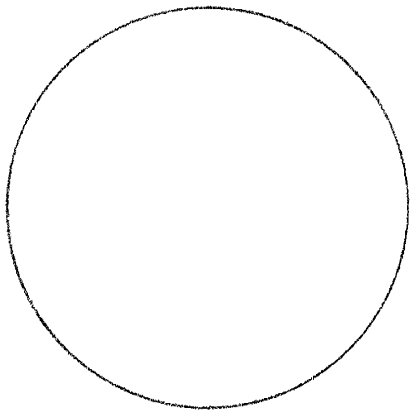

Mineralization

Rock Classification Mylonitic-Rhyolite

Possible Parentage Porphyritic Rhyolite

Discussion The unit crops out as a single dike, that is parallel with the axial plane of a regional antiform fold. Shearing along this plane has occurred, supported by the mylonitic texture. In addition, the unit has two facies, an outer aphanitic facies and an inner coarse grained facies. The latter one is described here.

Petrographic Description

DATE: 1-30-80

Sample #: 36

Essential Minerals	%
Quartz	40
Biotite and/or Chlorite	15
Orthoclase	20

Secondary or Alteration products	%
Sericite	5
Chlorite	
Magnetite	tr

Varietal Minerals	%
Microcline	10
Plagioclase	9

Plagioclase composition (Michel-Levy)

An 32 Andesine (3 samples)
negative

Metamorphic grade Lower Amphibolite? Retrograde

Accessory Minerals	%
Sphene	1
Zircon	tr

Textures

Petrofabric is mylonitic with porphyroblasts of orthoclase, microcline in a foliated matrix composed of biotite, quartz and feldspar. Porphyroblasts-are poikiloblastic. helicitic and they display weak pressure shadows, strain features and occasional exsolution textures (graphic).

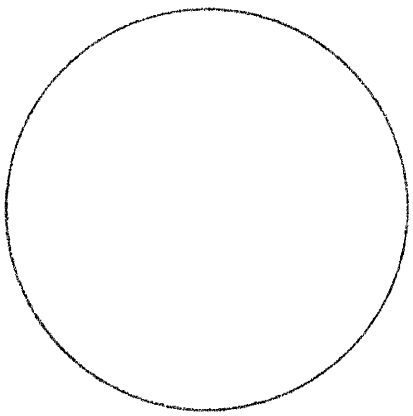

Mineralization

Rock Classification Mylonitic-Rhyolite

Possible Parentage Porphyritic-Rhyolite

Discussion Unit occurs as a dike that cross-cuts the peu foliation.

Petrographic Description

DATE: 2-3-80

Sample #: 37

Essential Minerals	%
Biotite and/or Chlorite	20
Orthoclase	25
Quartz	35

Secondary or Alteration products	%
Sericite (Muscovite)	5
Chlorite	
Magnetite	

Varietal Minerals	%
Plagioclase	5
Microcline	10

Plagioclase composition (Michel-Levy)

Not enough to determine composition

Accessory Minerals	%
Zircon (inclusion)	tr
Apatite (inclusion)	tr
Sphene	tr

Metamorphic grade Upper Greenschist Amphibolite(?) Retrograde?

Textures

Petrofabric is mylonitic with a pervasive foliation accented by mica flakes and alignment of porphyroblasts. The matrix is granoblastic and recrystallized and composed chiefly of quartz and feldspar. Porphyroblasts are poikilitic-helicitic and display pressure shadows with the matrix wrapping around them. They also show strain fractures, alteration, undulatory extinction and some graphic texture.

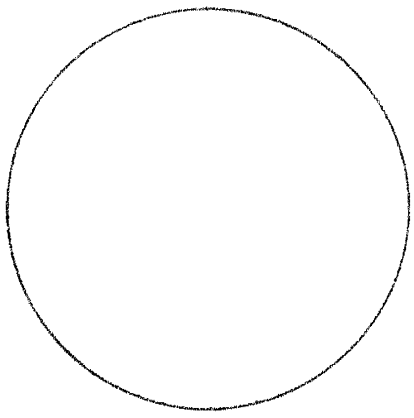

Mineralization

Rock Classification Mylonitic-Rhyolite

Possible Parentage Porphyritic Rhyolite

Discussion The unit is the coarse-grained outer facies of pemr unit which is located west of the Juno claim block.

Petrographic Description

DATE: 2-4-80

Sample #: 38

Essential Minerals	%
Biotite and/or Chlorite	20
Quartz	30
Orthoclase	25

Varietal Minerals	%
Plagioclase	10
Microcline	10

Accessory Minerals	%
Sphene	tr

Secondary or Alteration products	%
Sericite	5
Chlorite	
Magnetite	tr

Plagioclase composition (Michel-Levy)

Not enough to determine composition

Metamorphic grade Upper Green schist Lower Amphibolite Retrograde?

Textures

Petrofabric is mylonitic with a pervasive foliation accented by mica flakes. The matrix is fine-medium-grained and the porphyroblasts are less than 1mm. Porphyroblasts are poikiloblastic, altered, and display pressure shadows, strain fractures and undulatory extinction. Graphic texture and bent twin lamallae are occasionally present

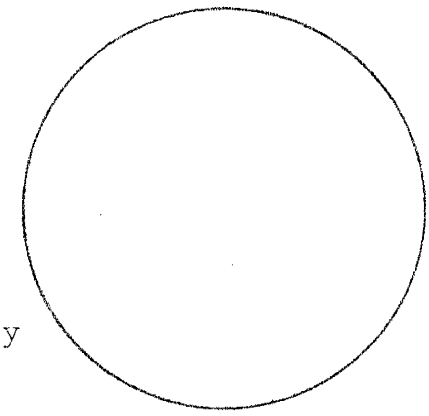

Mineralization

Rock Classification Mylonitic-Rhyolite

Possible Parentage Porphyritic Rhyolite

Discussion The unit is the coarse-grained outer facies of pemr unit which is located west of the Juno claim block.

Petrographic Description

DATE: 2-4-80

Sample #: 39

Essential Minerals	%
Chlorite and/or Biotite	25
Quartz	30
Orthoclase	20

Varietal Minerals	%
Plagioclase	4
Microcline	5

Accessory Minerals	%
Zircon	tr
Sphene	1

Secondary or Alteration products	%
Muscovite?	10
Sericite	5
Magnetite	tr

Plagioclase composition (Michel-Levy)

Not enough to determine composition

Metamorphic grade Upper Greenschist to Lower Amphibolite Retrograde?

Textures

Petrofabric is mylonitic with a strong pervasive foliation accented by mica flakes. Porphyroblasts are chiefly orthoclase that are poikiloblastic helictitic and show pressure shadows, alteration and undulatory extinction. Porphyroblasts are x 1mm. The matrix is fine grained, recrystallized and composed mainly of quartz, feldspar and biotite, ~ granoblastic.

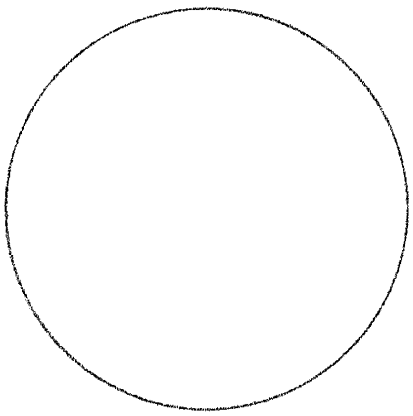

Mineralization

Rock Classification Mylonitic-Rhyolite

Possible Parentage Porphyritic Rhyolite

Discussion The unit is the fine-grained aphanitic inner facies of the pemr unit, which is located west of the Juno claim block.

Petrographic Description

DATE: 2-4-80

Sample #: 40

Essential Minerals	%
Quartz	30
Chlorite and/or Biotite	35
Orthoclase	20

Varietal Minerals	%
Microcline	5
Plagioclase	5
Unknown	

Accessory Minerals	%
Sphene	1

Secondary or Alteration products	%
Sericite & Muscovite(?)	5 >
Magnetite	tr

Plagioclase composition (Michel-Levy)

Not enough to determine composition

Metamorphic grade Upper Green schist Lower Amphibolite Retrograde?

Textures

Petrofabric is mylonitic with a strong pervasive foliation accented by mica flakes. Porphyroblasts are chiefly orthoclase with some microcline and plagioclase. Porphyroblasts are poikiloblastic, helicitic and show well-developed pressure shadows; they are <1mm in size. The matrix is fine-grained recrystallized and composed mainly of quartz, biotite and feldspar = granoblastic. Alteration of feldspar is common - sericitization

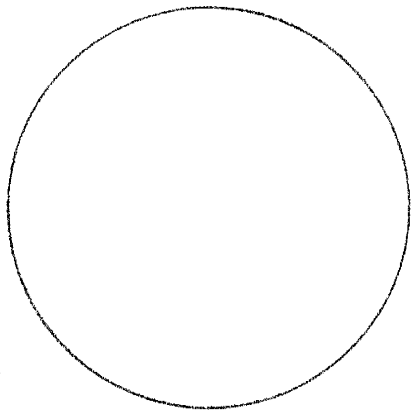

Mineralization

Rock Classification Mylonitic-Rhyolite

Possible Parentage Porphyritic Rhyolite

Discussion The unit is the fine-grained aphanitic inner facies of pEmr unit, which is located west of the Juno claim block.

Petrographic Description

DATE: 1-21-80

Sample #: 41

Essential Minerals	%
Quartz	25
Chlorite and/or	25
Biotite	

Secondary or Alteration products	%
Sericite	25
Alunite (biaxial +)	5
Magnetite	

Varietal Minerals	%
Microcline	10
Orthoclase	10
Pyroxene(?)	1

Plagioclase composition (Michel-Levy)

Not enough present

Accessory Minerals	%
Muscovite	tr
Apatite(?)	tr
Hornblende Lath	tr
Plagioclase	tr

Metamorphic grade Greenschist Facies Lower Amphibolite Retrograde

Textures

The petrofabric is mylonitic with a streaky foliation produced by micas (chlorite). Large porphyroblasts (max. 2mm) of feldspar display pressure shadows, strain fractures and a helicitic texture with alunite and sericite as the inclusions.

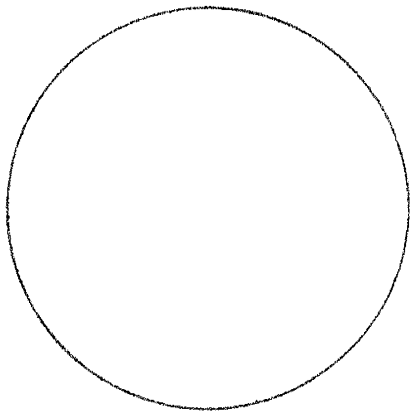

Mineralization

Rock Classification Mylonitic-Rhylite

Possible Parentage Porphyritic Rhyolite

Discussion The unit occurs as a dike-like structure that trends east-west and is parallel with the axial plane of a large (4mi) antiform fold plunging to the northeast. Apparently shearing has occurred along the axial plane of this fold.

Petrographic Description

DATE: 1-19-80

Sample #: 42

Essential Minerals	%
Plagioclase	40
Hornblende	30
Augite(?) pyx.	10

Varietal Minerals	%
Natrolite	2

Accessory Minerals	%
Quartz	tr
Calcite	tr

Secondary or Alteration products	%
Saussuritization of plag.	20
Hornblende after	
Pyroxene (uralization)	
Magnetite	

Plagioclase composition (Michel-Levy)

Too altered to determine composition

Metamorphic grade

Textures

Ophitic texture of plagioclase laths imbedded in hornblende. Twinning of pyroxene!

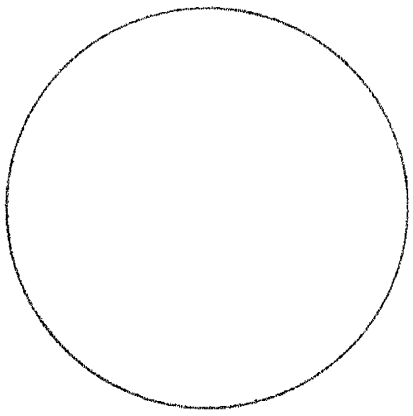

Mineralization

Rock Classification Diabase

Possible Parentage

Discussion Large phenocryst of magnetite surrounded by large subeuhedral crystals of feldspar and quartz is present. Composition of the plagioclase is too hard to determine with the intense seritization of the sample (i.e. the internal part of the plagioclase is almost completely altered).

Petrographic Description

DATE: 1-20-80

Sample #: 43

Essential Minerals	%
Plagioclase	20
Pyroxene (Augite)	20
Hornblende	20

Varietal Minerals	%
Quartz	3
Zeolite (Natrolite)	2

Accessory Minerals	%
Calcite	tr
Chlorite	tr
Actinolite-Tremolite	

Secondary or Alteration products	%
Saussuritization of plagioclase and sericitization of other feldspars	25
Actinolite-Tremolite after Pyroxene-	
Magnetite	10

Plagioclase composition (Michel-Levy)

An 42 Andesine

Metamorphic grade

Textures

Interlocking network of plagioclase and pyroxene resulting in an ophitic texture.

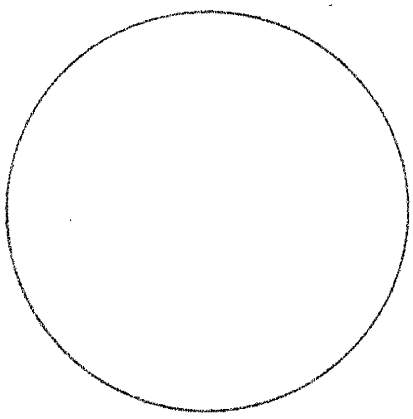

Mineralization

Rock Classification: Diabase

Possible Parentage

Discussion: Diabase dike with intense hydrothermal(?) alteration. Hand specimen shows epidote crystals on joint planes. Very altered unit.

Petrographic Description

DATE: 1-20-80

Sample #: 44

Essential Minerals	%
Microcline	20
Orthoclase	20
Quartz	20
Pyroxene (Augite)	20
Hornblende	

Varietal Minerals	%
Plagioclase	10

Accessory Minerals	%
Riebeckite	tr

Secondary or Alteration products	%
Saussuri tization	10
Uralitization	
Magnetite	tr

Plagioclase composition (Michel-Levy)

Not enough crystal to determine and too highly altered

Metamorphic grade

Textures

Graphic texture displayed in some feldspars. Clusters of sutured quartz grains are randomly distributed throughout the section, recrystallization is also found in certain areas. The overall texture of the section is ophitic with laths of altered plagioclase interlocked with altered pyroxene crystals. Feldspars display a poikiloblastic texture with quartz often filling the inclusions, they also show occasional crystal zoning.

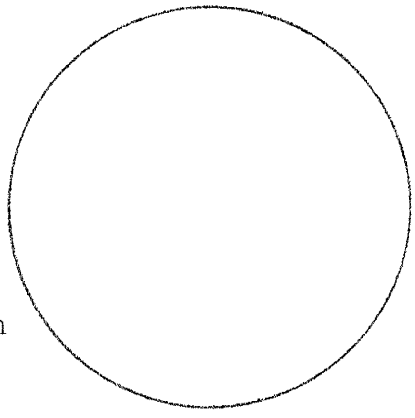

Mineralization

Rock Classification Diabase

Possible Parentage

Discussion The cluster of quartz crystal displays a low 2V biaxial figure, indicating strain has occurred with the unit.

Petrographic Description

DATE: 1-21-80

Sample #: 45

Essential Minerals	%
Quartz	95

Secondary or Alteration products	%
Sericitization	4

Varietal Minerals	%
Chalcedony	1

Plagioclase composition (Michel-Levy)

No plagioclase present

Metamorphic grade

Accessory Minerals %

Textures

Open space filling with the c-axis of euhedral quartz crystals growing perpendicular to the cavity. The open space is filled with later(?) fine-grained to microcrystalline quartz. Quartz crystals often show polygonal texture and the boundaries are often straight. Undulatory extinction is common.

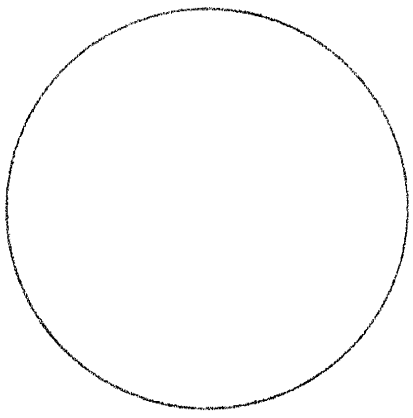

Mineralization Hematite - minor veinlets in the section

Rock Classification Hydrothermal quartz vein

Possible Parentage

Discussion

Petrographic Description

DATE: 1-27-80

Sample #: 46

Essential Minerals	%
Microcline	25
Quartz	40
Orthoclase	15

Secondary or Alteration products	%
Sericite	10
Magnetite	

Varietal Minerals	%
Analcite(?)	10(+)
Plagioclase	

Plagioclase composition (Michel-Levy)

Not enough to determine composition.

Metamorphic grade

Amphibolite

Accessory Minerals	%
Plagioclase	1
Zircon	tr

Textures

Petrofabric is cataclastic (i.e. there is no pronounced foliation) with porphyroblasts of orthoclase, microcline and lithic-fragments of chert(?). Porphyroblasts are sericitized, recrystallized poikiloblastic and show pressure shadows and minor graphic texture. Aggregates of quartz grains display sutured boundaries and undulatory extinction.

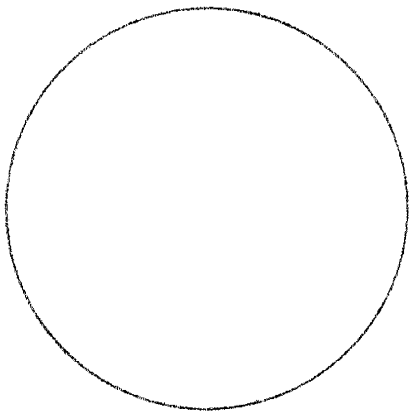

Mineralization

Rock Classification: Cataclastic granite (Alteration Zone)

Possible Parentage: Granite

Discussion: The rock is granitic facies of the ptu unit. Analcite looks like chert fragments, but it has a lower relief, however it is not fibrous. Analcite is believed to be a deuteric product.

Petrographic Description

DATE: 1-26-80

Sample #: 47

Essential Minerals	%
Quartz	30
Orthoclase	25
Chlorite	10

Secondary or Alteration products	%
Sericite (extensive) and muscovite	25
Magnetite	10

Varietal Minerals	%
Plagioclase(?)	?

Plagioclase composition (Michel-Levy)

Labradorite An 51, very difficult due to alteration

Accessory Minerals	%
Zircon	tr
Apatite (hi-relief)	

Metamorphic grade Lower amphibolite to upper green schist

Textures

Petrofabric is granoblastic to cataclastic with preferential alteration of plagioclase(?). This results in xenoblastic crystals of quartz and orthoclase in a sea of sericite. Most grain edges are sutured and some quartz crystals have a low 2V biaxial figure (strained). There are secondary cryptocrystalline quartz veins that cross-cut the petrofabric. Only a trace of graphic texture was observed and the orthoclase grains are seldom poikiloblastic.

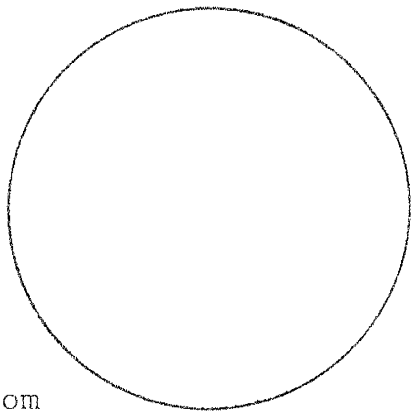

Mineralization

Rock Classification Sericitized - granite (pEu) (Alteration Zone)

Possible Parentage Granite

Discussion The rock unit is the granitic facies of the pEu unit, that has undergone intense hydrothermal alteration. The general trend of the alteration zone is east-west. Secondary quartz vein.

Petrographic Description

DATE: 2-1-80

Sample #: 48

Essential Minerals	%
Orthoclase (Altered)	22
Quartz (Crypto)	35

Secondary or Alteration products	%
Sericite (intense)	40
Magnetite	tr

Varietal Minerals	%
Microcline	3
Plagioclase	?

Plagioclase composition (Michel-Levy)

Too altered - no plag observed

Metamorphic grade

Accessory Minerals	%
Zircon	tr

Textures

Petrofabric is porphyritic with an aphanitic groundmass. Porphyroblasts are anhedral and the entire section is extremely sericitized.

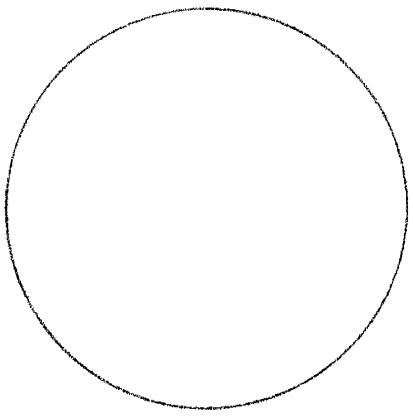

Mineralization

Rock Classification: Sericitic - Porphyritic Rhyolite(?)

Possible Parentage: Porphyritic Rhyolite(?)

Discussion

Sample locations and preparation
Appendix II and III

For sample locations see the airphoto on the following page.

Samples:

a, b, c, d = Chloride granite (analysis #2)

e, f, g, h = Precambrian granite (analysis #1 and 1-a)

At each location for the Chloride granite (a,b,c,d) three representative hand specimens were collected within a 200 yard radius. All of the samples for the Chloride granite (a,b,c,d) were homogenized, crushed and then fresh pieces were hand picked. The fresh pieces were again homogenized and then made into a fine powder for pelletization and X-ray analysis. Part of sample (a) was made into a thin section and stained for potassium. The same method was employed for the Precambrian granite samples (e,f,g,h), with part of sample (h) being made into a thin section.

Samples:

3, 4, 5, 6, 7, 8, 9, 10 = Amphibolite samples

At each location three representative hand specimens were collected within a 200 yard radius. For each sample location the hand specimens were crushed and homogenized, and then fresh pieces were picked. The fresh pieces were again homogenized and then made into a powder for pelletization and X-ray analyis. Two pellets were made from sample location seven (7, 7-a) for a duplicate run. Part of samples 3, 4, 6, 7, 8, 9, 10 were made into thin sections.

SAMPLE LOCATION

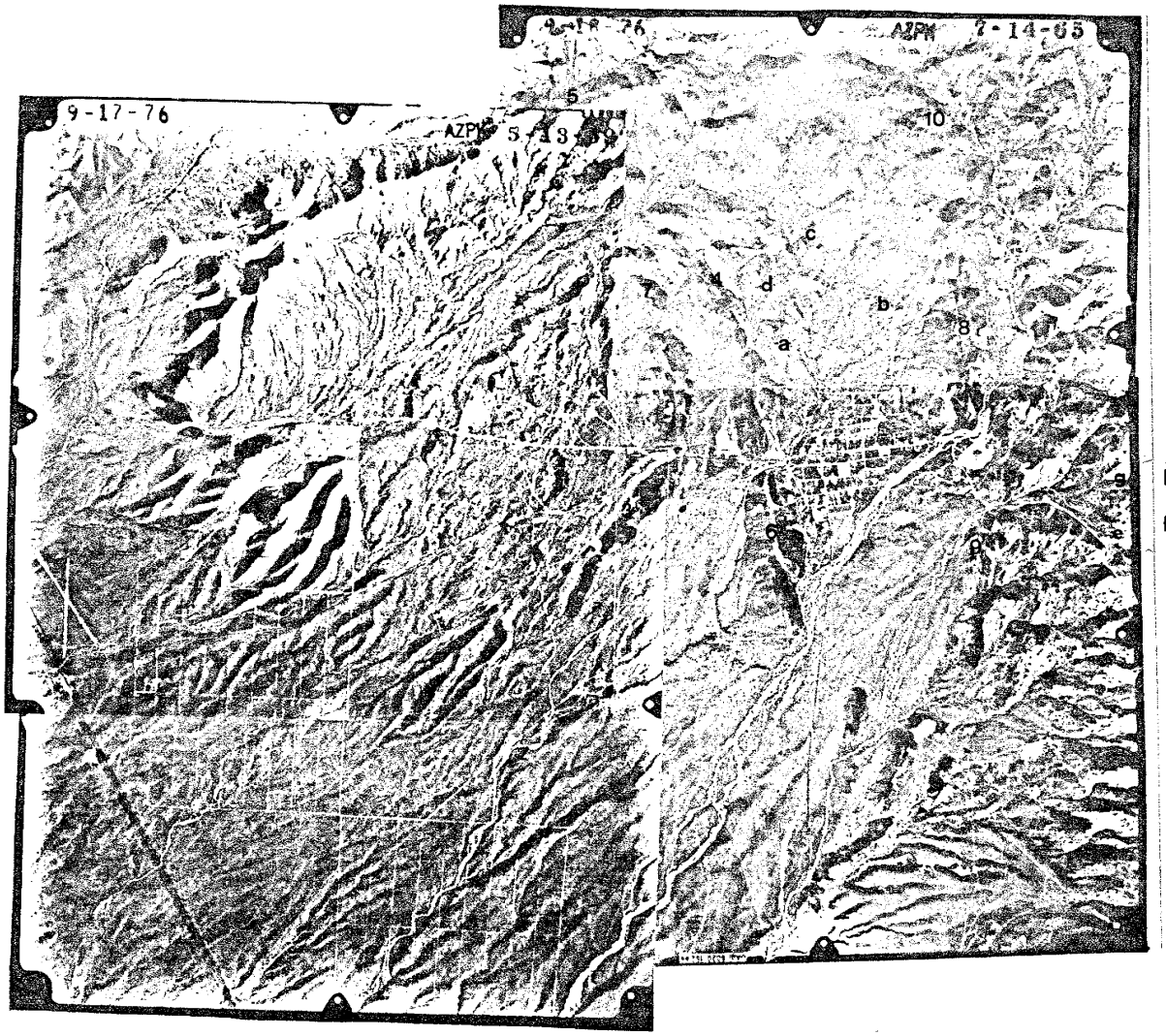

Appendix IV

X-ray Fluorescence settings and U.S.G.S. Standards

Machine: X-ray Fluorescence Universal Vacuum Spectrograph

Kv/Ma = 50/45 Tube: Cr Hv: 2100 Pha: .18 + .32

Elem.	Peak	Bkg.	Coll.	Crystal	Gain	Fix Time
Fe	33.62	34.60	F	Qtz	2.8x4	1 sec.
Ti	48.51	47.60	F	Qtz	3x4	2 sec.
Ca	60.27	59.30	F	Qtz	4x4	1 sec.
K	68.00	67.00	F	Qtz	4x4	2 sec.
Si	56.00	57.30	C	Gyp	3.5x8	5 sec.
Al	66.62	65.40	C	Gyp	3.5x8	10 sec.
Mg	81.35	80.50	C	Gyp	4.5x8	50 sec.
Na	103.30	105.00	C	Gyp	5x16	100 sec.

Machine: X-ray Fluorescence Universal Vacuum Spectrograph

Kv/Ma = 50/45 Tube: W Hv: 2100 Pha: .18 + .32

Elem.	Peak	Bkg.	Coll.	Crystal	Gain	Fix Time
Mn	36.67	37.70	F	Qtz	2.8x4	1 sec.

Std.	Basalt BRC-1	Basalt JB-1	Andesite BR	Andesite AGV-1	Diabase W-1	Granite G-2	Granite GH
SiO_2	54.50	52.09	38.20	59.00	52.64	69.11	75.80
TiO_2	2.20	1.34	2.60	1.04	1.07	0.50	0.08
Al_2O_3	13.61	14.53	10.20	17.25	15.00	15.40	12.50
Fe_2O_3	3.68	2.30	5.58	4.51			
FeO	8.80	6.06	6.57	2.05	1.04	1.08	0.41
Total Fe	13.40	9.04	12.88	6.76	8.72	2.65	0.84
MgO	3.46	7.70	13.28	1.53	11.09	2.65	1.34
CaO	6.92	9.21	13.80	4.90	10.96	1.94	0.69
Na_2O	3.27	2.79	3.05	4.26	2.15	4.07	3.85
K_2O	1.70	1.42	1.40	2.89	0.64	4.51	4.76
$H_2O^{(+)(-)}$	.77+.80	1.00+.98	2.30+.50	0.81+0.16	0.53+0.16	0.55+0.11	0.46+0.06
Loss on ignition							
MnO	0.18	0.16	0.20	0.097	0.17	0.34	0.05
P_2O_5	0.36	0.26	1.04	0.49	0.14	0.14	0.01
Total	100.28	100.03	99.64	99.91	100.26	99.73	99.86
Cu ppm	18.4	52	70	59.7	110	11.7	12
Ni	15.8	139	270	18.5	76	5.1	3
Co	38	39	150	14.1	47	5.5	1.5
Zn	120	83	160	84	86	85	80
Cr	17.6	417	420	12.2	114	7	6
S	392	50	-	<10	123	24	-

Appendix V

Original wt. pct. oxides

CIPW norm values

Thornton and Tuttle differentiation index

Barth's cations

Niggli values

GRANITES

ORIGINAL WT.PCT. OXIDES

SIO2	AL203	FE203	FEO	MGO	CAO	NA2O	K2O	H2O	TIO2	P2O5	MNO	ZRO2	CO2	SO3	CL	F	S	CR2O3	NIO	BAO
69.10	15.34	1.87	2.03	2.50	2.98	3.19	3.60	0.00	0.37	0.00	0.25	0.00	0.00	0.00	0.00	0.00	0.00	0.00	0.00	0.00

SUM OF ORIGINAL OXIDES=101.23

CIPW NORM FOR SAMPLE NO. 1

CONSTITUENTS	SIO2	AL2O3	FE2O3	FEO	MGO	CAO	NA2O	K2O	H2O	TIO2	P2O5	AL2O3/SIO2
PERCENTAGES	68.26	15.15	1.85	2.01	2.47	2.94	3.15	3.56	0.00	0.37	0.00	0.222
MOL. AMTS.	1.1361	0.1486	0.0116	0.0279	0.0613	0.0525	0.0508	0.0378	0.0000	0.0046	0.0000	

CONSTITUENTS	MNO	ZRO2	CO2	SO3	CL	F	S	CR2O3	NIO	BAO	FEO/FE2O3
PERCENTAGES	0.25	0.00	0.00	0.00	0.00	0.00	0.00	0.00	0.00	0.00	1.086
MOL. AMTS.	0.0035	0.0000	0.0000	0.0000	0.0000	0.0000	0.0000	0.0000	0.0000	0.0000	

MINERALS	Q	C	Z	OR	AB	AN	LC	NE	KP	HL	TH	NC
MOL.AMTS.	0.4230	0.0075	0.0000	0.0378	0.0508	0.0525	0.0000	0.0000	0.0000	0.0000	0.0000	0.0000
PERCENTAGES	25.416	0.768	0.000	21.015	26.665	14.604	0.000	0.000	0.000	0.000	0.000	0.000

MINERALS	AC	NS	KS	WO	EN	FS	FO	FA	CS	MT	CM	HM
MOL.AMTS.	0.0000	0.0000	0.0000	0.0000	0.0613	0.0153	0.0000	0.0000	0.0000	0.0116	0.0000	0.0000
PERCENTAGES	0.000	0.000	0.000	0.000	6.151	2.012	0.000	0.000	0.000	2.678	0.000	0.000

MINERALS	IL	TN	PF	RU	AP	FR	PR	CC	MG	TOTAL	SALIC	FEMIC
MOL.AMTS.	0.0046	0.0000	0.0000	0.0000	0.0000	0.0000	0.0000	0.0000	0.0000			
PERCENTAGES	0.694	0.000	0.000	0.000	0.000	0.000	0.000	0.000	0.000	100.003	88.468	11.535

MINERALS	DI	DI-WO	DI-EN	DI-FS	HY	HY-EN	HY-FS	OL	OL-FO	OL-FA	WOL
MOL. AMTS.	0.0000	0.0000	0.0000	0.0000	0.0765	0.0613	0.0153	0.0000	0.0000	0.0000	0.0000
PERCENTAGES	0.000	0.000	0.000	0.000	8.163	6.151	2.012	0.000	0.000	0.000	0.000

THORNTON & TUTTLE DIFFERENTIATION INDEX = 73.096

BARTHS CATIONS	SI	AL	FE+3	FE+2	MG	CA	NA	K	H	TI	P	MN
	63.70	16.67	1.30	1.57	3.44	2.94	5.70	4.23	0.00	0.26	0.00	0.20

	ZR	C	S1	CL	F	S2	CR	NI	BA
	0.00	0.00	0.00	0.00	0.00	0.00	0.00	0.00	0.00

NIGGLI VALUES	AL*	FM*	C*	ALK*	SI	RI	P	H	K	MG	SI'	QZ
	36.65	28.56	12.95	21.85	280.16	1.13	0.00	0.00	0.43	0.53	187.39	92.77

GRANITES

ORIGINAL WT.PCT. OXIDES

SIO2	AL203	FE203	FEO	MGO	CAO	NA2O	K2O	H2O	TIO2	P2O5	MNO	ZRO2	CO2	SO3	CL	F	S	CR2O3	NIO	BAO
69.70	15.34	1.86	2.10	2.42	2.97	3.16	3.62	0.00	0.36	0.00	0.23	0.00	0.00	0.00	0.00	0.00	0.00	0.00	0.00	0.00

SUM OF ORIGINAL OXIDES=101.76

CIPW NORM FOR SAMPLE NO. 1-a

CONSTITUENTS	SIO2	AL203	FE203	FEO	MGO	CAO	NA2O	K2O	H2O	TIO2	P2O5	AL203/SIO2
PERCENTAGES	68.56	15.07	1.83	2.06	2.38	2.92	3.11	3.56	0.00	0.35	0.00	0.220
MOL. AMTS.	1.1400	0.1479	0.0114	0.0287	0.0590	0.0520	0.0501	0.0378	0.0000	0.0044	0.0000	

CONSTITUENTS	MNO	ZRO2	CO2	SO3	CL	F	S	CR2O3	NIO	BAO	FEO/FE2O3
PERCENTAGES	0.22	0.00	0.00	0.00	0.00	0.00	0.00	0.00	0.00	0.00	1.129
MOL. AMTS.	0.0032	0.0000	0.0000	0.0000	0.0000	0.0000	0.0000	0.0000	0.0000	0.0000	

MINERALS	Q	C	Z	OR	AB	AN	LC	NF	KP	HL	TH	NC
MOL.AMTS.	0.4337	0.0079	0.0000	0.0378	0.0501	0.0520	0.0000	0.0000	0.0000	0.0000	0.0000	0.0000
PERCENTAGES	26.058	0.809	0.000	21.022	26.277	14.480	0.000	0.000	0.000	0.000	0.000	0.000

MINERALS	AC	NS	KS	WO	EN	FS	FO	FA	CS	NT	CM	BM
MOL.AMTS.	0.0000	0.0000	0.0000	0.0000	0.0590	0.0160	0.0000	0.0000	0.0000	0.0114	0.0000	0.0000
PERCENTAGES	0.000	0.000	0.000	0.000	5.923	2.112	0.000	0.000	0.000	2.650	0.000	0.000

MINERALS	IL	LN	PF	RU	AP	FR	PR	CC	MG	TOTAL	SALIC	FEMIC
MOL.AMTS.	0.0044	0.0000	0.0000	0.0000	0.0000	0.0000	0.0000	0.0000	0.0000			
PERCENTAGES	0.672	0.000	0.000	0.000	0.000	0.000	0.000	0.000	0.000	100.003	88.646	11.357

MINERALS	DI	DI-WO	DI-EN	DI-FS	HY	HY-EN	HY-FS	OL	OL-FO	OL-FA	WOL
MOL. AMTS.	0.0000	0.0000	0.0000	0.0000	0.0750	0.0590	0.0160	0.0000	0.0000	0.0000	0.0000
PERCENTAGES	0.000	0.000	0.000	0.000	8.035	5.923	2.112	0.000	0.000	0.000	0.000

THORNTON & TUTTLE DIFFERENTIATION INDEX = 73.357

BARTHS CATIONS	SI	AL	FE+3	FE+2	MG	CA	NA	K	H	TI	P	MN
	63.98	16.60	1.28	1.61	3.31	2.92	5.62	4.24	0.00	0.25	0.00	0.18

	ZR	C	S1	CL	F	S2	CR	NI	BA
	0.00	0.00	0.00	0.00	0.00	0.00	0.00	0.00	0.00

NIGGLI VALUES	AL*	FM*	C*	ALK*	SI	RI	P	H	K	MG	SI'	QZ
	36.82	28.33	12.96	21.88	283.91	1.10	0.00	0.00	0.43	0.52	187.53	96.38

GRANITES

ORIGINAL WT.PCT. OXIDES

SIO2	AL203	FE203	FEO	MGO	CAO	NA2O	K2O	H2O	TIO2	P2O5	MNO	ZRO2	CO2	SO3	CL	F	S	CR2O3	NIO	BAO
74.87	15.37	1.53	0.22	1.61	1.51	2.95	5.26	0.00	0.03	0.00	0.23	0.00	0.00	0.00	0.00	0.00	0.00	0.00	0.00	0.00

SUM OF ORIGINAL OXIDES=103.57

CIPW NORM FOR SAMPLE NO. 2

CONSTITUENTS	SIO2	AL2O3	FE2O3	FEO	MGO	CAO	NA2O	K2O	H2O	TIO2	P2O5	AL2O3/SIO2
PERCENTAGES	72.29	14.84	1.48	0.21	1.55	1.46	2.85	5.08	0.00	0.03	0.00	0.205
MOL. AMTS.	1.2031	0.1455	0.0093	0.0030	0.0385	0.0260	0.0459	0.0539	0.0000	0.0004	0.0000	

CONSTITUENTS	MNO	ZRO2	CO2	SO3	CL	F	S	CR2O3	NIO	BAO	FEO/FE2O3
PERCENTAGES	0.22	0.00	0.00	0.00	0.00	0.00	0.00	0.00	0.00	0.00	0.144
MOL. AMTS.	0.0031	0.0000	0.0000	0.0000	0.0000	0.0000	0.0000	0.0000	0.0000	0.0000	

MINERALS	Q	C	Z	OR	AB	AN	LC	NE	KP	HL	TH	NC
MOL.AMTS.	0.5137	0.0197	0.0000	0.0539	0.0459	0.0260	0.0000	0.0000	0.0000	0.0000	0.0000	0.0000
PERCENTAGES	30.868	2.013	0.000	30.011	24.077	7.228	0.000	0.000	0.000	0.000	0.000	0.000

MINERALS	AC	NS	KS	WO	EN	FS	FO	FA	CS	MI	CM	HM
MOL.AMTS.	0.0000	0.0000	0.0000	0.0000	0.0385	0.0000	0.0000	0.0000	0.0000	0.0057	0.0000	0.0036
PERCENTAGES	0.000	0.000	0.000	0.000	3.864	0.000	0.000	0.000	0.000	1.310	0.000	0.574

MINERALS	IL	TN	PF	RU	AP	FR	PR	CC	MG	TOTAL	SALIC	FEMIC
MOL.AMTS.	0.0004	0.0000	0.0000	0.0000	0.0000	0.0000	0.0000	0.0000	0.0000			
PERCENTAGES	0.057	0.000	0.000	0.000	0.000	0.000	0.000	0.000	0.000	100.003	94.198	5.805

MINERALS	DI	DI-WO	DI-EN	DI-FS	HY	HY-EN	HY-FS	OL	OL-FO	OL-FA	WOL
MOL. AMTS.	0.0000	0.0000	0.0000	0.0000	0.0385	0.0385	0.0000	0.0000	0.0000	0.0000	0.0000
PERCENTAGES	0.000	0.000	0.000	0.000	3.864	3.864	0.000	0.000	0.000	0.000	0.000

THORNTON & TUTTLE DIFFERENTIATION INDEX = 84.956

BARTHS CATIONS	SI	AL	FE+3	FE+2	MG	CA	NA	K	H	TI	P	MN
	67.47	16.32	1.04	0.17	2.16	1.46	5.15	6.05	0.00	0.02	0.00	0.17
		ZR	C	S1	CL	F	S2	CR	NI	BA		
		0.00	0.00	0.00	0.00	0.00	0.00	0.00	0.00	0.00		

NIGGLI VALUES	AL*	FM*	C*	ALK*	SI	RI	P	H	K	MG	SI'	QZ
	43.53	18.85	7.77	29.85	359.81	0.11	0.00	0.00	0.54	0.61	219.41	140.40

AMPHIBOLITES

ORIGINAL WT.PCT. OXIDES

SIO2	AL203	FE203	FEO	MGO	CAO	NA2O	K2O	H2O	TIO2	P2O5	MNO	ZRO2	CO2	SO3	CL	F	S	CR2O3	NIO	BAO
47.30	13.46	2.41	8.21	9.23	14.03	2.25	0.21	0.00	0.91	0.00	0.21	0.00	0.00	0.00	0.00	0.00	0.00	0.00	0.00	0.00

SUM OF ORIGINAL OXIDES= 96.23

CIPW NORM FOR SAMPLE NO. 3

CONSTITUENTS	SIO2	AL203	FE203	FEO	MGO	CAO	NA2O	K2O	H2O	TIO2	P2O5	AL203/SIO2
PERCENTAGES	48.15	13.70	2.45	8.36	9.40	11.28	2.29	0.22	0.00	0.93	0.00	0.285
MOL. AMTS.	0.8014	0.1344	0.0154	0.1163	0.2331	0.2547	0.0370	0.0023	0.0000	0.0116	0.0000	

CONSTITUENTS	MNO	ZRO2	CO2	SO3	CL	F	S	CR2O3	NIO	BAO	FEO/FE2O3
PERCENTAGES	0.22	0.00	0.00	0.00	0.00	0.00	0.00	0.00	0.00	0.00	3.407
MOL. AMTS.	0.0031	0.0000	0.0000	0.0000	0.0000	0.0000	0.0000	0.0000	0.0000	0.0000	

MINERALS	Q	C	Z	UR	AB	AN	LC	NE	KP	HL	TH	NC
MOL.AMTS.	0.0000	0.0000	0.0000	0.0023	0.0303	0.0951	0.0000	0.0065	0.0006	0.0000	0.0000	0.0000
PERCENTAGES	0.000	0.000	0.000	1.281	15.905	26.466	0.000	1.883	0.000	0.000	0.000	0.000

MINERALS	AC	NS	KS	WO	EN	FS	FO	FA	CS	MT	CM	HM
MOL.AMTS.	0.0000	0.0000	0.0000	0.1596	0.1143	0.0453	0.0594	0.0236	0.0000	0.0154	0.0000	0.0000
PERCENTAGES	0.000	0.000	0.000	18.534	11.472	5.974	8.363	4.800	0.000	3.557	0.000	0.000

MINERALS	IL	PF	RU	AP	FR	PR	CC	MG	TOTAL	SALIC	FEMIC
MOL.AMTS.	0.0116	0.0000	0.0000	0.0000	0.0000	0.0000	0.0000	0.0000			
PERCENTAGES	1.767	0.000	0.000	0.000	0.000	0.000	0.000	0.000	100.003	45.535	54.467

MINERALS	DI	DI-AO	DI-EN	DI-FS	HY	HY-EN	HY-FS	OL	OL-FO	OL-FA	WOL
MOL. AMTS.	0.1596	0.1596	0.1143	0.0453	0.0000	0.0000	0.0000	0.0830	0.0594	0.0236	0.0000
PERCENTAGES	35.981	18.534	11.472	5.974	0.000	0.000	0.000	13.162	8.363	4.800	0.000

THORNTON & TUTTLE DIFFERENTIATION INDEX = 19.070

BARTHS CATIONS	SI	AL	FE+3	FE+2	MG	CA	NA	K	H	TI	P	MN
	44.56	14.95	1.71	6.47	12.96	14.16	4.11	0.26	0.00	0.65	0.00	0.17

	ZR	C	SI	CL	F	S2	CR	NI	BA
	0.00	0.00	0.00	0.00	0.00	0.00	0.00	0.00	0.00

NIGGLI VALUES	AL*	FM*	C*	ALK*	SI	FI	P	H	K	MG	SI*	QZ
	16.56	47.22	31.38	4.84	98.74	1.43	0.00	0.00	0.06	0.61	119.35	-20.61

AMPHIBOLITES

ORIGINAL WT.PCT. OXIDES

SIO2	AL2O3	FE2O3	FEO	MGO	CAO	NA2O	K2O	H2O	TIO2	P2O5	MNO	ZRO2	CO2	SO3	CL	F	S	CR2O3	NIO	BAO
47.85	13.24	2.58	7.98	9.25	14.03	2.01	0.23	0.00	1.08	0.00	0.24	0.00	0.00	0.00	0.00	0.00	0.00	0.00	0.00	0.00

SUM OF ORIGINAL OXIDES= 98.48

CIPW NORM FOR SAMPLE NO. 4

CONSTITUENTS	SIO2	AL2O3	FE2O3	FEO	MGO	CAO	NA2O	K2O	H2O	TIO2	P2O5	AL2O3/SIO2
PERCENTAGES	48.59	13.44	2.62	8.10	9.39	14.25	2.04	0.23	0.00	1.10	0.00	0.277
MOL. AMTS.	0.8086	0.1319	0.0164	0.1128	0.2330	0.2540	0.0329	0.0025	0.0000	0.0137	0.0000	

CONSTITUENTS	MNO	ZRO2	CO2	SO3	CL	F	S	CR2O3	NIO	BAO	FEO/FE2O3
PERCENTAGES	0.24	0.00	0.00	0.00	0.00	0.00	0.00	0.00	0.00	0.00	3.093
MOL. AMTS.	0.0034	0.0000	0.0000	0.0000	0.0000	0.0000	0.0000	0.0000	0.0000	0.0000	

MINERALS	Q	C	Z	OR	AB	AN	LC	NE	KP	HL	TH	NC
MOL.AMTS.	0.0000	0.0000	0.0000	0.0025	0.0329	0.0955	0.0000	0.0000	0.0000	0.0000	0.0000	0.0000
PERCENTAGES	0.000	0.000	0.000	1.368	17.236	26.856	0.000	0.000	0.000	0.000	0.000	0.000

MINERALS	AC	NS	KS	WO	EN	FS	FO	FA	CS	MT	CM	HM
MOL.AMTS.	0.0000	0.0000	0.0000	0.1575	0.1265	0.0467	0.0533	0.0197	0.0000	0.0164	0.0000	0.0000
PERCENTAGES	0.000	0.000	0.000	8.296	12.699	6.165	7.493	4.009	0.000	3.798	0.000	0.000

MINERALS	IL	TN	PF	RU	AP	FR	PR	CC	MG	TOTAL	SALIC	FEMIC
MOL.AMTS.	0.0137	0.0000	0.0000	0.0000	0.0000	0.0000	0.0000	0.0000	0.0000			
PERCENTAGES	2.083	0.000	0.000	0.000	0.000	0.000	0.000	0.000	0.000	100.003	45.460	54.543

MINERALS	DI	DI-WO	DI-EN	DI-FS	HY	HY-EN	HY-FS	OL	OL-FO	OL-FA	WOL
MOL. AMTS.	0.1575	0.1575	0.1150	0.0425	0.0157	0.0115	0.0042	0.0729	0.0533	0.0197	0.0000
PERCENTAGES	35.449	18.296	11.547	5.605	1.711	1.152	0.559	11.502	7.493	4.009	0.000

THORNTON & TUTTLE DIFFERENTIATION INDEX = 18.604

BARTHS CATIONS	SI	AL	FE+3	FE+2	MG	CA	NA	K	H	TI	P	MN
	45.11	14.71	1.83	6.29	13.00	14.17	3.67	0.27	0.00	0.77	0.00	0.19
		ZR	C	S1	CL	F	S2	CR	NI	BA		
		0.00	0.00	0.00	0.00	0.00	0.00	0.00	0.00	0.00		

NIGGLI VALUES	AL*	FM*	C*	ALK*	SI	RI	P	H	K	MG	SI'	QZ
	16.42	47.56	31.63	4.40	100.67	1.71	0.00	0.00	0.07	0.61	117.59	-16.92

AMPHIBOLITES

ORIGINAL WT.PCT. OXIDES

SIO2	AL2O3	FE2O3	FEO	MGO	CAO	NA2O	K2O	H2O	TIO2	P2O5	MNO	ZRO2	CO2	SO3	CL	F	S	CR2O3	NIO	BAO
47.98	13.03	2.48	8.34	9.11	13.06	2.20	0.00	0.00	0.98	0.00	0.24	0.06	0.00	0.00	0.00	0.00	0.00	0.00	0.00	0.00

SUM OF ORIGINAL OXIDES= 97.40

CIPW NORM FOR SAMPLE NO. 5

CONSTITUENTS	SIO2	AL2O3	FE2O3	FEO	MGO	CAO	NA2O	K2O	H2O	TIO2	P2O5	AL2O3/SIO2
PERCENTAGES	49.26	13.38	2.55	8.56	9.38	13.35	2.26	0.00	0.00	1.01	0.00	0.272
MOL. AMTS.	0.8199	0.1312	0.0159	0.1192	0.2328	0.2380	0.0365	0.0000	0.0000	0.0126	0.0000	

CONSTITUENTS	MNO	ZRO2	CO2	SO3	CL	F	S	CR2O3	NIO	BAO	FEO/FE2O3
PERCENTAGES	0.25	0.00	0.00	0.00	0.00	0.00	0.00	0.00	0.00	0.00	3.363
MOL. AMTS.	0.0035	0.0000	0.0000	0.0000	0.0000	0.0000	0.0000	0.0000	0.0000	0.0000	

MINERALS	Q	C	Z	OR	AB	AN	LC	NE	KP	NS	TN	NC
MOL.AMTS.	0.0000	0.0000	0.0000	0.0000	0.0365	0.0947	0.0000	0.0000	0.0000	0.0000	0.0000	0.0000
PERCENTAGES	0.000	0.000	0.000	0.024	19.122	26.348	0.000	0.000	0.000	0.000	0.000	0.000

MINERALS	AC	NS	KS	WO	EN	FS	FO	FA	CS	MI	CM	HM
MOL.AMTS.	0.0000	0.0000	0.0000	0.1433	0.1491	0.0603	0.0418	0.0169	0.0000	0.0159	0.0000	0.0000
PERCENTAGES	0.000	0.000	0.000	16.647	14.969	7.952	5.888	3.447	0.000	3.692	0.000	0.000

MINERALS	IL	TN	PF	RU	AP	FR	PR	CC	MG	TOTAL	SALIC	FEMIC
MOL.AMTS.	0.0126	0.0000	0.0000	0.0000	0.0000	0.0000	0.0000	0.0000	0.0000			
PERCENTAGES	1.913	0.000	0.000	0.000	0.000	0.000	0.000	0.000	0.000	100.003	45.494	54.509

MINERALS	DI	DI-WO	DI-EN	DI-FS	HY	HY-EN	HY-FS	OL	OL-FO	OL-FA	WOL
MOL. AMTS.	0.1433	0.1433	0.1021	0.0413	0.0661	0.0470	0.0190	0.0588	0.0418	0.0169	0.0000
PERCENTAGES	32.336	16.647	10.246	5.443	7.233	4.724	2.509	9.335	5.888	3.447	0.000

THORNTON & TUTTLE DIFFERENTIATION INDEX = 19.146

BARTHS CATIONS	SI	AL	FE+3	FE+2	MG	CA	NA	K	H	TI	P	MN
	45.72	14.63	1.78	6.65	12.98	13.27	4.07	0.00	0.00	0.70	0.00	0.19

	ZR	C	S1	CL	F	S2	CR	NI	BA
	0.00	0.00	0.00	0.00	0.00	0.00	0.00	0.00	0.00

NIGGLI VALUES	AL*	FM*	C*	ALK*	SI	RI	P	H	K	MG	SI*	QZ
	16.54	48.84	30.01	4.60	103.38	1.59	0.00	0.00	0.00	0.60	118.41	-15.03

AMPHIBOLITES

ORIGINAL WT.PCT. OXIDES

SIO2	AL2O3	FE2O3	FEO	MGO	CAO	NA2O	K2O	H2O	TIO2	P2O5	MNO	ZRO2	CO2	SO3	CL	F	S	CR2O3	NIO	BAO
47.71	14.19	2.89	6.70	8.20	13.36	2.48	0.27	0.00	1.39	0.00	0.23	0.00	0.00	0.00	0.00	0.00	0.00	0.00	0.00	0.00

SUM OF ORIGINAL OXIDES= 97.42

CIPW NORM FOR SAMPLE NO. 6

CONSTITUENTS	SIO2	AL2O3	FE2O3	FEO	MGO	CAO	NA2O	K2O	H2O	TIO2	P2O5	AL2O3/SIO2
PERCENTAGES	48.97	14.57	2.97	5.88	8.42	13.71	2.55	0.28	0.00	1.43	0.00	0.297
MOL. AMTS.	0.8150	0.1429	0.0186	0.0957	0.2088	0.2445	0.0411	0.0030	0.0000	0.0179	0.0000	

CONSTITUENTS	MNO	ZRO2	CO2	SO3	CL	F	S	CR2O3	NIO	BAO	FE2O/FE2O3
PERCENTAGES	0.24	0.00	0.00	0.00	0.00	0.00	0.00	0.00	0.00	0.00	2.318
MOL. AMTS.	0.0033	0.0000	0.0000	0.0000	0.0000	0.0000	0.0000	0.0000	0.0000	0.0000	

MINERALS	Q	C	Z	OR	AB	AN	LC	NE	KP	HL	TN	NC
MOL.AMTS.	0.0000	0.0000	0.0000	0.0030	0.0408	0.0988	0.0000	0.0003	0.0000	0.0000	0.0000	0.0000
PERCENTAGES	0.000	0.000	0.000	1.656	21.387	27.484	0.000	0.028	0.000	0.000	0.000	0.000

MINERALS	AC	NS	KS	WO	EN	FS	FO	FA	CS	MI	CM	KM
MOL.AMTS.	0.0000	0.0000	0.0000	0.1457	0.1121	0.0336	0.0463	0.0145	0.0000	0.0186	0.0000	0.0000
PERCENTAGES	0.000	0.000	0.000	16.930	11.257	4.436	6.801	2.954	0.000	4.301	0.000	0.000

MINERALS	IL	IN	PF	RU	AP	FR	PR	CC	MG	TOTAL	SALIC	FEMIC
MOL.AMTS.	0.0179	0.0000	0.0000	0.0000	0.0000	0.0000	0.0000	0.0000	0.0000			
PERCENTAGES	2.710	0.000	0.000	0.000	0.000	0.000	0.000	0.000	0.000	100.003	50.614	49.389

MINERALS	DI	DI-WO	DI-EN	DI-FS	HY	HY-EN	HY-FS	OL	OL-FO	OL-FA	WOL
MOL. AMTS.	0.1457	0.1457	0.1121	0.0336	0.0000	0.0000	0.0000	0.0628	0.0483	0.0145	0.0000
PERCENTAGES	32.623	16.930	11.257	4.436	0.000	0.000	0.000	9.755	6.801	2.954	0.000

THORNTON & TUTTLE DIFFERENTIATION INDEX = 23.130

BARTHS CATIONS.	SI	AL	FE+3	FE+2	MG	CA	NA	K	H	TI	P	MN
	45.37	15.91	2.07	5.33	11.62	13.61	4.57	0.33	0.00	0.99	0.00	0.19

	ZR	C	S1	CL	F	S2	CR	NI	BA
	0.00	0.00	0.00	0.00	0.00	0.00	0.00	0.00	0.00

NIGGLI VALUES	AL*	FM*	C*	ALK*	SI	PI	P	H	K	MG	SI'	QZ
	18.40	44.43	31.49	5.67	104.97	2.30	0.00	0.00	0.07	0.61	122.70	-17.73

AMPHIBOLITES

ORIGINAL WT.PCT. OXIDES

SIO2	AL203	FE203	FEO	MGO	CAO	NA2O	K2O	P2O	TIO2	P2O5	MNO	ZRO2	CO2	SO3	CL	F	S	CR2O3	NIO	BAO
45.75	13.50	2.69	8.24	8.90	14.73	1.72	0.48	0.00	1.19	0.00	0.10	0.00	0.00	0.00	0.00	0.00	0.00	0.00	0.00	0.00

SUM OF ORIGINAL OXIDES= 97.30

CIPW NORM FOR SAMPLE NO. 7

CONSTITUENTS	SIO2	AL203	FE203	FEO	MGO	CAO	NA2O	K2O	H2O	TIO2	P2O5	AL203/SIO2
PERCENTAGES	47.02	13.87	2.76	8.47	9.15	15.14	1.77	0.49	0.00	1.22	0.00	0.295
MOL. AMTS.	0.7825	0.1361	0.0173	0.1179	0.2269	0.2699	0.0285	0.0052	0.0000	0.0153	0.0000	

CONSTITUENTS	MNO	ZRO2	CO2	SO3	CL	F	S	CR2O3	NIO	BAO	FEO/FE2O3
PERCENTAGES	0.10	0.00	0.00	0.00	0.00	0.00	0.00	0.00	0.00	0.00	3.063
MOL. AMTS.	0.0015	0.0000	0.0000	0.0000	0.0000	0.0000	0.0000	0.0000	0.0000	0.0000	

MINERALS	Q	C	Z	OR	AB	AN	LC	NE	KP	HL	TH	RC
MOL.AMTS.	0.0000	0.0000	0.0000	0.0052	0.0203	0.1023	0.0000	0.0082	0.0000	0.0000	0.0000	0.0000
PERCENTAGES	0.000	0.000	0.000	2.971	10.637	28.463	0.000	2.341	0.000	0.000	0.000	0.000

MINERALS	AC	NS	KS	WO	EN	FS	FO	FA	CS	MT	CM	HM
MOL.AMTS.	0.0000	0.0000	0.0000	0.1676	0.1213	0.0464	0.0528	0.0202	0.0000	0.0173	0.0000	0.0000
PERCENTAGES	0.000	0.000	0.000	19.474	12.177	6.115	7.430	4.112	0.000	4.008	0.000	0.000

MINERALS	IL	TN	PF	RU	AP	FR	PR	CC	MG	TOTAL	SALIC	FEMIC
MOL.AMTS.	0.0153	0.0000	0.0000	0.0000	0.0000	0.0000	0.0000	0.0000	0.0000			
PERCENTAGES	2.323	0.000	0.000	0.000	0.000	0.000	0.000	0.000	0.000	100.001	44.361	55.640

MINERALS	DI	DI-WO	DI-EN	DI-FS	HY	HY-EN	HY-FS	OL	OL-FO	OL-FA	WOL
MOL. AMTS.	0.1676	0.1676	0.1213	0.0464	0.0000	0.0000	0.0000	0.0730	0.0528	0.0202	0.0000
PERCENTAGES	37.766	19.474	12.177	6.115	0.000	0.000	0.000	11.543	7.430	4.112	0.000

THORNTON & TUTTLE DIFFERENTIATION INDEX = 15.899

BARTHS CATIONS	SI	AL	FE+3	FE+2	MG	CA	NA	K	H	TI	P	MN
	43.76	15.22	1.64	6.59	12.69	15.09	3.19	0.59	0.00	0.86	0.00	0.08

	ZR	C	S1	CL	F	S2	CR	NI	BA
	0.00	0.00	0.00	0.00	0.00	0.00	0.00	0.00	0.00

NIGGLI VALUES	AL*	FM*	C*	ALK*	SI	RI	P	H	K	MG	SI'	QZ
	16.58	46.41	32.89	4.11	95.36	1.87	0.00	0.00	0.16	0.60	116.46	-21.10

AMPHIBOLITES

ORIGINAL WT.PCT. OXIDES

SIO2	AL2O3	FE2O3	FEO	MGO	CAO	NA2O	K2O	H2O	TIO2	P2O5	MNO	ZRO2	CO2	SO3	CL	F	S	CR2O3	NIO	BAO
45.81	13.47	2.67	8.25	8.93	14.76	1.63	0.45	0.00	1.17	0.00	0.11	0.00	0.00	0.00	0.00	0.00	0.00	0.00	0.00	0.00

SUM OF ORIGINAL OXIDES= 97.25

CIPW NORM FOR SAMPLE NO. 7-a

CONSTITUENTS	SIO2	AL2O3	FE2O3	FEO	MGO	CAO	NA2O	K2O	H2O	TIO2	P2O5	AL2O3/SIO2
PERCENTAGES	47.10	13.85	2.75	8.48	9.18	15.18	1.68	0.46	0.00	1.20	0.00	0.294
MOL. AMTS.	0.7840	0.1358	0.0172	0.1181	0.2278	0.2706	0.0271	0.0049	0.0000	0.0151	0.0000	

CONSTITUENTS	MNO	ZRO2	CO2	SO3	CL	F	S	CR2O3	NIO	BAO	FEO/FE2O3
PERCENTAGES	0.11	0.00	0.00	0.00	0.00	0.00	0.00	0.00	0.00	0.00	3.090
MOL. AMTS.	0.0016	0.0000	0.0000	0.0000	0.0000	0.0000	0.0000	0.0000	0.0000	0.0000	

MINERALS	Q	C	Z	OR	AB	AN	LC	NE	KP	HL	TH	MC
MOL.AMTS.	0.0000	0.0000	0.0000	0.0049	0.0212	0.1038	0.0000	0.0059	0.0000	0.0000	0.0000	0.0000
PERCENTAGES	0.000	0.000	0.000	2.734	11.121	28.884	0.000	1.677	0.000	0.000	0.000	0.000

MINERALS	AC	NS	KS	WO	EN	FS	FO	FA	CS	MT	CM	HM
MOL.AMTS.	0.0000	0.0000	0.0000	0.1668	0.1206	0.0463	0.0536	0.0206	0.0000	0.0172	0.0000	0.0000
PERCENTAGES	0.000	0.000	0.000	19.378	12.103	6.103	7.544	4.192	0.000	3.981	0.000	0.000

MINERALS	IL	TN	PF	RU	AP	FR	PR	CC	MC	TOTAL	SALIC	FEMIC
MOL.AMTS.	0.0151	0.0000	0.0000	0.0000	0.0000	0.0000	0.0000	0.0000	0.0000			
PERCENTAGES	2.285	0.000	0.000	0.000	0.000	0.000	0.000	0.000	0.000	100.001	44.416	55.585

MINERALS	DI	DI-WO	DI-EN	DI-FS	HY	HY-EN	HY-FS	OL	OL-FO	OL-FA	WOL
MOL. AMTS.	0.1668	0.1668	0.1206	0.0463	0.0000	0.0000	0.0000	0.0742	0.0536	0.0206	0.0000
PERCENTAGES	37.584	19.378	12.103	6.103	0.000	0.000	0.000	11.736	7.544	4.192	0.000

THORNTON & TUTTLE DIFFERENTIATION INDEX = 15.532

BARTHS CATIONS	SI	AL	FE+3	FE+2	MG	CA	NA	K	H	TI	P	MN
	43.87	15.20	1.92	6.61	12.75	15.14	3.03	0.55	0.00	0.84	0.00	0.09
		ZR	C	S1	CL	F	S2	CR	NI	BA		
		0.00	0.00	0.00	0.00	0.00	0.00	0.00	0.00	0.00		

NIGGLI VALUES	AL*	FM*	C*	ALK*	SI	RI	P	H	K	MG	SI'	QZ
	16.56	46.55	32.99	3.90	95.57	1.84	0.00	0.00	0.15	0.60	115.61	-20.05

AMPHIBOLITES

ORIGINAL WT.PCT. OXIDES

SIO2	AL2O3	FE2O3	FEO	MGO	CAO	NA2O	K2O	P2O	TIO2	P2O5	MNO	ZRO2	CO2	SO3	CL	F	S	CR2O3	NIO	BAO
46.44	12.28	2.88	10.02	8.22	12.92	2.35	0.50	0.00	1.38	0.00	0.05	0.00	0.00	0.00	0.00	0.00	0.00	0.00	0.00	0.00

SUM OF ORIGINAL OXIDES= 97.04

CIPW NORM FOR SAMPLE NO. 6

CONSTITUENTS	SIO2	AL2O3	FE2O3	FEO	MGO	CAO	NA2O	K2O	H2O	TIO2	P2O5	AL2O3/SIO2
PERCENTAGES	47.86	12.65	2.97	10.33	8.47	13.31	2.42	0.51	0.00	1.42	0.00	0.264
MOL. AMTS.	0.7965	0.1241	0.0186	0.1437	0.2101	0.2374	0.0391	0.0055	0.0000	0.0178	0.0000	

CONSTITUENTS	MNO	ZRO2	CO2	SO3	CL	F	S	CR2O3	NIO	BAO	FEO/FE2O3
PERCENTAGES	0.05	0.00	0.00	0.00	0.00	0.00	0.00	0.00	0.00	0.00	3.479
MOL. AMTS.	0.0008	0.0000	0.0000	0.0000	0.0000	0.0000	0.0000	0.0000	0.0000	0.0000	

MINERALS	Q	C	Z	OR	AB	AN	LC	NE	KP	HL	TH	NC
MOL.AMTS.	0.0000	0.0000	0.0000	0.0055	0.0326	0.0796	0.0000	0.0065	0.0000	0.0000	0.0000	0.0000
PERCENTAGES	0.000	0.000	0.000	3.039	17.114	22.135	0.000	1.834	0.000	0.000	0.000	0.000

MINERALS	AC	NS	KS	WO	EN	FS	FO	FA	CS	MT	CM	HM
MOL.AMTS.	0.0000	0.0000	0.0000	0.1578	0.1042	0.0536	0.0529	0.0272	0.0000	0.0166	0.0000	0.0000
PERCENTAGES	0.000	0.000	0.000	18.336	10.464	7.074	7.450	5.551	0.000	4.303	0.000	0.000

MINERALS	IL	TN	PF	RU	AP	FR	PR	CC	MG	TOTAL	SALIC	FEMIC
MOL.AMTS.	0.0178	0.0000	0.0000	0.0000	0.0000	0.0000	0.0000	0.0000	0.0000	100.001	44.121	55.879
PERCENTAGES	2.701	0.000	0.000	0.000	0.000	0.000	0.000	0.000	0.000			

MINERALS	DI	DI-WO	DI-EN	DI-FS	HY	HY-EN	HY-FS	OL	OL-FO	OL-FA	WOL
MOL. AMTS.	0.1578	0.1578	0.1042	0.0536	0.0000	0.0000	0.0000	0.0802	0.0529	0.0272	0.0000
PERCENTAGES	35.874	18.336	10.464	7.074	0.000	0.000	0.000	13.001	7.450	5.551	0.000

THORNTON & TUTTLE DIFFERENTIATION INDEX = 21.986

BARTHS CATIONS	SI	AL	FE+3	FE+2	MG	CA	NA	K	H	TI	P	MN
	44.73	13.94	2.09	8.07	11.80	13.33	4.39	0.61	0.00	1.00	0.00	0.04
		ZR	C	S1	CL	F	S2	CR	NI	BA		
		0.00	0.00	0.00	0.00	0.00	0.00	0.00	0.00	0.00		

NIGGLI VALUES	AL*	FM*	C*	ALK*	SI	EI	P	H	K	MG	SI'	QZ
	15.56	49.10	29.76	5.58	99.83	2.23	0.00	0.00	0.12	0.54	122.33	-22.51

AMPHIBOLITES

ORIGINAL WT.PCT. OXIDES

SIO2	AL2O3	FE2O3	FEO	MGO	CAO	NA2O	K2O	H2O	TIO2	P2O5	MNO	ZRO2	CO2	SO3	CL	F	S	CR2O3	NIO	BAO
46.59	12.56	2.81	9.22	8.62	13.05	2.40	0.20	0.00	1.31	0.00	0.22	0.00	0.00	0.00	0.00	0.00	0.00	0.00	0.00	0.00

SUM OF ORIGINAL OXIDES= 98.98

CIPW NORM FOR SAMPLE NO. 9

CONSTITUENTS	SIO2	AL2O3	FE2O3	FEO	MGO	CAO	NA2O	K2O	H2O	TIO2	P2O5	AL2O3/SIO2
PERCENTAGES	48.04	12.95	2.90	9.51	8.89	13.46	2.47	0.21	0.00	1.35	0.00	0.270
MOL. AMTS.	0.7995	0.1270	0.0181	0.1323	0.2205	0.2399	0.0399	0.0022	0.0000	0.0169	0.0000	

CONSTITUENTS	MNO	ZRO2	CO2	SO3	CL	F	S	CR2O3	NIO	BAO	FEO/FE2O3
PERCENTAGES	0.23	0.00	0.00	0.00	0.00	0.00	0.00	0.00	0.00	0.00	3.261
MOL. AMTS.	0.0032	0.0000	0.0000	0.0000	0.0000	0.0000	0.0000	0.0000	0.0000	0.0000	

MINERALS	Q	C	Z	OR	AB	AN	LC	NE	KP	ND	TH	UC
MOL.AMTS.	0.0000	0.0000	0.0000	0.0022	0.0359	0.0849	0.0000	0.0040	0.0000	0.0000	0.0000	0.0000
PERCENTAGES	0.000	0.000	0.000	1.243	18.816	23.626	0.000	1.132	0.000	0.000	0.000	0.000

MINERALS	AC	NS	KS	WO	EN	FS	FO	FA	CS	MT	CM	HM
MOL.AMTS.	0.0000	0.0000	0.0000	0.1550	0.1065	0.0485	0.0570	0.0260	0.0000	0.0181	0.0000	0.0000
PERCENTAGES	0.000	0.000	0.000	18.008	10.691	6.402	8.023	5.295	0.000	4.201	0.000	0.000

MINERALS	IL	TN	PF	RU	AP	FR	PR	CC	MG	TOTAL	SALIC	FEMIC
MOL.AMTS.	0.0169	0.0000	0.0000	0.0000	0.0000	0.0000	0.0000	0.0000	0.0000			
PERCENTAGES	2.565	0.000	0.000	0.000	0.000	0.000	0.000	0.000	0.000	100.003	44.816	55.187

MINERALS	DI	DI-WO	DI-EN	DI-FS	HY	HY-EN	HY-FS	OL	OL-FO	OL-FA	WOL
MOL. AMTS.	0.1550	0.1550	0.1065	0.0485	0.0000	0.0000	0.0000	0.0830	0.0570	0.0260	0.0000
PERCENTAGES	35.102	18.008	10.691	6.402	0.000	0.000	0.000	13.319	8.023	5.295	0.000

THORNTON & TUTTLE DIFFERENTIATION INDEX = 21.190

BARTHS CATIONS	SI	AL	FE+3	FE+2	MG	CA	NA	K	H	TI	P	MN
	44.74	14.22	2.03	7.40	12.34	13.43	4.46	0.25	0.00	0.95	0.00	0.18
		ZR	C	S1	CL	F	S2	CR	NI	BA		
		0.00	0.00	0.00	0.00	0.00	0.00	0.00	0.00	0.00		

NIGGLI VALUES	AL*	FM*	C*	ALK*	SI	RI	P	H	K	MG	SI'	QZ
	15.85	48.96	29.94	5.25	99.76	2.11	0.00	0.00	0.05	0.56	121.01	-21.25

AMPHIBOLITES

ORIGINAL WT.PCT. OXIDES

SIO2	AL203	FE203	FEO	MGO	CAO	NA2O	K2O	H2O	TIO2	P2O5	MNO	ZRO2	CO2	SO3	CL	F	S	CR2O3	NIO	BAO
46.95	13.20	2.44	7.81	9.80	15.13	1.79	0.19	0.00	0.94	0.00	0.02	0.00	0.00	0.00	0.00	0.00	0.00	0.00	0.00	0.00

SUM OF ORIGINAL OXIDES= 98.26

CIPW NORM FOR SAMPLE NO. 10

CONSTITUENTS	SIO2	AL203	FE2O3	FEO	MGO	CAO	NA2O	K2O	H2O	TIO2	P2O5	AL2O3/SIO2
PERCENTAGES	47.78	13.43	2.48	7.95	9.97	15.40	1.82	0.19	0.00	0.95	0.00	0.281
MOL. AMTS.	0.7952	0.1318	0.0156	0.1106	0.2474	0.2746	0.0294	0.0020	0.0000	0.0119	0.0000	

CONSTITUENTS	MNO	ZRO2	CO2	SO3	CL	F	S	CR2O3	NIO	BAO	FEO/FE2O3
PERCENTAGES	0.02	0.00	0.00	0.00	0.00	0.00	0.00	0.00	0.00	0.00	3.201
MOL. AMTS.	0.0003	0.0000	0.0000	0.0000	0.0000	0.0000	0.0000	0.0000	0.0000	0.0000	

MINERALS	Q	C	Y	OR	AB	AN	LC	NE	KP	HL	TN	NC
MOL.AMTS.	0.0000	0.0000	0.0000	0.0029	0.0242	0.1003	0.0000	0.0052	0.0000	0.0000	0.0000	0.0000
PERCENTAGES	0.000	0.000	0.000	1.175	12.702	27.912	0.000	1.474	0.000	0.000	0.000	0.000

MINERALS	AC	NS	FS	AG	EN	FS	FO	FA	CS	MT	CM	RM
MOL.AMTS.	0.0000	0.0000	0.0000	0.1743	0.1303	0.0439	0.0585	0.0197	0.0000	0.0156	0.0000	0.0000
PERCENTAGES	0.000	0.000	0.000	20.242	13.082	5.798	8.236	4.023	0.000	3.600	0.000	0.000

MINERALS	IL	TN	PF	RU	AP	FR	PR	CC	MG	TOTAL	SALIC	FEMIC
MOL.AMTS.	0.0119	0.0000	0.0000	0.0000	0.0000	0.0000	0.0000	0.0000	0.0000			
PERCENTAGES	1.807	0.000	0.000	0.000	0.000	0.000	0.000	0.000	0.000	100.000	43.212	56.788

MINERALS	DI	DI-WO	DI-EN	DI-FS	HY	HY-EN	HY-FS	OL	OL-FO	OL-FA	WOL
MOL. AMTS.	0.1743	0.1743	0.1303	0.0439	0.0000	0.0000	0.0000	0.0783	0.0585	0.0197	0.0000
PERCENTAGES	39.122	20.242	13.082	5.798	0.000	0.000	0.000	12.258	8.236	4.023	0.000

THORNTON & TUTTLE DIFFERENTIATION INDEX = 15.301

BARTHS CATIONS	SI	AL	FE+3	FE+2	MG	CA	NA	K	H	TI	P	MN
	44.24	14.66	1.73	6.15	13.76	15.28	3.27	0.22	0.00	0.66	0.00	0.01
		ZR	C	S1	CL	F	S2	CR	NI	BA		
		0.00	0.00	0.00	0.00	0.00	0.00	0.00	0.00	0.00		

NIGGLI VALUES	AL*	FM*	C*	ALK*	SI	RI	P	H	K	MG	SI*	QZ
	15.93	47.07	33.20	3.80	96.15	1.44	0.00	0.00	0.06	0.64	115.20	-19.05

Appendix VI

Computer programs used in this thesis

Program	Capabilities	Source
XRFMAJ.FOR	X-ray data is converted into oxide percentages	Rewritten for Dec-20 by Gary Anderson, Dec. 3, 1979
USGS.FOR	Calculates CIPW values, Niggli values, Barth's cations and Thornton and Tuttle diff. index.	Rewritten for Dec-20 by Gary Anderson, last update 4/5/80

Appendix VII

ACF
Values

Initial oxide percentages for the amphibolite samples were converted to molecular percentages, then corrected for accessory minerals - biotite and magnetite. For biotite a Mg:Fe ratio was assumed = 1.

Corrected molecular percentages for iron and magnesium are:

samples	3	4	6	7	8	9	10
Fe_2O_3	.59	-	-	-	-	-	-
FeO	6.47	6.2	3.88	5.31	7.5	5.79	5.94
MgO	8.19	8.63	7.16	8.11	8.98	7.71	7.34

$A = (Al_2O_3) + (Fe_2O_3) - ((Na_2O) + (K_2O))$

$C = (CaO) - 3.3(P_2O_5)$

$F = (MgO) = (MnO) + (FeO)$

ACF values calculated with corrected iron and magnesium values are:

Samples	3	4	6	7	8	9	10
A	9.92	9.5	9.62	9.95	7.72	8.24	9.85
C	25.06	25.05	23.86	26.3	23.06	23.3	27.01
F	29.77	30.53	23.61	27.8	32.94	27.63	26.63

The ACF values were recalculated to 100% for ternary plots.

This thesis is accepted on behalf of the faculty of the Institute by the following committee:

Clay T. Smith

James M. Rubin

David L. Norman

Date 9-30-80